**NORTHWESTERN UNIVERSITY**

# The N-Terminus of Tau in Filament Formation and the Regulation of Axonal Transport: A Perspective on Tau Assembly and Toxicity

**A DISSERTATION**

**SUBMITTED TO THE GRADUATE SCHOOL**

**IN PARTIAL FULFILLMENT OF THE REQUIREMENTS**

**for the degree**

**DOCTOR OF PHILOSOPHY**

**Field of Cell and Molecular Biology**

**By**

**Nichole E. M. LaPointe**

**EVANSTON, ILLINOIS**

**June 2008**

© Copyright by Nichole LaPointe 2008
All Rights Reserved

## Abstract

**The N-Terminus of Tau in Filament Formation and the Regulation of Axonal Transport: A Perspective on Tau Assembly and Toxicity**

**Nichole E. M. LaPointe**

In several neurodegenerative diseases, the microtubule-associated protein tau self-aggregates to form filaments that accumulate in neurons and/or glia, although the relationship between tau aggregation and cell death is a subject of debate. The amino terminus of tau is involved in conformational changes that appear critical for filament formation, hinting at a regulatory role for this part of the protein in aggregation. The amino terminus may also be important to the study of physiological tau function, as it is implicated in a number of interactions between tau and various other cellular proteins. In this dissertation, we hypothesize that the amino terminus plays a critical role in the regulation of tau filament formation and toxicity. We examine the regulatory role of the amino terminus in filament formation using an *in vitro* polymerization assay, and address its involvement in filament toxicity in isolated axoplasm. We demonstrate that polymerization of full-length tau is inhibited when an excess of amino terminus is added to the reaction mixture, either in the form of recombinant N-terminal constructs or as the short, naturally occurring 6D and 6P isoforms. Our results are consistent with a model of soluble tau in which the amino terminus and the carboxy terminus are in close proximity. We also demonstrate that the amino terminus triggers a signaling cascade resulting in

the inhibition of kinesin-dependent axonal transport. This effect is present in soluble 6D and 6P tau isoforms, which lack the C-terminal half of canonical tau, but is absent from full-length monomer. The folded conformation described above may explain why soluble full-length tau has no effect on transport in this system. In contrast, full-length tau triggers transport inhibition when in filamentous form, suggesting that filament formation locks canonical tau in a conformation in which the N-terminus is more accessible. Collectively, this dissertation proposes that the toxic effects of tau filaments result when the amino terminus is repositioned and "unmasked" during polymerization. Our work not only reveals a novel role for the amino terminus in the regulation of filament formation, but highlights the cell biological consequences of tau aggregation.

## Acknowledgement

I would like to thank my P.I., Skip Binder, for the support and encouragement he's given me over the years. Skip's been around since the beginning of my graduate career; he interviewed me when I applied to Northwestern, and gave me a job the summer before classes started. My education also owes a good deal to Dr. Robert Berry, who co-ran the lab for most of my graduate career, and whose presence in lab has been sorely missed this past year and a half. Moving to a new city is never easy, but the friendly crew in the Binder-Berry Lab, and their policy of Friday happy hours, eased the transition to Chicago quite a bit. I feel very fortunate to have found a home with them.

I could not have accomplished the work in this dissertation without the help of many lab members, past and present. In particular, I would like to thank Drs. Chris Gamblin and Angie Guillozet-Bongaarts, for the invaluable advice and guidance they've given me during their time in the lab and beyond. I would also like to acknowledge my fellow graduate students; Dr. Mathew Reynolds, Dr. Peleg Horowitz, who co-authored the work presented in Chapter 2, and especially Dr. Sarita Lagalwar, who joined the Binder Lab at the same time I did and weathered the storm that is graduate school with me. I am also deeply grateful Dr. Yifan Fu, lab manager, research associate, and antibody expert; without her, the lab would grind to a halt.

I would also like to acknowledge Drs. Scott Brady and Gerardo Morfini (UIC), who made the work in Chapter Four possible, and Dr. Sarah Rice, for serving on my thesis committee and for her help in the preparation of this dissertation. I would also like to thank Dr. Adriana Ferreira for her work on my thesis committee. Finally, I would like to thank my friends and

family for their love and support over the years, especially my parents, Jean and Dudley LaPointe, who instilled in me a love of learning, and my husband, Justin Ziegler.

**Table of Contents**

## List of figures

## List of Tables

## Abbreviations

| | |
|---|---|
| **0N, 1N, 2N** | Zero, one, and two alternatively spliced amino terminal exons |
| **3R, 4R** | Three and four microtubule-binding repeats |
| **AA** | Arachidonic acid |
| **Aβ** | Beta-amyloid |
| **AD** | Alzheimer's disease |
| **CNS** | Central nervous system |
| **CMC** | Critical micelle concentration |
| **CREBpp** | cAMP response element-binding protein phosphopeptide |
| **DIC** | Differential interference contrast |
| **DTT** | Dithiothreitol |
| **E2, E3, E10** | Exons two, three, and ten |
| **EGTA** | Ethylene glycol bis(β-aminoethylether)- N,N,N',N'-tetraacetic acid |
| **ELISA** | Enzyme linked immunosorbent assay |
| **EM** | Electron microscopy |
| **FAT** | Fast axonal transport |
| **FRET** | Florescence resonance energy transfer; FTD, fronto-temporal dementia |
| **FTDP-17** | Frontotemporal dementia and Parkinsonism linked to chromosome 17 |
| **GSK3** | Glycogen synthase kinase-3 |
| **HEPES** | N-(2-hydroxyethyl)piperazine-N'-2-ethanesulfonic acid |
| **hTau23** | Shortest human brain tau isoform, with no alternatively-spliced exons |
| **hTau40** | Longest human brain tau isoform, with alternatively-spliced exons 2, 3, and 10 |

| | |
|---|---|
| **$i_s$** | Intensity of scattered light |
| **JNK** | cJun N-terminal kinase |
| **K23** | Tau construct based on hTau23, but containing no MTBRs |
| **KHC** | Kinesin heavy chain |
| **KLC** | Kinesin light chain |
| **LLS** | Laser light scattering |
| **MAP** | Microtubule-associated protein |
| **MARK** | Microtubule affinity regulating kinase |
| **MBO** | Membrane bound organelle |
| **MBTR** | Microtubule binding repeat |
| **MT** | Microtubule |
| **NFT** | Neurofibrillary tangle |
| **PHF** | Paired helical filament |
| **PP1** | Protein phosphatase-1 |
| **PP1c** | Protein phosphatase-1 catalytic subunit |
| **PP2A** | Protein phosphatase 2A |
| **SAPK** | Stress-activated protein kinase |

# CHAPTER ONE

## INTRODUCTION

Tau is a microtubule-associated protein (MAP) originally identified as a factor that stimulated microtubule formation in tubulin preparations *in vitro* (Weingarten, Lockwood, Hwo, & Kirschner, 1975). Roughly a decade after its initial discovery, several groups reported that aggregated tau is the major component of neurofibrillary tangles (NFT), one of the defining neuropathological features of Alzheimer's disease (AD) (Grundke-Iqbal et al., 1986; Kosik, Joachim, & Selkoe, 1986; Wood, Mirra, Pollock, & Binder, 1986). The revelation of tau's prominent role in disease sparked renewed interest in this protein, and initiated efforts to understand the mechanics and consequences of tau aggregation (reviewed in (T. C. Gamblin, R. W. Berry, & L. I. Binder, 2003) and (Ballatore, Lee, & Trojanowski, 2007)).

Although tau aggregates via interactions of its repeat regions, cis-acting control elements exist within the molecule as well. Of these, the amino terminus has emerged as an area involved in conformational changes that appear critical for tau filament formation, hinting at a regulatory role for this part of the protein in tau aggregation. This portion of the protein may also be important to the study of physiological tau function, as it is implicated in a number of interactions between tau and various other cellular proteins. It is not known whether the interaction of tau with these other proteins is affected by the conformational rearrangements in the amino terminus that accompany filament formation, but this question lies at the intersection of the studies of tau form and function.

In this dissertation, we hypothesized that the amino terminus of tau plays a critical role in the regulation of filament formation and toxicity. First, we used an *in vitro* polymerization assay to examine the regulatory role that this part of the molecule plays in filament formation The results of these experiments lead to a better understanding of the positioning of the amino terminus when tau is in a soluble state, and the conformational changes involving the amino

terminus that accompany polymerization. Next, we extended our study of the N-terminus in filament formation to naturally occurring isoforms (Tau6D and Tau6P) that lack the MTBR region and the C-terminus of canonical tau. Our work suggests that these N-terminal isoforms may be potential endogenous regulators of filament formation. Finally, we examined the involvement of the amino terminus in filament toxicity using isolated squid axoplasm. Our results in this system highlight the consequences of filament formation, and suggest a mechanism through which changes in the amino terminus may contribute to neuronal dysfunction.

The following sections of this chapter review the basics of tau biochemistry, and cover a number of its hypothetical physiological functions, including the regulation of microtubule-dependent transport. Tau neuropathology is also discussed, as well as the controversial relationship between aggregation and neurodegeneration. This chapter also covers several *in vitro* and *in vivo* factors that influence tau filament formation, including background information on the role of the N-terminus in this process.

## TAU PRODUCTION AND LOCALIZATION

Tau is encoded by a single gene on chromosome 17 (Neve, Harris, Kosik, Kurnit, & Donlon, 1986). This gene gives rise to three major transcripts; a 2 kb transcript that targets tau to the nucleus, a 6 kb transcript that encodes neuronal tau, and a 9 kb transcript expressed in the retina and the peripheral nervous system (reviewed in (Andreadis, 2005)).

In the adult human central nervous system (CNS), alternative splicing of the 6 kb transcript produces six canonical tau isoforms that differ according to the presence or absence of exons 2, 3, and 10. Exons 2 and 3 encode regions that extend the acidic amino terminus of the protein, often referred to as the projection domain. The N-terminal domain is followed by a

proline-rich region that is thought to confer a great deal of flexibility to the protein. The C-terminal portion of the protein contains three or four (if exon 10 is present) imperfect repeats of 18 amino acids, termed microtubule binding repeats (MTBR), separated by inter-repeat regions of 13 or 14 amino acids. The alternative splicing of tau is developmentally regulated, with the shortest isoform (lacking exons 2, 3, and 10) predominating early in development. In the healthy adult CNS, the six isoforms are expressed at roughly equal levels (reviewed in (V. M. Lee, Goedert, & Trojanowski, 2001).

In the six major tau isoforms described above, exon 6 is entirely removed from the transcript prior to translation. However, other tau isoforms include part or all of this exon. Isoforms in which the entire exon is included are designated 6+, and have been detected in fetal and adult brain at the mRNA (Leroy et al., 2006; Wei & Andreadis, 1998) and protein level (Luo, Tse, Memmott, & Andreadis, 2004). The domain encoded by exon 6 is proline-rich, and inclusion of this exon extends the proline-rich region of the protein. It is not known how the presence of exon 6 modifies tau's physiological functions, but expression of 6+ tau in neuronal cell culture inhibits neurite extension (Luo et al., 2004).

In addition to its normal 3' splice site, exon 6 contains two additional 3' splice sites, designated 6p and 6d according to whether the location is proximal or distal to the 5' border of exon 6. Initially believed to be cryptic, subsequent work detected evidence that these sites are utilized in various human tissues, including brain (Leroy et al., 2006; Luo et al., 2004; Wei & Andreadis, 1998). The use of either of these sites causes a frame shift, which introduces a unique eleven amino acid sequence followed by a stop codon. The resulting tau proteins contain the amino terminus of the canonical isoforms, but lack most of the proline-rich region, the MTBR

domain, and the C-terminal tail (Luo et al., 2004). These isoforms, Tau6D and Tau6P, are discussed further in Chapters Three, Four, and Five.

**Tau localization in normal brain**

Estimates have placed the concentration of tau in neurons at 1-10 μM (Drubin, Feinstein, Shooter, & Kirschner, 1985; Khatoon, Grundke-Iqbal, & Iqbal, 1992). Although tau was originally labeled an axonal protein (Binder, Frankfurter, & Rebhun, 1985), further work demonstrated its presence throughout the somato-dentritic compartment (Papasozomenos & Binder, 1987). Tau is also present in the nucleus, where it is associated with the nucleolus (Loomis, Howard, Castleberry, & Binder, 1990), although its function there remains largely mysterious. Tau expression is not restricted to neurons, but also occurs in oligodendrocytes (LoPresti, Szuchet, Papasozomenos, Zinkowski, & Binder, 1995), astrocytes (Papasozomenos & Binder, 1987), and microglia (Ghoshal et al., 2001; Odawara et al., 1995).

Although the six canonical tau isoforms are ubiquitous throughout the adult human brain, expression of the 6D/6P isoforms appears to be less evenly distributed. For example, 6D protein levels are particularly high in the cerebellum, and low in the hippocampus and cerebral cortex. This expression pattern means that 6D levels are highest in an area that is relatively protected from developing tau-based neuropathology in Alzheimer's disease, and lowest in the most severely affected areas. Furthermore, even within affected areas, 6D expression did not co-localize with markers of filamentous tau pathology on a cell-by-cell basis (Luo et al., 2004). Based on these observations, we examined the potential of the 6D/6P isoforms as inhibitors of tau filament formation. That work is presented in Chapter Three.

## PHYSIOLOGICAL TAU FUNCTIONS

### Microtubule binding and dynamics

The best-studied function of tau is as a regulator of microtubule assembly and dynamics. Microtubules are tubular polymers composed of alpha and beta tubulin subunits. They are a major component of the neuronal cytoskeleton, where they provide structure, support neurite outgrowth, and serve as tracks for intracellular transport. Microtubules are structures constantly in flux, and exhibit both treadmilling and dynamic instability. Treadmilling refers to the process by which tubulin subunits attach preferentially to the "plus" end of the polymer, resulting in net growth at that end, and are simultaneously lost from the "minus" end. The plus end of the microtubule is also the site of dynamic instability, in which periods of sustained growth are interrupted by rapid shortening events, termed "catastrophes". Conversely, the transition from shortening to growth at the plus end is referred to as a "rescue" (see (Margolis & Wilson, 1998) and (Desai & Mitchison, 1997) for review). Microtubule dynamics are regulated by a number of MAPs, as well as naturally occurring and synthetic compounds (reviewed in (L. Wilson, Panda, & Jordan, 1999)).

Tau promotes microtubule assembly, effectively lowering the critical concentration of tubulin (Cleveland, Hwo, & Kirschner, 1977; Weingarten et al., 1975). At steady state, tau suppresses microtubule dynamics; it increases the time that microtubules spend in an attenuated state (neither growing nor shortening), increases the rescue frequency, and suppresses the catastrophe frequency (Panda, Goode, Feinstein, & Wilson, 1995). The effect of tau on microtubule dynamics is similar to taxol, although their binding sites on tubulin probably do not overlap (reviewed in (L. Wilson et al., 1999)). Like taxol, tau most likely acts by inducing conformational changes in tubulin subunits local to the binding site, which are communicated to

more distal tubulin subunits (Panda et al., 1995). As a result, even low ratios of tau to tubulin have dramatic effects on microtubule morphology (Felgner et al., 1997) and behavior (Panda et al., 1995; L. Wilson et al., 1999).

Tau binds predominately at the microtubule surface, although a fraction appears to be incorporated into the tubulin lattice during microtubule polymerization (Makrides, Massie, Feinstein, & Lew, 2004). Four-repeat tau binds to microtubules with a stronger affinity than three-repeat tau (Butner & Kirschner, 1991; Gustke, Trinczek, Biernat, Mandelkow, & Mandelkow, 1994). Partly due to this observation, initial models proposed that tau-microtubule binding occurred exclusively through the MTBRs, and that the presence of multiple tandem MTBR domains allowed tau to link individual tubulin dimers together (reviewed in (Chau et al., 1998)) However, subsequent research demonstrated that the individual repeats do not contribute equally to microtubule binding. Furthermore, a strong contribution to binding is made by the inter-repeat region between MTBRs 1 and 2, which is present only in four-repeat tau isoforms (Goode & Feinstein, 1994). In three-repeat tau, the analogous region between repeats 1 and 3 makes a similar but lesser contribution (Goode, Chau, Denis, & Feinstein, 2000).

Another blow to the tandem repeat model of tau-microtubule interaction was the discovery that constructs consisting of the repeat domain alone bind poorly to microtubules. Affinity is dramatically increased by the presence of the proline rich region and the C-terminal tail, areas of tau that directly flank the MTBR domain (Gustke et al., 1994; Mukrasch et al., 2007). Current models of tau-microtubule interaction suggest that tau adopts an “induced fit” conformation on the microtubule surface, in which initial binding through the MTBRs is followed by a conformational change in tau that stabilizes the interaction (Goode et al., 2000). Intramolecular interactions between the parts of the proline rich region and the C-terminus that

flank the MTBR domain (Lichtenberg-Kraag et al., 1992) may be part of this stabilizing conformation (Goode et al., 2000). The contribution of the MTBR flanking regions differs between three- and four-repeat tau, indicating that there are isoform-specific differences in the mode of microtubule binding (Goode et al., 2000; Goode & Feinstein, 1994). This hypothesis is supported by the recent discovery that three- and four-repeat isoforms have subtly different effects on microtubule dynamics (Levy et al., 2005).

The affinity of tau for microtubules is negatively regulated by phosphorylation, especially at sites within and around the MTBR region (see (V. M. Lee et al., 2001) for a review). Of these sites, phosphorylation at KXGS motifs in the MTBR region by the microtubule affinity regulating kinase (MARK)/Par 1 family of kinases appears to be particularly important in inducing the detachment of tau from microtubules (Drewes, Ebneth, & Mandelkow, 1998; Drewes, Ebneth, Preuss, Mandelkow, & Mandelkow, 1997). Tau is highly phosphorylated in fetal brain (Bramblett et al., 1993; Goedert et al., 1993; Kanemaru, Takio, Miura, Titani, & Ihara, 1992) and in disease (Goedert et al., 1993; Hoffmann, Lee, Leight, Varga, & Otvos, 1997; Morishima-Kawashima et al., 1995; Zheng-Fischhofer et al., 1998), which likely contributes to reduced microtubule affinity in both states. For a review of other kinases involved in tau phosphorylation, see (Mazanetz and Fischer).

**Tau and microtubule-dependent transport**

Microtubule-dependent transport is the process by which cellular materials are moved from the soma to the periphery (anterograde direction), and back again (retrograde direction). Cargos transported in this manner include mitochondria and other membrane-bound organelles (MBO), synaptic components, and some cytoskeletal material. Transport is accomplished by

molecular "motor" proteins that move along microtubule tracks by converting the chemical energy of adenosine triphosphate (ATP) to mechanical energy. The primary anterograde motor is kinesin, while the retrograde motor is dynein. Neurons are particularly vulnerable to disruptions in intracellular transport; their extended morphology means that components necessary for proper function must be transported long distances (reviewed in (Gunawardena & Goldstein, 2004)).

Because of its ability to bind to the microtubule surface, many investigators have examined the effects of tau on microtubule-dependent transport. The anterograde motor kinesin seems particularly affected by the presence of tau. In *in vitro* systems consisting of only tau, microtubules, and kinesin, high ratios of tau to tubulin impair the attachment of the kinesin to the microtubule surface (Hagiwara, Yorifuji, Sato-Yoshitake, & Hirokawa, 1994; Seitz et al., 2002). Although tau inhibits the initial attachment of kinesin to microtubules, it has no effect once the motor is attached (Seitz et al., 2002). Further supporting an effect of tau on kinesin-microtubule attachment, recent research has demonstrated that tau reduces the number of kinesin molecules engaged in moving a single cargo (Vershinin, Carter, Razafsky, King, & Gross, 2007). Finally, some groups have observed partial overlap in the binding sites of tau and kinesin on the microtubule surface, which may explain the apparent binding interference (reviewed in (Marx, Muller, Mandelkow, Hoenger, & Mandelkow, 2006)).

Although tau competes with kinesin *in vitro*, the importance of this effect *in vivo* is a subject of debate. Certainly, high level expression of tau in cell culture results in decreased anterograde transport of membrane-bound organelles, suggesting that tau interferes with kinesin in these systems (Ebneth et al., 1998; Stamer, Vogel, Thies, Mandelkow, & Mandelkow, 2002). Furthermore, anterograde transport in cells overexpressing tau is restored by MARK kinase (E.

M. Mandelkow, Thies, Trinczek, Biernat, & Mandelkow, 2004), which induces the detachment of tau from the microtubule surface (Drewes et al., 1998; Drewes et al., 1997; E. M. Mandelkow et al., 2004). However, not all investigators have observed an effect of tau on anterograde transport. For example, the introduction of tau to isolated axoplasm at physiological concentrations had no effect on anterograde or retrograde transport, despite the fact that the majority of tau bound to microtubules. In this system, tau was ineffective even at high tau to tubulin ratios (3:1), suggesting that tau-microtubule binding does not directly affect kinesin-dependent transport (Morfini, Pigino, Mizuno, Kikkawa, & Brady, 2007).

In this dissertation we take a new approach to the study of tau and microtubule-dependent transport. Instead of focusing exclusively on soluble full-length tau, we also examine the effects of tau filaments and naturally occurring tau isoforms that lack the C-terminal half of canonical tau, including the MTBR region. Our use of isolated squid axoplasm for these experiments also allowed us to ask novel questions about the mechanism of action. The results of these experiments are discussed in Chapter Four.

**Other functions of tau**

Tau interacts with many other cellular proteins in addition to microtubules. Tau binds several kinases and phosphatases (Sobue et al., 2000; Sontag et al., 1999; Sun et al., 2002), including the serine/throenine phosphatase PP1 (protein phosphatase-1) (Liao, Li, Brautigan, & Gundersen, 1998), and may target these enzymes to the microtubule surface. Tau has also been found in association with ribosomes (Papasozomenos & Binder, 1987), and interacts with components of the neural plasma membrane (Brandt, Leger, & Lee, 1995; Hwang, Jhon, Bae, Kim, & Rhee, 1996; G. Lee, Newman, Gard, Band, & Panchamoorthy, 1998; Maas,

Eidenmuller, & Brandt, 2000) and the actin cytoskeleton (Fulga et al., 2007). Although the purpose of most of these interactions remains unknown, the number and variety of interaction partners hint at the complexity of the physiological role of tau in the cell.

Many of the interactions between tau and other cellular components take place via sequences in the amino terminal half of the tau protein (Brandt et al., 1995; Hwang et al., 1996; G. Lee et al., 1998; Maas et al., 2000). The amino terminus has also been implicated in several signaling cascades (Amadoro et al., 2006; Amadoro et al., 2004; Hwang et al., 1996), including the response to beta-amyloid (Barbato et al., 2005; King et al., 2006), a major protein in AD pathogenesis. If the assembly of tau into filaments affects the ability of the amino terminus to interact with other proteins, it may provide insights into the link between filament formation and disease. In Chapter Four, we present evidence suggesting that polymerization "unmasks" the amino terminus of the protein, and that this conformational rearrangement confers a toxic gain-of-function to filamentous tau.

## TAU NEUROPATHOLOGY

A number of diseases are characterized by intracellular filamentous aggregates of tau. Collectively, these diseases are termed "tauopathies". The list of neurodegenerative tauopathies is diverse, and includes corticobasal degeneration, progressive supranuclear palsy, Down's syndrome, and Pick's disease (see (V. M. Lee et al., 2001) for a review). Two tauopathies of particular interest are Alzheimer's disease (AD), and frontotemporal dementia and parkinsonism linked to chromosome-17 (FTDP-17).

### Tau pathology in Alzheimer's disease

Alzheimer's disease is characterized by intra- and extracellular protein deposits in the brain. The extracellular aggregates, or "amyloid plaques", consist of beta-amyloid (Aß), which is produced by cleavage of a larger amyloid precursor protein (APP). The intracellular deposits are filamentous aggregates of tau (Grundke-Iqbal et al., 1986; Kosik et al., 1986; Wood et al., 1986). In contrast to amyloid plaques, the number of tau deposits correlates with AD severity (Arriagada, Growdon, Hedley-Whyte, & Hyman, 1992; Arriagada, Marzloff, & Hyman, 1992), a point often cited to argue the relative importance of tau vs. amyloid pathology.

Neuropathological tau aggregates in AD are classified as one of three types based on morphology and subcellular localization: neurofibrillary tangles (NFT) are flame-shaped deposits in the neuronal cell body and proximal axon, neuropil threads consist of tau deposits in dendrites and the axon proper, and neuritic plaques are beta-amyloid deposits invaded by neuronal processes that contain filamentous tau (Goedert, Spillantini, & Davies, 1998). Filamentous tau deposits also appear in glia, although these accumulations are more abundant in other disorders (e.g. corticobasal degeneration and progressive supranuclear palsy) than in AD (R.W. Berry et al., 2001; R. W. Berry et al., 2004). Ultrastructurally, tau filaments purified from AD brain can be "straight" or "paired helical" in morphology (SF and PHF, respectively) (Buee, Bussiere, Buee-Scherrer, Delacourte, & Hof, 2000).

The appearance of tau pathology in AD follows a characteristic progression through the distinct anatomical regions of the brain that underlie the cognitive symptoms of the disease. For instance, the first lesions appear in anatomical regions associated with learning and memory, consistent with the fact that the disease initially presents with short term memory deficits (reviewed in (Ghoshal et al., 2002)). The ordered temporal and spatial progression of tau neuropathology has made it possible to develop a concept of tangle evolution (reviewed in

(Binder, Guillozet-Bongaarts, Garcia-Sierra, & Berry, 2005)). The basis of tangle evolution is that in tissue from any given case, the oldest tau pathology is found in the entorhinal cortex, while the youngest lesions are found in the parietal and frontal cortices. A second important component in the study of tangle evolution is the existence of a number of antibodies that recognize specific tau modifications (e.g. phosphorylation and truncation events).

Within this framework, it has been possible to determine the chronology of the myriad changes that tau undergoes during AD progression. In one of the earliest changes, tau adopts the conformation recognized by the antibody Alz-50, which precedes the formation of filamentous pathology (Garcia-Sierra, Ghoshal, Quinn, Berry, & Binder, 2003). In this conformation, the amino terminus of the protein is in close proximity to the MTBR region (Carmel, Mager, Binder, & Kuret, 1996). Subsequently, caspase cleavage of the extreme C-terminus (T. C. Gamblin, F. Chen et al., 2003) and loss of the amino terminus (Horowitz et al., 2004) are followed by another conformational rearrangement, in which the proline-rich region folds over the MTBRs (Tau-66 conformation; (Ghoshal et al., 2001)). In the oldest "end stage" tangles, tau has undergone further truncations, and little more than the MTBR region, thought to make up the filament core, remains (Garcia-Sierra et al., 2002).

**Frontotemporal dementia and parkinsonism linked to chromosome-17**

Mutations in the tau gene are responsible for FTDP-17, a group of autosomally dominant neurodegenerative dementias (reviewed in (Goedert & Jakes, 2005; V. M. Lee et al., 2001)). The discovery of these mutations was an important landmark in understanding the role of tau in disease, because they demonstrated that changes in tau are sufficient to cause neurodegeneration. FTDP-17 mutations can be exonic or intronic. With few exceptions, exonic mutations cluster in

and around the MTBR region. Individual exonic FTDP-17 mutations vary in their effects on tau biochemistry, but many reduce tau's microtubule binding affinity and increase its propensity to form filamentous aggregates. The intronic mutations cluster around the exon 10 splice site, where they disrupt the ratio of 3-repeat to 4-repeat tau. That The fact that this shift in the balance of tau isoforms results in neurodegeneration underscores the importance of the proper regulation of tau alternative splicing. Although neuropathological and biochemical features differ between mutations, all FTDP-17 cases are characterized by the presence of filamentous tau aggregates.

L266V is an FTDP-17 mutation that illustrates many clinical, neuropathological, and tau biochemical features of this group of dementias. The patient presented in his early thirties with inappropriate behavior, personality changes, and apathy, followed by a relatively quick (< 6 year) decline. Autopsy revealed severe neuronal atrophy throughout much of the cerebral cortex (Hogg et al., 2003).

L266V occurs in exon 9 (MTBR 1) and produces Pick's disease-like neuropathology, a common feature of exon 9 mutations (e.g. G272V and K257T). Biochemical analysis of L266V brain homogenate revealed that the pathology in this case was composed primarily of three-repeat tau. Consistent with this finding, experiments with recombinant L266V demonstrated that this mutation increased the ability of three-repeat tau to form filaments, but did not affect the polymerization of four-repeat tau. In contrast to the isoform-specific effects on aggregation, L266V decreased the ability of both three- and four-repeat tau isoforms to promote microtubule assembly (Hogg et al., 2003).

## THE RELATIONSHIP BETWEEN FILAMENT FORMATION AND TOXICITY

Despite multiple links between tau filament formation and disease, the role that tau aggregation plays in neurodegeneration remains controversial. FTDP-17 mutations that increase tau aggregation suggest that filament formation represents a toxic gain-of-function (reviewed in (V. M. Lee et al., 2001)), as does the fact that tau pathology in AD correlates with the severity of disease (Arriagada, Growdon et al., 1992; Arriagada, Marzloff et al., 1992). A direct link is also supported by studies of tau aggregation in cultured cells, where the appearance of aggregates is associated with cell death (Bandyopadhyay, Li, Yin, & Kuret, 2007; Y. P. Wang, Biernat, Pickhardt, Mandelkow, & Mandelkow, 2007).

Although tau filament formation correlates with neurodegeneration in many experimental systems, this is not always the case. For example, dramatic neurodegeneration in the absence tau deposits was observed in a drosophila model of tauopathy (Wittmann et al., 2001). Similarly, in a transgenic mouse model, cognitive improvement was observed when tau expression was suppressed, although NFTs continued to accumulate (Santacruz et al., 2005). A disconnect between tau aggregation and toxicity was also observed in a mouse model expressing P301L tau, a potent FTDP-17 mutation that drives tau aggregation; here, synapse loss occurred prior to tangle formation (Yoshiyama et al., 2007).

These and other studies have lead some to propose that tau filaments do not precede the onset of toxicity and are not directly toxic. Instead, neurodegeneration may result from the loss of normal tau functions, which may be driven by abnormal phosphorylation, or by filaments acting as sinks that remove otherwise functional tau from essential functions (reviewed in (Ballatore et al., 2007). It is likely that the loss of tau's microtubule-associated functions contributes to neurodegeneration in AD, since some of the earliest morphological changes in this disease are consistent with disruptions in the microtubule network. Also supporting the loss-of-

function hypothesis, the microtubule-stabilizing drug paclitaxel reversed signs of microtubule loss and neurodegeration in a tau transgenic mouse model of AD (Zhang et al., 2005).

Another possibility is that smaller tau aggregates, such as oligomers, are the toxic species. Oligomeric species of other proteins have been implicated in disease, including beta-amyloid and alpha-synuclein (reviewed in (Caughey & Lansbury, 2003)). Oligomeric tau species have been isolated in two mouse models of tauopathy, and the appearance of these oligomers correlated with functional deficits and memory loss (Berger et al., 2007). Tau oligomers have also been detected in human AD (Berger et al., 2007; Maeda et al., 2007; Maeda et al., 2006) and FTDP-17 tissue (Berger et al., 2007). Tau oligomers may be difficult to detect in some systems, and could explain animal models in which a disconnect has been observed between toxicity and detectable tau aggregates.

In this dissertation, we examine the issue of filament toxicity by comparing the effects of soluble and filamentous tau on microtubule-dependent transport in isolated axoplasm. Our results indicate that tau filaments disrupt transport in this system at concentrations where soluble tau has no effect, and that the mechanism involves the amino terminus of the protein. These results are presented in Chapter Four.

## REGULATION OF TAU FILAMENT FORMATION

Tau is a remarkably soluble protein under many conditions, including high temperatures and salt concentrations. Given that solubility, an important question in the field is how this soluble protein forms the insoluble polymers found in disease. In solution, tau monomer has little detectable secondary structure, and is thought to exist in a relatively extended conformation (Schweers, Schonbrunn-Hanebeck, Marx, & Mandelkow, 1994; Syme et al., 2002). In contrast,

tau filaments are highly ordered structures with a strong beta-sheet component. The evidence for this beta-sheet content is supported by x-ray diffraction studies, as well as the strong reactivity of tau filaments to compounds that fluoresce in the presence of beta structure, such as thioflavin S (reviewed in (T. C. Gamblin, R. W. Berry et al., 2003) and (Kuret et al., 2005)). The beta-sheet signal is likely traceable to the filament core, which is thought to be composed of stacked MTBRs of individual tau proteins. Sequences in this region of the protein are essential for *in vitro* filament formation (Abraha et al., 2000; von Bergen, Friedhoff, Biernat, Heberle, & Mandelkow, 2000), and constructs consisting of only the MTBR region can assemble into filament-like structures (von Bergen et al., 2000). Although the MTBR region plays a central role in filament formation, many other factors influence this process.

**Heparin and arachidonic acid**

Tau does not readily aggregate into filaments *in vitro*; rather, filament formation must be triggered through the addition of inducer molecules. The two most commonly used are the polyanionic compound heparin and arachidonic acid, a fatty acid that forms micelles under physiological buffer conditions.

Although the mechanism of action by which heparin facilitates filament assembly is incompletely understood, it is thought to promote a conformational shift toward beta-sheet in the MTBR region of the molecule (Barghorn, Davies, & Mandelkow, 2004; Mukrasch et al., 2007; von Bergen, Barghorn, Biernat, Mandelkow, & Mandelkow, 2005). The mechanism may involve interactions between heparin and the many positively charged lysine residues in this region (Mukrasch et al., 2007). Heparin-induced polymerization is optimal at slightly higher tau concentrations and lower pH than those found *in vivo*, but the filaments produced recapitulate all

of the major morphological types found endogenously (i.e. straight, twisted, and paired-helical). Although tau constructs containing only the MTBR region assemble rapidly in the presence of heparin, polymerization of wild-type tau by this method is slow, with a half time of around three days (reviewed in (T. C. Gamblin, R. W. Berry et al., 2003)).

In contrast to heparin, arachidonic acid-induced tau assembly is rapid at room temperature, with half times on the order of hours, and occurs readily at physiological pH and tau concentrations (reviewed in (T. C. Gamblin, R. W. Berry et al., 2003)). Filaments formed under these conditions are mostly straight filaments, although paired helical filaments are observed with longer incubation times (King, Ahuja, Binder, & Kuret, 1999). Like heparin, arachidonic acid is thought to induce a transition to beta-sheet in the MTBR region (C. N. Chirita, Congdon, Yin, & Kuret, 2005).

Induction of polymerization is not limited to arachidonic acid, but can be triggered by other fatty acids as well (D. M. Wilson & Binder, 1997). Research into the mechanism of fatty acid-induced polymerization has determined that micelle formation and the concentration of negative charges at the micelle surface are important factors in this process (C. N. Chirita, Necula, & Kuret, 2003). Tau filament formation is also triggered by anionic-coated microspheres, underscoring the importance of a negatively charged surface for the growth of tau polymers. However, microspheres are less potent inducers than fatty acids, indicating that additional qualities of the fatty acid inducers are necessary for robust polymerization (C. N. Chirita & Kuret, 2004). By extension, this research suggests that naturally occurring cellular components that resemble negatively-charged micelles, such as lipid vesicles or the plasma membrane, may support filament formation *in vivo* (C. N. Chirita et al., 2003). This idea was previously proposed based on an electron microscopic study of PHF in AD tissue. In this study,

filaments were often observed originating or terminating at membranous structures (Gray, Paula-Barbosa, & Roher, 1987).

The rapid timetable of arachidonic acid-induced polymerization makes it possible to monitor this process in real time through right angle laser-light scattering (LLS). As filaments form, light passing through the polymerization mixture is deflected. A camera placed at a 90 degree angle to the path of the laser is used to measure this scattered light, which is directly proportional to the amount of polymer. This technique allows the rapid biochemical evaluation of the effects of tau modifications on its polymerization profile (Gamblin, King, Dawson et al., 2000).

Tau aggregation has traditionally been thought to proceed through a nucleation-elongation mechanism (Barghorn & Mandelkow, 2002; C. N. Chirita et al., 2005; C. N. Chirita & Kuret, 2004; Friedhoff, von Bergen, Mandelkow, & Davies, 1998; King et al., 1999; Kuret et al., 2005). However, recent work challenges this model, suggesting that tau filaments do not nucleate per se. In this more complex mechanism, heparin and arachidonic acid induce allosteric changes in tau that promote aggregation, but the inducers do not remain associated with the filaments. This model is consistent with several observations, including the complex relationships between tau concentration, inducer concentration, and the amount of polymer formed (Carlson et al., 2007).

### *In vivo* regulators of polymerization

Although arachidonic and heparin may contribute to tau aggregation *in vivo*, their low concentration in the brain suggests that they are not the most important driving factors (reviewed in (Carlson et al., 2007)). Instead, the search for *in vivo* regulators of tau polymerization has

focused on mutations, posttranslational modifications, and regulatory elements within the protein itself. Some of the major factors that influence tau filament formation are discussed below.

*The amino terminus*: One of the first indications that the amino terminus was involved in filament formation came from the conformation-dependent antibody Alz-50. The Alz-50 epitope is discontinuous, and involves residues in the extreme amino terminus and the MTBR region. The affinity of this antibody for filamentous tau is roughly two orders of magnitude higher than its affinity for tau monomer, suggesting that filament formation brings the two regions that constitute the Alz-50 epitope, the N-terminus and the MTBR region, into close proximity (Carmel et al., 1996). Further *in vitro* studies demonstrated that removal of the amino terminal portion of the Alz-50 epitope impaired filament formation; this truncated tau construct (Δ2-18) forms multiple small aggregates, but rarely elongated filaments (Gamblin, King, Kuret, Berry, & Binder, 2000). These observations lead to the idea that adoption of the Alz-50 conformation represents an initial step in filament formation. However, more recent evidence indicates that the Alz-50 conformation does not necessarily lead to filament formation; nitration of tau monomer at sites that increase Alz-50 affinity also inhibits polymerization (Reynolds, Berry, & Binder, 2005b). The work presented in Chapter 2 of this dissertation uncovers an added layer of complexity in the role of the amino terminus in filament formation.

*The carboxy terminus:* While association of the amino terminus with the MTBR region encourages polymerization, association of the carboxy terminus with the MTBRs inhibits polymerization. When the C-terminal tail of the protein is removed, the resulting truncated tau

construct (1-421) assembles more rapidly than wild-type tau, and to a greater extent. Remarkably, polymerization levels are returned to normal when a peptide corresponding to the missing amino acids (422-441) is added back to the reaction mixture. Further work demonstrated that the function of this peptide depends on its ability to form an alpha helix, and that residues in the MTBR are required for its effect. These results suggest that association of the C-terminus with the MTBR region inhibits polymerization, and that this conformation promotes tau solubility (R. W. Berry et al., 2003).

*Caspase cleavage:* Caspases are effectors of apoptotic cell death, and play an important role in the developing nervous system. There is also growing evidence that they are involved in neurodegenerative conditions such as AD. The carboxy terminus of tau contains a caspase recognition motif ($^{418}$DMVD$^{421}$) that is highly conserved across species, suggesting that caspases cleave this portion of tau *in vivo*. Cleavage at Asp421 results in the removal of the last twenty amino acids of the protein, and the generation of a truncated tau product (1-421) (T. C. Gamblin, F. Chen et al., 2003). Because 1-421 assembles more rapidly and to a greater extent than wild-type tau, cleavage at this site may drive filament formation *in vivo* (R. W. Berry et al., 2003; T. C. Gamblin, F. Chen et al., 2003).

To examine the role of caspase cleavage of tau in AD, we generated an antibody that is specific for tau cleaved at Asp421 (Tau-C3). This antibody recognizes a subset of neuropathology in AD brain tissue, indicating that caspase cleavage may contribute to the formation of neurofibrillary pathology in this disease. Furthermore, Tau-C3 also recognizes tau in cultured neurons that have been exposed to the toxic fragment of beta-amyloid ($A\beta_{1-42}$), suggesting that caspase cleavage of tau may represent an important link between amyloid

plaques and NFTs, the two neuropathological features of AD (T. C. Gamblin, F. Chen et al., 2003).

*FTDP-17 mutations*: Many of the FTDP-17 mutations increase the ability of tau to aggregate. Most of these mutations occur in and around the MTBR region, highlighting the importance of that part of the molecule to filament formation. Other FTDP-17 mutations occur in intronic sequences near the exon 10 splice site, and disrupt the alternative splicing of this exon. The fact that these intronic mutations are associated with the pathological aggregation of tau suggests that alterations of the natural balance between three- and four-repeat tau can drive filament formation. In support of this idea, *in vitro* studies have demonstrated that four-repeat tau has a greater propensity to aggregate than three-repeat tau (King, Gamblin, Kuret, & Binder, 2000). In addition to effects on filament formation and tau splicing, many FTDP-17 mutations decrease the affinity of tau for microtubules, which could encourage filament formation by increasing the pool of cytoplasmic tau (reviewed in (Goedert & Jakes, 2005; V. M. Lee et al., 2001)).

*Phosphorylation:* The level of tau phosphorylation is elevated in AD, although many of these phosphorylation events are thought to occur in healthy brain as well as disease. It is estimated that tau in AD has 2-3 times the phosphate content of normal tau; as a result, tau in AD is often said to be phosphorylated to an abnormal extent, or "hyperphosphorylated". Hyperphosphorylation is not unique to AD tau, but occurs in FTDP-17 tau pathology as well (reviewed in (Brandt, Hundelt, & Shahani, 2005)).

There is conflicting evidence regarding the role that phosphorylation plays in the transition of tau from monomer to filament (reviewed in (Brandt et al., 2005)).

Hyperphosphorylation is an early change in the development of AD (E. Braak, Braak, & Mandelkow, 1994), and was thought to represent a driving force behind the formation of tau aggregates. In support of this model, Alonso et al. found that hyperphosphorylated tau isolated from AD brain assembles in the absence of polymerization inducers, and that dephosphorylation eliminates this ability (Alonso, Zaidi, Novak, Grundke-Iqbal, & Iqbal, 2001). In addition, the inhibition of glycogen synthase kinase-3 (GSK-3), a major tau kinase, alleviates tau aggregation and symptoms in some mouse models of tauopathy (Noble et al., 2005; Perez, Hernandez, Lim, Diaz-Nido, & Avila, 2003).

Additional evidence suggesting an intimate link between tau phosphorylation aggregation comes from *in vitro* experimental systems. In recombinant tau, pseudophosphorylation at Ser396 and Ser404 stimulates filament formation, possibly by interfering with the folding of the C-terminus over the MTBR region (Abraha et al., 2000). Also, phosphorylation of recombinant tau *in vitro* promotes the aggregation of filaments into higher-ordered NFT-like structures (Rankin, Sun, & Gamblin, 2005). However, other studies of *in vitro* filament assembly have found that phosphorylation inhibits filament formation (Schneider, Biernat, von Bergen, Mandelkow, & Mandelkow, 1999). Taken together, it appears that the specific effect of phosphorylation on tau aggregation depends on the location and number of phosphorylation events.

Phosphorylation induces conformational changes in tau, and these conformational changes may result in tau toxicity without necessarily leading to aggregation. For instance, expression of pseudophosphorylated tau constructs in neuronal cell culture triggered caspase activation and apoptotic cell death, but no tau aggregation (Fath, Eidenmuller, & Brandt, 2002). Toxicity of hyperphosphorylated tau in the absence of large tau aggregates has been reported in several other systems as well (reviewed in (Brandt et al., 2005)).

*Nitration:* In contrast to phosphorylation, the effects of nitration on filament formation are largely inhibitory. Tau contains five tyrosine residues; $^{18}$Y, $^{29}$Y, $^{197}$Y, $^{310}$Y, and $^{394}$Y, and all but one of these residues ($^{310}$Y) can be nitrated *in vitro* by peroxynitrite treatment (Reynolds, Berry, & Binder, 2005a). Using constructs singly-nitrated at each of these sites, Reynolds et al. examined the effects of nitration on tau filament formation. Nitration at each site inhibited tau polymerization, although the magnitude of the effect varied in a site-specific manner, with nitration at $^{29}$Y and $^{394}$Y showing the strongest inhibition. Tau nitration at $^{18}$Y (Reyes et al., submitted) and $^{29}$Y (Reynolds, Reyes et al., 2006) has been detected in the fibrillar lesions of AD brain, suggesting that nitration at these sites may play some role in the disease process.

## SUMMARY AND PREVIEW

Tau is a cytoskeleton-associated protein potentially involved in several cellular processes, including the regulation of microtubule dynamics and microtubule-dependent transport. In a variety of disease states, tau forms insoluble filamentous aggregates that correlate with neuronal dysfunction and death. Therefore, uncovering the factors that influence tau aggregation is important to understanding these diseases. Finally, although many lines of evidence link filament formation to neurodegeneration, it is unclear whether filamentous tau itself is directly toxic.

In Chapter Two, we examine the role of the amino terminus of tau in filament formation using an *in vitro* polymerization assay. We discover that tau fragments consisting of the amino terminus inhibit the polymerization of full-length tau. These N-terminal fragments appear to act by stabilizing full-length tau in a soluble conformation in which the N- and C-termini are in close

proximity. In Chapter Three, we extend our *in vitro* analysis of this phenomenon to naturally occurring short isoforms of tau, Tau6D and 6P. These isoforms contain the N-terminus of canonical tau, but lack most of the proline-rich region, the MTBR region, and the C-terminus. Like the N-terminal fragments of Chapter Two, which they resemble, we demonstrate that 6D and 6P isoforms inhibit the polymerization of full-length tau. Furthermore, we demonstrate that this ability is affected by alternative splicing events and by posttranslational modifications in crucial N- and C-terminal regions.

Finally, in Chapter Four we examine the consequences of filament formation by comparing the effects of monomeric and filamentous tau on microtubule-dependent transport in isolated squid axoplasm. We find that tau filaments inhibit anterograde (kinesin-dependent) transport, and that this effect depends on the extreme amino terminus of tau. Transport is also inhibited by soluble (as opposed to filamentous) forms of the 6D/6P isoforms. In contrast, inhibition is absent from soluble forms of canonical tau, suggesting that the N-terminus is inaccessible when full-length tau is free in the cytoplasm. These results support the model of soluble tau conformation proposed in Chapter Two. Collectively, the work presented in the following chapters sheds light on the conformational changes that the amino terminus undergoes during filament formation. It also suggests that repositioning of the amino terminus during polymerization allows tau filaments to trigger the disruption of microtubule-dependent transport, a process critical to neuronal survival.

# CHAPTER TWO

## N-TERMINAL FRAGMENTS OF TAU INHIBIT FULL-LENGTH TAU POLYMERIZATION *IN VITRO*

**Reproduced with permission from Biochemistry 45(42):12859-12866.**

**Copyright 2006 American Chemical Society**

## ABSTRACT

The polymerization of the microtubule-associated protein, tau, into insoluble filaments is a common thread in Alzheimer's disease and in a variety of frontotemporal dementias. The conformational change required for tau to transition from an extended monomeric state to a filamentous state with a high β-sheet content involves the extreme N-terminus coming into contact with distal portions of the molecule; however, these exact interactions are incompletely understood. Here we report that a construct representing amino acids 1-196 (Tau196), which itself does not polymerize, inhibits polymerization of full-length tau (hTau40) *in vitro*. In addition, we trace the inhibitory effect of Tau196 to amino acids 18-42 of the construct. We also provide evidence that the N-terminal tau fragments require a specific C-terminal region of tau (residues 392-421) to exert their inhibitory effect. The fragments are most effective at inhibiting polymerization when present during the initial five minutes, they remain in the soluble fraction of the polymerization reaction, and they increase the amount of soluble hTau40. The fragments also reduce the number and average length of filaments formed. Taken together, these results suggest that the N-terminal tau fragments inhibit hTau40 polymerization by interacting with a specific C-terminal sequence, thereby stabilizing a soluble conformation of tau.

# INTRODUCTION

Tau polymerization is a characteristic pathological feature of Alzheimer's disease (AD) (Binder et al., 2005; Duyckaerts, Colle, Dessi, Piette, & Hauw, 1998; Johnson & Hartigan, 1998; Johnson & Jenkins, 1996), several frontotemporal dementias (FTDs) (V. M. Lee et al., 2001), and various hereditary tauopathies (Hutton, 2001; V. M. Lee et al., 2001; Poorkaj et al., 2002). In AD, the appearance of filamentous tau pathology follows a spatial and temporal progression through the brain regions that underlie cognitive systems affected in AD (H. Braak & Braak, 1995; Ghoshal et al., 2002; Mitchell et al., 2002). Therefore, it is widely recognized that an understanding of the biochemical mechanisms underlying tau polymerization may lead to a deeper understanding of disease progression.

In solution, tau monomers have little discernible secondary structure (Schweers et al., 1994), although isolated regions of the tau protein, specifically the third microtubule binding repeat (Minoura et al., 2002) and the C-terminus (R. W. Berry et al., 2003; Esposito, Viglino, Novak, & Cattaneo, 2000), exhibit secondary structure detectible by NMR and / or circular dichroism. When not bound to microtubules, monomeric tau is thought to either exist in a largely extended state (Syme et al., 2002), exhibit high mobility in a globally folded state (Jeganathan, von Bergen, Brutlach, Steinhoff, & Mandelkow, 2006), or transition rapidly between several conformations (Minoura et al., 2005; Minoura et al., 2004). In contrast, tau filaments are highly ordered structures, with β-sheets predominating in the MTBR region (Barghorn et al., 2004; Eliezer et al., 2005; Tokimasa et al., 2005; von Bergen et al., 2000). The transition of tau from a monomeric to a filamentous state therefore must involve extensive conformational rearrangement.

Several lines of evidence suggest that the transition of tau from soluble monomer to insoluble filaments involves a folding event in which the N-terminus comes in close proximity to the MTBR region (Carmel et al., 1996; Jeganathan et al., 2006). Insights into the structures of filamentous tau have come from immunological studies with the conformation-dependent monoclonal antibodies Alz-50 (Carmel et al., 1996) and Tau-66 (Ghoshal et al., 2001). Both antibodies recognize tau conformations in which an N-terminal portion of tau is folded over the microtubule binding repeat (MTBR) region. The Alz-50 antibody recognizes a discontinuous epitope involving the extreme amino terminus and the third MTBR (residues 5-15 and 312-322) (Carmel et al., 1996; Jicha, Berenfeld, & Davies, 1999) and labels early tau lesions in AD brain (Garcia-Sierra et al., 2003; Hyman et al., 1988). In contrast, the epitope recognized by Tau-66 involves a different N-terminal region and a similar sequence in the third MTBR (residues 155-244 and 305-314) (Ghoshal et al., 2001), and Tau-66 decorates tau pathology at a later stage of maturation (Garcia-Sierra et al., 2003; Ghoshal et al., 2002).

Although immunological evidence suggests that the amino terminus is an integral part of filamentous tau conformations, little is known about how this region regulates the polymerization of tau. We have previously proposed that the N- and C- termini exert antagonistic effects on polymerization by competing for the same region in the MTBRs (R. W. Berry et al., 2003; Binder et al., 2005; T. C. Gamblin, R. W. Berry et al., 2003; T.C. Gamblin, R.W. Berry, & L. I. Binder, 2003). The C-terminus appears to be in close proximity to the MTBRs in the absence of polymerization inducers (Jeganathan et al., 2006), and removing the C-terminus increases the rate and extent of polymerization *in vitro* (Abraha et al., 2000; R. W. Berry et al., 2003). In contrast, folding of the extreme N-terminus into proximity with the MTBR region may be an early step in polymerization (King et al., 1999), and removal of amino

acids 2-18 of tau decreases, but does not abolish, polymerization *in vitro* (T.C. Gamblin et al., 2003). Because we have postulated that polymerization involves a folding event that brings the N-terminus and the MTBR region together (T. C. Gamblin, R. W. Berry et al., 2003; T.C. Gamblin et al., 2003), we hypothesized that a protein fragment containing only the N-terminus and not the MTBRs would inhibit polymerization of the full-length protein. However, we have previously shown that application of an N-terminal peptide consisting of amino acids 1-15 of tau did not affect polymerization *in vitro* (T.C. Gamblin et al., 2003), suggesting that a different or larger polypeptide fragment may be necessary to observe such an effect. Therefore we chose to begin our investigations with a construct representing nearly the entire N-terminal half of the protein.

Here we report that an N-terminal tau fragment truncated after residue 196 (Tau196, which lacks the MTBRs and is therefore assembly-incompetent) inhibits polymerization of full-length human tau (hTau40) in a dose-dependent manner. We show that the inhibitory effect requires amino acids 18-42 in the N-terminal fragment and residues 392-421 of the full-length protein. Furthermore, we provide evidence that the primary effect of the fragments is to inhibit polymerization at an early stage of the reaction, most likely by interacting with and stabilizing a monomeric or soluble oligomeric tau species.

## EXPERIMENTAL PROCEDURES

*Materials* – Arachidonic acid (AA) was obtained from Cayman Chemical (Ann Arbor, MI) and stored at -20°C. Working solutions were prepared in 100 % ethanol immediately prior to use. Synthetic peptides were supplied by Cell Essentials (Boston, MA). The peptide 18-42 represents amino acids 18-42 of hTau40 (YGLGDRKDQGGYTMHQDQEGDTDAG), and was supplied at >90% purity. A peptide with the same amino acid composition in a randomized order (KDQLDGGQQGGDTMHEGRAYDDGTY) was also synthesized.

*Recombinant proteins* – The full-length tau used in this study (hTau40) is the longest isoform in the human central nervous system and contains 441 amino acids, including both alternatively spliced N-terminal exons (e2 and e3) and four microtubule binding repeats (m1-m4; Fig. 1). The generation and purification of this construct and several others used in this study have been described elsewhere: hTau40, Δ2-18, Δ9-155, Δ155-244, Δ321-441, Δ430-441 (Carmel et al., 1996); Δ18-42, Δ18-30, Δ24-36, Δ30-42 (Horowitz et al., 2004); hTau23, hTau24 (King et al., 2000); Δ291-349, Δ376-441, Δ392-441 (Abraha et al., 2000); and Δ422-441 (T. C. Gamblin, F. Chen et al., 2003). The Tau196 construct was generated as previously described (Reynolds et al., 2005a). The Tau196 internal deletion mutant library was generated by restriction digestion and ligation of Tau196 with the various N-terminal deletions listed above, with the exception of Tau196 Δ104-147 ("Tau196B"), which was created using the Tau196 template and phosphorylated primers flanking the desired deletion. All proteins were expressed in *E. coli* and purified by means of an N-terminal poly-histidine tag (Abraha et al., 2000; Carmel et al., 1996).

*Epitope Mapping of Tau-7* – Internal deletion mutants of hTau40 were diluted to 2 ng/µl in Tris buffered saline (pH 7.6) and attached in quadruplicate to Costar 96-well plates overnight at 4° C. ELISAs were performed as previously described (Ghoshal et al., 2001) using the mouse monoclonal C-terminal tau antibody Tau-7 (40 ng/mL). Results of these ELISAs (Fig. 1) confirm that removal of amino acids 430-441 of tau abolish Tau-7 binding.

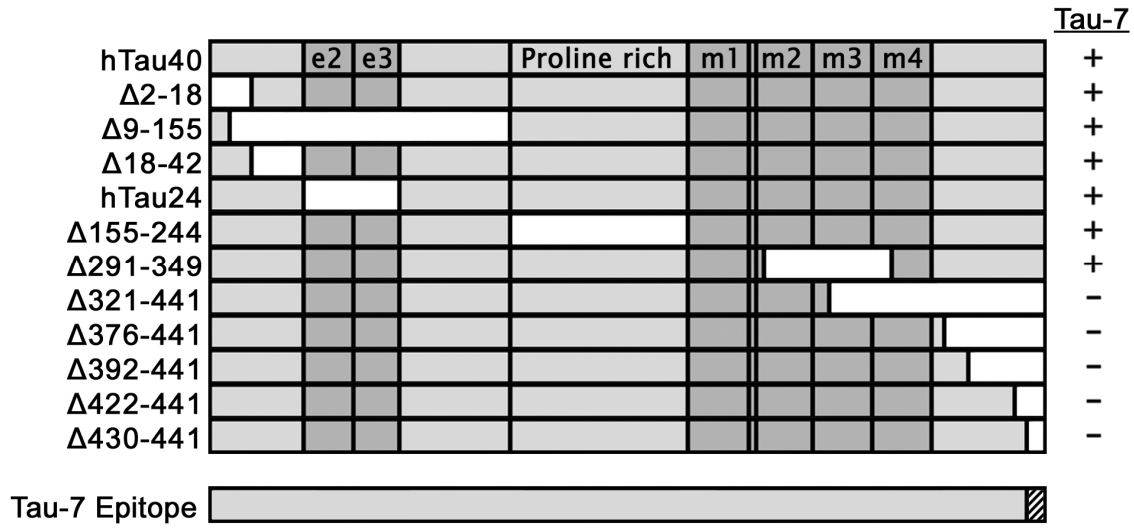


**Figure 1. The monoclonal antibody Tau-7 recognizes the extreme C-terminus of tau.** hTau40 is the longest isoform of tau in the human central nervous system (441 amino acids). Labeled boxes represent (from left to right): alternatively spliced N-terminal exons (e2 and e3), the proline-rich region, and the microtubule-binding repeats (m1-m4). The ability of Tau-7 to react with full-length hTau40 and tau harboring deletions (white; numbers on left) was assayed by ELISA. Data are expressed as plus (O.D. > 3.5) or minus (O.D. at background levels). The epitope was defined as the smallest deletion which completely abolished Tau-7 binding (hatched; Δ430-441).

*Polymerization reactions* – Tau polymerization was induced by arachidonic acid as previously described (Gamblin, King, Dawson et al., 2000). Briefly, tau protein (4 µM) was incubated at room temperature in reaction buffer (final buffer conditions: 10 mM HEPES, pH 7.6, 100 mM NaCl, 0.1 mM EGTA, 5mM DTT) in the presence of 75 µM arachidonic acid. The final volume

of ethanol in these reactions was 3.8 %, and this volume was added to control reactions in the absence of AA. Unless otherwise noted, N-terminal constructs were added at a concentration of 8 μM to the polymerization reaction, prior to the addition of 4 μM full-length tau and arachidonic acid. Reaction progress was monitored by the intensity of right angle laser-light scattering ($i_s$). End-point (t = 300 min) laser light scatter data from at least three independent experiments were analyzed for statistical significance by one-way ANOVA and protected t-tests, and time course data were fit with curves using GraphPad Prism 3.0 software. Error bars in all figures and tables represent plus or minus one standard error of the mean.

*Arachidonic acid critical micelle concentration (CMC)* – Arachidonic acid was diluted in polymerization buffer at a range of concentrations and incubated ten minutes at room temperature in the presence or absence of 8 μM protein. Intensity of right-angle laser light scattering was plotted as a function of arachidonic acid concentration, and linear regression was performed to determine the x-intercept (Brito & Vaz, 1986; C. N. Chirita et al., 2003). The data presented here are the combined results of five separate experiments, analyzed using a one-tailed t-test (GraphPad 3.0).

*N-terminal Fragment Centrifugation* – Reactions polymerized for five hours were centrifuged at 355,000 x g for 15 minutes at 25° C over a 40% glycerol cushion. Supernatant and pellet were boiled in Laemmli buffer and proteins were separated by SDS-PAGE electrophoresis before transfer to nitrocellulose membranes. N-terminal fragments (Tau196B) were probed with the amino terminal antibody Tau-12 (4 ng/mL) (Ghoshal et al., 2002; Horowitz et al., 2004), while

full-length tau was probed with Tau-7 (see Fig. 1). HRP-conjugated goat-anti-mouse secondary antibody (Vector) and ECL (Amersham) were used for detection.

*Electron microscopy* – Polymerization reactions were allowed to proceed at least four hours, fixed with 2% glutaraldehyde (Electron Microscopy Sciences, EMS), spotted onto 300 mesh formvar/carbon coated copper grids (EMS), and negatively stained with 2% uranyl acetate (EMS) as previously described (King et al., 1999). Grids were examined using a JEOL JEM-1220 electron microscope at 60kV and 12,000x magnification, and photographed using a MegaScan 794/20 digital camera and DigitalMicrograph software version 3.9.3 (Gatan). Optimas 6.0 imaging software (Media Cybernetics) was used to automatically identify and measure filaments (defined as objects ≥20 nm in length). At least five fields from each grid were chosen for quantitation under low illumination to prevent bias. Results from three separate experiments were analyzed by two-tailed t-test (GraphPad Prism 3.0 software).

*Tau Critical Concentration Assay* – Reactions polymerized for five hours were centrifuged at 355,000 x g for 15 minutes at 25° C. To determine the effectiveness of these sedimentation conditions at removing polymerized material from the supernatant, the supernatant fractions were analyzed by electron microscopy as above. The amount of tau in supernatant fractions was quantified by diluting samples in Laemmli sample buffer and spotting onto nitrocellulose membranes, alongside a series of hTau40 standards of known concentrations. Full-length tau was visualized with Tau-7 (which does not react with the N-terminal fragment) and HRP-conjugated goat-anti-mouse secondary antibody. The amount of protein per spot was quantified using Adobe Photoshop: a box of fixed size was centered on each spot, and the average pixel

intensity was determined using the histogram function. The tau standard curve and GraphPad Prism 3.0 software were used to determine tau concentrations in the soluble fractions of the polymerization reactions.

## RESULTS

*N-terminal tau fragments inhibit full-length tau polymerization* in vitro – To determine whether an amino terminal fragment of tau would inhibit polymerization of full-length tau (hTau40), a protein construct corresponding to the N-terminal half of hTau40 was generated by changing the tyrosine at position 197 to a stop codon. The resulting construct ("Tau196"; Fig. 2A) lacks the MTBR region, including the sequence required for arachidonic acid-induced filament assembly (residues 314-320) (Abraha et al., 2000). As predicted, Tau196 itself failed to polymerize in the presence of arachidonic acid (data not shown). When Tau196 was added at a two- or four-fold molar ratio, this N-terminal fragment of tau inhibited the polymerization of full-length tau protein as measured by right-angle laser light scattering (Fig. 2B).

*Inhibition of polymerization depends on amino acids 18-42 of Tau196* – In order to identify the specific sequence in Tau196 responsible for interfering with hTau40 polymerization, we generated a library of internal deletions on the Tau196 background (Fig. 2A) and screened these proteins for their ability to inhibit hTau40 polymerization. Tau196 mutants harboring deletions of residues 2-18, 41-103 (exons 2 and 3), or 104-147 reduced hTau40 polymerization by 57-63% ($p < 0.01$) at a two-fold molar ratio. However, removal of residues 18-42 resulted in loss of the inhibition (Fig. 2C; $p < 0.01$ vs. other deletions, not significant vs. hTau40 control). Constructs containing smaller deletions in the 18-42 region (18-30, 24-36, or 30-42) also failed to significantly decrease hTau40 polymerization (Fig. 2D; not significant vs. hTau40 control), indicating that this entire sequence may be required for inhibition. The inhibition caused by Tau196 Δ104-147 was more robust than for Tau196, and for this reason it was used as a positive

**Figure 2. N-terminal fragments of tau specifically inhibit arachidonic-acid induced tau polymerization as measured by laser light scattering.** (A) Schematic of the N-terminal tau constructs used in this study. A tau construct containing a stop codon at Y197 ("Tau196") and several internal deletion mutations on the Tau196 background were created and purified, including Tau196 Δ104-147 (herein called "Tau196B"). Constructs that inhibited (+) or failed to inhibit (–) polymerization (shown below) are indicated, as is the specific N-terminal sequence required for inhibition (hatched, residues 18-42). (B) Tau196 was added at a one-, two-, or four-fold molar ratio to a polymerization reaction of 4 μM full-length tau (hTau40). Polymerization was significantly inhibited in the presence of 8 μM ($p < 0.05$) and 16 μM ($p < 0.01$) concentrations of Tau196. (C) Internal deletion mutations in Tau196 (8 μM) were utilized to map the sequence specificity of the inhibitory effect. Only the Tau196 Δ18-42 fragment failed to significantly inhibit hTau40 polymerization ($p < 0.01$ vs. other deletion constructs, not significant vs. hTau40 control). (D) Smaller deletions in the 18-42 region of the tau fragment also eliminate the inhibitory effect of the fragment ($p < 0.01$ vs. Tau196B, not significant vs. hTau40 control), suggesting that this entire sequence is necessary to inhibit hTau40 polymerization.

**Figure 2**

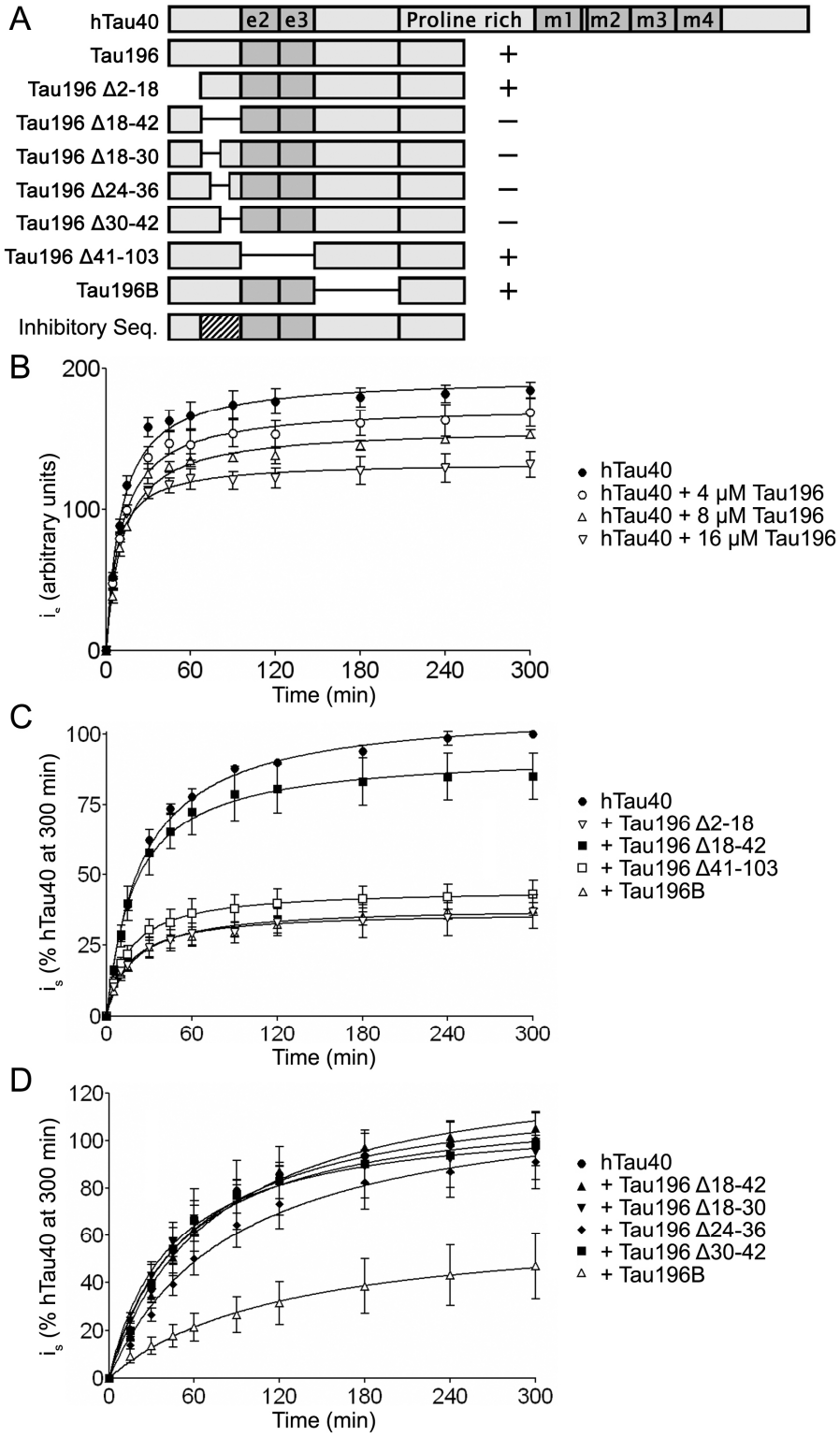
A
hTau40
e2
e3
Proline rich
m1
m2
m3
m4
Tau196
+
Tau196 Δ2-18
+
Tau196 Δ18-42
−
Tau196 Δ18-30
−
Tau196 Δ24-36
−
Tau196 Δ30-42
−
Tau196 Δ41-103
+
Tau196B
+
Inhibitory Seq.
B
200
100
0
$i_c$ (arbitrary units)
0
60
120
180
240
300
Time (min)
hTau40
hTau40 + 4 μM Tau196
hTau40 + 8 μM Tau196
hTau40 + 16 μM Tau196
C
100
75
50
25
0
$i_s$ (% hTau40 at 300 min)
0
60
120
180
240
300
Time (min)
hTau40
+ Tau196 Δ2-18
+ Tau196 Δ18-42
+ Tau196 Δ41-103
+ Tau196B
D
120
100
80
60
40
20
0
$i_s$ (% hTau40 at 300 min)
0
60
120
180
240
300
Time (min)
hTau40
+ Tau196 Δ18-42
+ Tau196 Δ18-30
+ Tau196 Δ24-36
+ Tau196 Δ30-42
+ Tau196B

control for polymerization inhibition in this experiment ($p < 0.01$) and for the remainder of the study, and Tau196 Δ104-147 was renamed to "Tau196B".

Since these data suggested a crucial role for residues 18-42, we next asked whether a peptide corresponding to these residues would also inhibit hTau40 polymerization. A second peptide containing the same amino acids in a randomized order was used as a control. At a 10-fold molar ratio (40 μM), neither peptide inhibited hTau40 polymerization as measured by laser light scattering and electron microscopy (data not shown). This result is consistent with our previous report that another N-terminal peptide (residues 1-15) does not affect hTau40 polymerization (T.C. Gamblin et al., 2003). The failure of these peptides to inhibit polymerization may indicate that a larger sequence is necessary to stabilize a direct interaction with hTau40, or to recapitulate the native conformation of the N-terminus of tau.

*N-terminal fragments require residues 392-421 of hTau40 to inhibit polymerization* – In our working model of tau polymerization, the N-terminus and C-terminus interact with the MTBR region of the full-length protein, with the N-terminus promoting polymerization and the C-terminus promoting solubility (R. W. Berry et al., 2003; Binder et al., 2005; T. C. Gamblin, R. W. Berry et al., 2003; T.C. Gamblin et al., 2003). We therefore hypothesized that the N-terminal fragments likewise interact with the MTBRs of hTau40, blocking the intramolecular interaction of these two regions that facilitates polymerization. If this is the case, removal of the MTBR binding site on hTau40 should ameliorate the inhibitory effects of the N-terminal fragment.

In order to identify this site, we employed a series of C-terminally truncated tau constructs (Δ321-441, Δ376-441, Δ392-441, Δ422-441), the last two of which are also found in AD brains (T. C. Gamblin, F. Chen et al., 2003; Novak, Kabat, & Wischik, 1993). All of these truncated tau proteins are known to polymerize effectively *in vitro* (Abraha et al., 2000; T. C. Gamblin, F. Chen et al., 2003). These C-terminally deleted tau proteins were polymerized in the absence or presence of twice-molar Tau196B, and the extent of polymerization was measured by laser light scattering. Tau196B inhibited polymerization of full-length tau and tau truncated at aspartic acid 421 (Fig. 3; $p < 0.01$). However, the N-terminal fragment failed to inhibit polymerization of tau proteins truncated prior to residue 392 ($p < 0.01$), suggesting that residues 392-421 are required for N-terminal inhibition. The simplest explanation for this result is that the N-terminus interacts directly with residues 392-421, although more complicated scenarios are possible. Because we have previously shown that residues 321-375 (and not 376-441) are required for C-terminal inhibition of polymerization (R. W. Berry et al., 2003), this result suggests that different regions of tau are required for polymerization regulation by the N- and C-termini.

*N-terminal fragments are most effective at early time points* – Once the specific sequences involved in the inhibition were identified, we turned our attention to the mechanism of tau polymerization and its inhibition. We began by examining the efficacy of the N-terminal fragments at various time points in tau polymerization. Specifically, Tau196B (8 μM) was added to an hTau40 polymerization reaction just prior to the induction of polymerization, or five minutes, 15 minutes, or 24 hours after induction. Tau196B was equally effective when added prior to polymerization induction or five minutes after induction (Fig. 4A); however, when the fragment was added 15 minutes after induction, it was 44% less effective at inhibiting

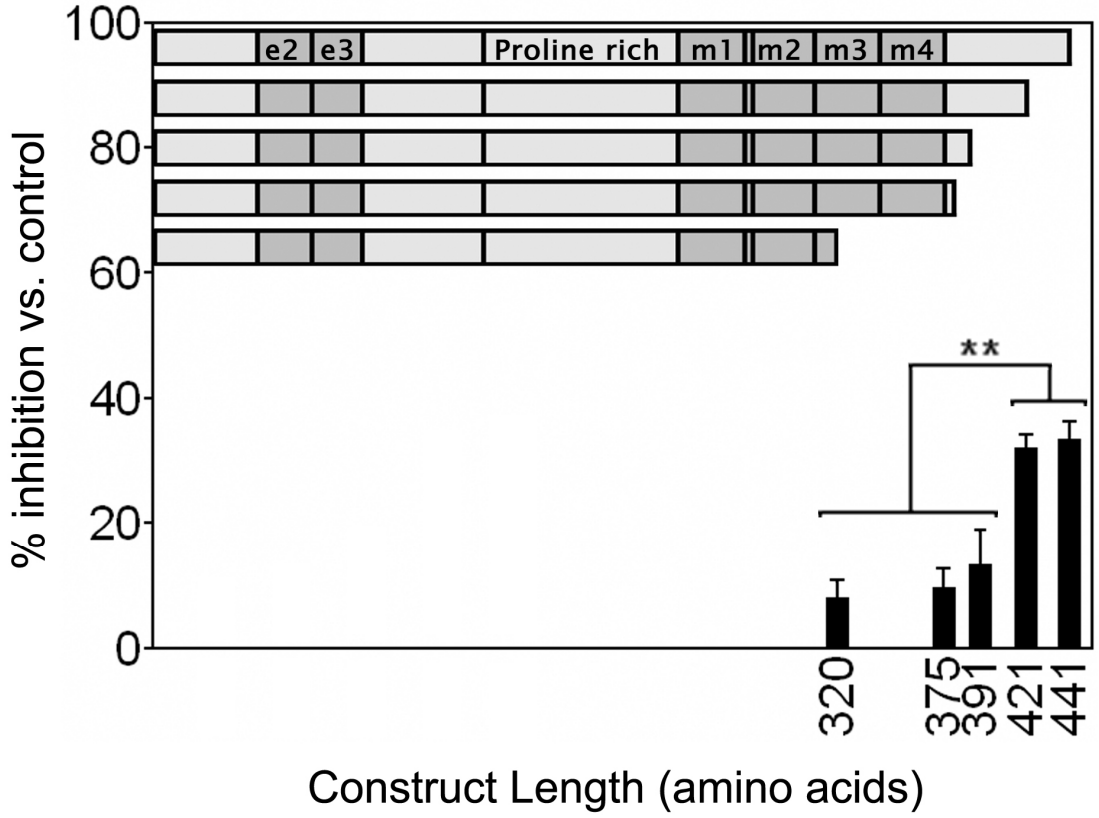


**Figure 3. Inhibition requires the C-terminal 392-421 region of hTau40.** A schematic of full-length tau and the C-terminal deletion constructs used is shown above. Tau196B inhibits full-length hTau40 and Δ422-441 tau polymerization ($p < 0.01$) but not the polymerization of Δ321-441, Δ376-441, or Δ392-441 tau ($p < 0.01$ vs. hTau40 and Δ422-441; not significant vs. control).

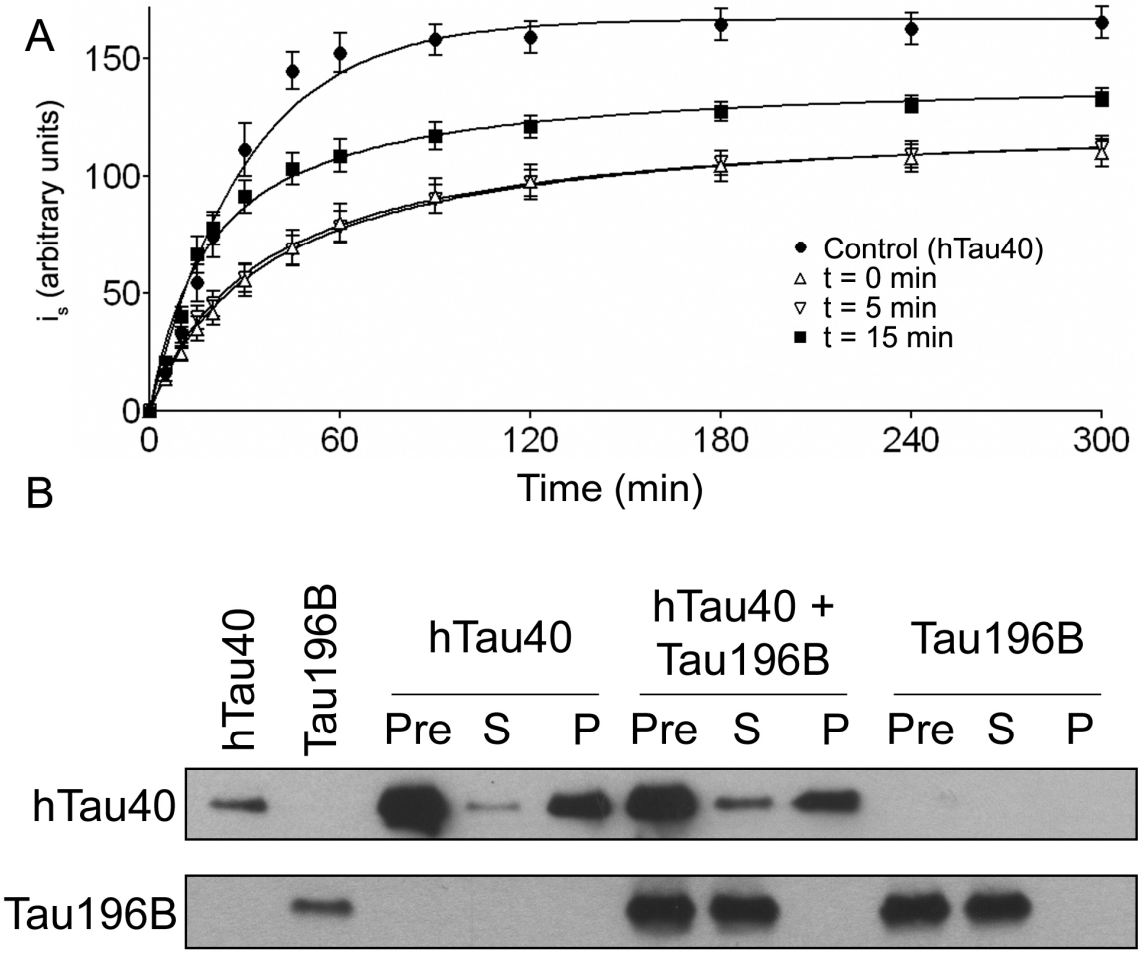


**Figure 4. N-terminal fragments act at an early step in polymerization and remain in the soluble fraction.** (A) Tau196B was added just prior to (t=0 min), or after induction of polymerization (t=5 or 15 min). Delaying addition of the fragment by 5 minutes did not reduce its efficacy; however, 15 minutes after induction the fragment was significantly less effective ($p < 0.05$). (B) Polymerized samples were subjected to ultracentrifugation over a 40% glycerol cushion and separated by gel electrophoresis. From left to right: hTau40 and Tau196B standards; hTau40 polymerization; hTau40 polymerization with twice molar Tau196B; Tau196B alone. Pre: pre-spin polymerization reaction; S: supernatant; P: pellet. N-terminal fragments (Tau196B) were probed with the amino terminal antibody Tau-12, while full-length tau was probed with the carboxy terminal antibody Tau-7. Tau196B does not pellet with the mass of polymerized hTau40, but instead remains in the supernatant.

polymerization ($p < 0.05$). Addition of Tau196B to fully polymerized hTau40 (24 hours after induction) did not result in depolymerization of hTau40 filaments six hours later, as measured by laser light scattering and quantitative electron microscopy (data not shown). Overall, the results of this experiment indicate that the N-terminal tau fragments are most effective at an early step in polymerization, suggesting that they hinder the generation or elongation of nascent polymers rather than destabilize existing filaments.

*N-terminal fragments remain in the soluble fraction* – Next, we asked whether the fragments associate with the mass of polymerized material or with a soluble component of the reaction. To address this question, hTau40 polymerization reactions were subjected to ultracentrifugation, and the pre-spin reactions and post-spin supernatants and pellets were analyzed by Western blotting (Fig. 4B). While the majority of the hTau40 in the polymerization reaction sediments under these conditions, we found no evidence of Tau196B in the pellet. As predicted, more hTau40 remains in the supernatant in the presence of the fragment, and the fragment does not sediment in the absence of hTau40. Our results strongly suggest that the fragments do not incorporate into the growing filaments, but rather exert their effects on a soluble component of the polymerization reaction.

*The 18-42 region does not affect arachidonic acid critical micelle concentration (CMC)* –Since the fragments remain in the soluble fraction and act at an early step in polymerization, we suspected they may interact with the polymerization inducer, arachidonic acid (AA). AA forms micelles under physiological buffer conditions, and tau filaments are thought to nucleate at the micelle surface (C. Chirita, Necula, & Kuret, 2004; C. N. Chirita et al., 2005; C. N. Chirita &

Kuret, 2004; C. N. Chirita et al., 2003). Tau lowers the CMC of AA and other anionic detergents, and this effect correlates with the ability of these detergents to induce tau polymerization (C. N. Chirita et al., 2003); however, the regions of tau that mediate the effect on AA CMC remain unidentified. If the N-terminal fragments also lower the AA CMC, they could coat the AA micelles or sequester AA and thereby have a substantial effect on filament nucleation.

To determine whether the inhibitory effect of the fragment involves such an interaction with arachidonic acid, we measured the AA CMC in the absence of protein, in the presence of an inhibitory fragment (Tau196), and in the presence of a fragment that failed to inhibit polymerization (Tau196 Δ18-42). Although both fragments lowered the AA CMC, the effects of Tau196 and Tau196 Δ18-42 did not differ significantly (Table 1). These results suggest that the observed inhibition of polymerization cannot be explained simply by an effect on arachidonic acid.

| Condition | AA CMC (μM) |
|---|---|
| No protein | 80.03 ± 5.79 |
| Tau196 | 55.54 ± 8.80 * |
| Tau196 Δ18-42 | 38.88 ± 12.50 * |

**Table 1.** The critical micelle concentration of arachidonic acid is depressed in the presence of either Tau196 or Tau196 Δ18-42 ($p < 0.05$ vs. no protein).

*Tau196B decreases the number and average length of filaments* – Electron microscopy is a useful tool for verifying results obtained by laser light scattering and further examining the effects of molecules that regulate polymerization (T.C. Gamblin et al., 2003). Filaments formed in the absence or presence of 8 μM Tau196B were visualized by electron microscopy. The filaments formed under these two conditions appeared morphologically similar (Fig. 5A). However, quantitative analysis (Fig. 5B) revealed several differences: the addition of the N-terminal tau fragment greatly reduced the number of filaments per field (to 51.0 ± 5.6 % of control; $p < 0.01$) and had a small but significant effect on average filament length (to 81.8 ± 1.9 % of control; $p < 0.05$). Under both conditions, exponential length distributions were observed (data not shown). Combined, the effects on filament number and length resulted in a substantial decrease in the mass of polymerized material (to 41.8 ± 5.2 % of control; $p < 0.01$), consistent with the light-scattering data (Fig. 2C-D). The electron microscopy data suggest that the N-terminal fragments primarily act by reducing the number of filaments formed, but also slightly decrease the average length of filaments.

*N-terminal fragments raise tau critical concentration* – Since Tau196B increased the amount of hTau40 in the supernatant of the polymerization reaction (Fig. 4B), we sought to quantify this result to determine the effect of N-terminal tau fragments on the hTau40 critical concentration. Though critical concentration measurements are frequently used as reflections of the growth constant (Timasheff, 1981), there is debate in the literature on how to best estimate the amount of unpolymerized, soluble tau in a polymerization reaction (T. C. Gamblin, R. W. Berry et al., 2003). We chose as our measure of tau critical concentration the amount of tau remaining in the supernatant fraction following ultracentrifugation. Since the centrifugal force required to

sediment all of the polymerized material (oligomeric and filamentous) is not known, electron microscopic analysis was performed to determine the efficacy of the protocol used here at sedimenting polymerized material (Fig. 5A). The micrographs demonstrate that the vast majority of polymerized protein is removed from the supernatant under the conditions employed (see Experimental Procedures). Furthermore, this protocol is externally validated by noting that the critical concentration of hTau40 measured by this method (0.45 ± .03 μM; Fig. 5C) is comparable to several previously published values for hTau40 critical concentration (0.50 ± 0.09 μM and 0.47 ± 0.14 μM) as estimated by laser light scattering (King et al., 1999; Reynolds et al., 2005b).

To determine the effect of Tau196B on hTau40 critical concentration, the amount of full-length tau in the supernatants was quantified with the monoclonal antibody Tau-7 (Fig. 5C), which recognizes only the C-terminus of hTau40 (and therefore not the N-terminal fragment). The presence of twice molar Tau196B significantly increased the hTau40 critical concentration to 0.56 ± 0.05 μM ($p < 0.01$). Since the tau critical concentration is inversely proportional to the growth constant (Timasheff, 1981), this signifies a 19.6 % decrease in the growth constant for hTau40 filament elongation. This data supports the quantitative electron microscopy findings that the fragments exert a small but significant effect on filament length, in addition to a primary effect on the number of filaments.

**Figure 5. N-terminal tau fragments decrease mass of polymerized material and increase the hTau40 critical concentration.** (A) Left: Representative electron microscopy fields from polymerization reactions of hTau40 in the absence and presence of Tau196B. Right: Electron microscopy confirms that ultracentrifugation removes the vast majority of polymerized material from the supernatant fraction. Scale bars represent 200 nm. (B) Quantitation of 5-hour polymerization reactions reveals that Tau196B caused a significant reduction in the number of filaments per field (to 51.0 ± 5.6 % of control, $p < 0.01$) as well as a smaller decrease in average length per filament (to 81.8 ± 1.9 % of control; $p < 0.05$). The combined effects on filament number and length resulted in a reduced overall mass of polymerized material per field (to 41.8 ± 5.2 % of control; $p < 0.01$). Black bars: hTau40 alone; white bars: hTau40 + Tau196B. (C) The hTau40 critical concentration in the absence and presence of Tau196B was quantified by blotting the supernatant fraction with the Tau-7 C-terminal antibody. T: hTau40 alone; T+F: hTau40 plus N-terminal fragments (Tau196B). The hTau40 critical concentration (0.45 ± .03 μM) is similar to previously published results. Tau196B increased the tau critical concentration to 0.56 ± 0.05 μM ($p < 0.01$).

**Figure 5**

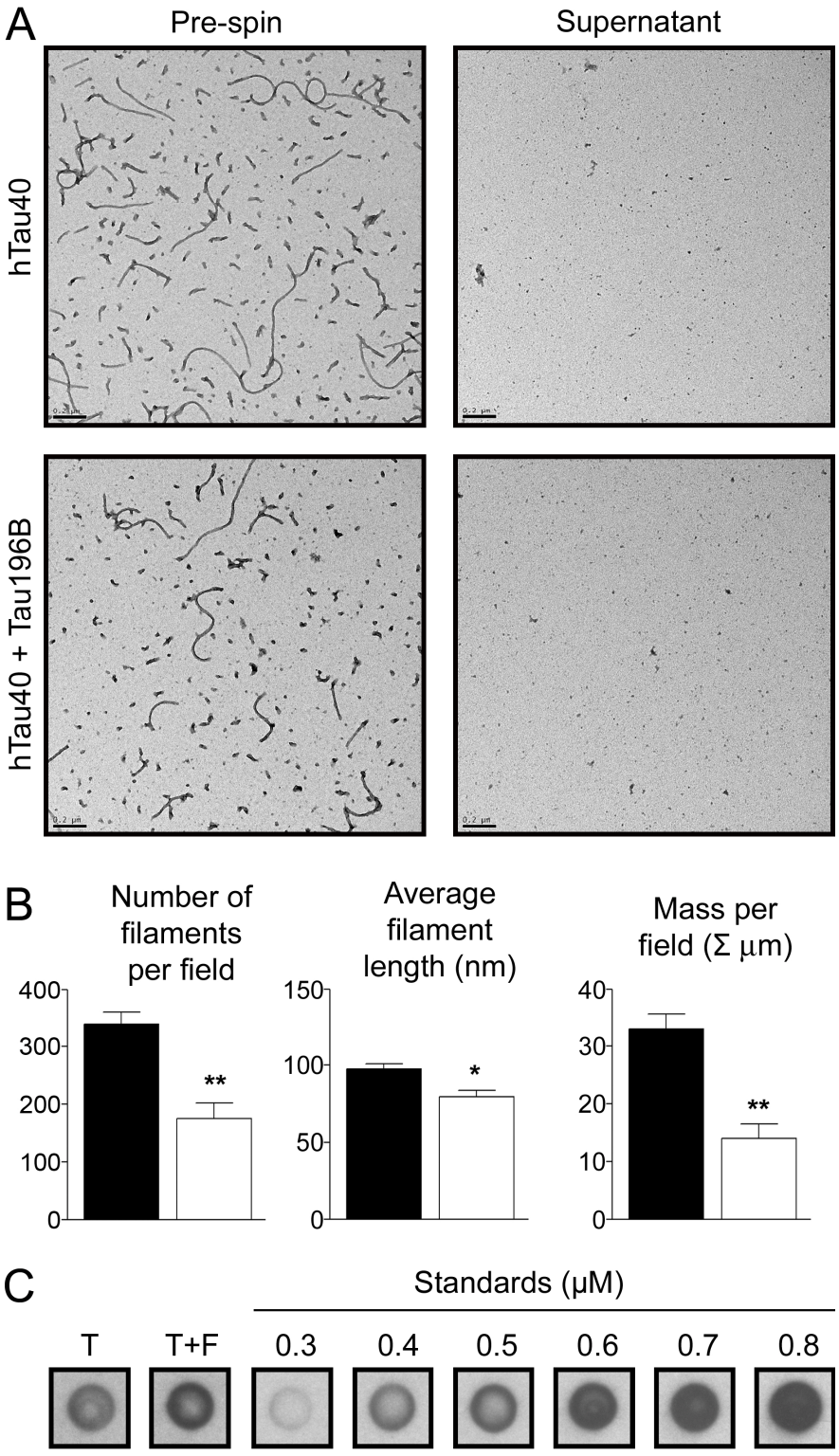
A
Pre-spin
Supernatant
hTau40
hTau40 + Tau196B
B
Number of filaments per field
Average filament length (nm)
Mass per field (Σ μm)
400
300
200
100
0
150
100
50
0
40
30
20
10
0
**
*
**
C
Standards (μM)
T
T+F
0.3
0.4
0.5
0.6
0.7
0.8

## DISCUSSION

Although the path from tau monomer to filament is incompletely understood, a picture of the regions of the tau protein governing this transition is beginning to emerge. A salient feature of this model is competition between the extreme termini of the protein for proximity to the MTBR region. The MTBR region of tau (specifically residues 314-320) (Abraha et al., 2000) is required for arachidonic acid induced polymerization, and folding of distal parts of tau onto the MTBRs is an important regulator of tau solubility and polymerization (R. W. Berry et al., 2003; T. C. Gamblin, R. W. Berry et al., 2003; T.C. Gamblin et al., 2003). Interaction of the extreme C-terminus with the MTBRs promotes solubility (R. W. Berry et al., 2003). Conversely, polymerization is favored when the N-terminus is in close proximity to the MTBRs, as recognized by the Alz-50 antibody (Carmel et al., 1996; King et al., 1999). The goal of the present study was to further characterize the role of the N-terminus by assessing the effects of a truncated construct representing the N-terminal half of tau (Tau196) in an *in vitro* polymerization assay. Our results demonstrate that a specific N-terminal tau region inhibits polymerization of the full-length protein, suggesting a novel regulatory role for the amino terminus of tau.

We initially hypothesized that an excess of Tau196, which contains the N-terminal portion of the Alz-50 epitope (residues 1-15) but lacks the corresponding MTBR portion, would inhibit polymerization of hTau40 by binding to nascent filaments and preventing the addition of full-length tau. However, our data show that both N- and C-terminal sequences that are required for the fragments to inhibit hTau40 polymerization (18-42 and 392-421; Figs. 2 and 3) differ considerably from the sequences required for Alz-50 binding (1-15 and 312-322) (Carmel et al., 1996). Furthermore, the filament “capping” mechanism is unlikely given that we were unable to detect any N-terminal fragments associated with tau filaments in the pellet of a polymerization

reaction following ultracentrifugation. Moreover, a "capping" mechanism would be expected to produce a pronounced effect on elongation, which seems not to be the case. Overall, these results suggest that if filament capping occurs, it is not the primary mechanism by which the N-terminal fragments inhibit polymerization.

Instead, the data presented here are consistent with a mechanism in which the N-terminal fragments act on a soluble component of the polymerization reaction. The fragments increase the amount of soluble tau in the polymerization reaction and are most effective when present at the induction of polymerization. Furthermore, the fragments are not incorporated into or associated strongly with filaments; instead, they remain in the soluble fraction. Since the inhibitory effect of the fragments cannot be explained by an effect on the arachidonic acid critical micelle concentration and instead requires specific sequences of both hTau40 and the N-terminal fragments, our results are most consistent with a mechanism in which the fragments interact with full-length soluble tau. Collectively, these results suggest that the N-terminal fragments stabilize full-length tau in a soluble conformation, removing hTau40 molecules from the pool of polymerizable protein.

One known conformation of soluble tau involves folding of the C-terminus of tau onto the MTBR region (R. W. Berry et al., 2003). Stabilizing this interaction could conceivably increase hTau40 solubility in the face of polymerization inducers. Recently, fluorescence resonance energy transfer (FRET) analysis of tau in solution has shown that residue 432 of the C-terminus and residue 310 of the third MTBR are in close proximity, confirming that the C-terminus of tau folds over the MTBRs in the absence of polymerization inducers (Jeganathan et al., 2006). However, the N-terminus has also been implicated in this C-terminal / MTBR folding: while the N-terminus and MTBRs have low FRET efficiency, residues 17-18 of the N-

terminus are in close proximity to residue 432 of the C-terminus (Jeganathan et al., 2006). Thus, in this "paperclip folded" conformation of soluble tau, the N-terminus is near the C-terminus as the C-terminus associates with the MTBRs.

The N-terminal fragment data presented here are consistent with the N-terminal involvement in the folding of the C-terminus over the MTBR region (Jeganathan et al., 2006). The association of residues 17-18 and 432 of the N- and C-termini in the paperclip folding of soluble tau (Jeganathan et al., 2006) suggests that residues 18-42 and 392-421, which have yet to be investigated by FRET, may also be in close proximity in this conformation. We therefore propose a scenario in which the N-terminal fragments bind to the C-terminus of hairpin-folded soluble tau and stabilize the C-terminal / MTBR interaction (Fig. 6). This explanation is consistent with our observations that the fragments increase the amount of soluble tau while the fragments themselves remain in the soluble fraction (Figs. 4 and 5). Furthermore, this interpretation, along with evidence from other structural studies (Jeganathan et al., 2006), places the extreme N-terminus of soluble tau in a precarious location, near the MTBR "core" of polymerization. It is easy to imagine how the N-terminus of tau could be induced to replace the carboxy terminus as the binding partner of the MTBR "core" to form the Alz-50 conformation (Carmel et al., 1996). However, the influence of the N-terminus on the polymerization of tau is complex, and further experimentation is needed to fully understand its involvement in the conformational shifts that take place during tau polymerization.

Although we have shown that residues 18-42 are necessary for polymerization inhibition, a peptide corresponding to this sequence alone was not sufficient to recapitulate the inhibitory effect of the N-terminal fragments. This contrasts with a C-terminal tau peptide (residues 422-441) which we have shown inhibits polymerization of the full-length protein (R. W. Berry et al.,

2003). In the latter case, the C-terminal 'tail' peptide is thought to inhibit polymerization by forming an amphipathic alpha helix (Esposito et al., 2000). Unlike the tail peptide, the N-terminus has little predicted secondary structure, and the N-terminal peptide may be unable to adopt a stable conformation outside the context of the larger N-terminal fragment. Alternatively, a longer sequence of the N-terminal fragment may be required to promote a stable interaction with the full-length molecule and thereby inhibit polymerization.

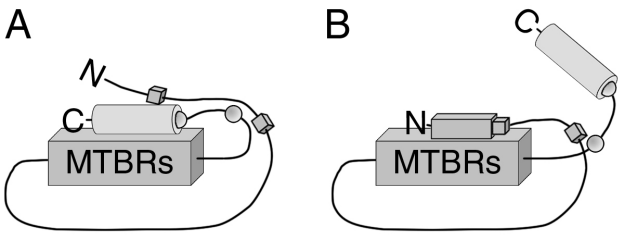


**Figure 6. Diagrammatic representations of the proposed conformations of tau in soluble and polymerized states.** (A) Association of the MTBR region with the extreme C-terminus (cylinder) promotes solubility (R. W. Berry et al., 2003), while the N-terminal region between residues 18 and 42 (both cubes) may stabilize this conformation by associating with the C-terminal region between residues 392 and 421 (both spheres). This arrangement of the MTBRs and both termini of tau has also been demonstrated independently by structural analyses of soluble tau (Jeganathan et al., 2006). (B) When the C-terminus vacates its position along the MTBRs, the extreme N-terminus may be allowed access to the MTBR "core" of polymerization. This conformation, recognized by the Alz-50 antibody (Carmel et al., 1996), is associated with early tau polymerization both *in vitro* (King et al., 1999) and *in vivo* (Garcia-Sierra et al., 2003; Hyman et al., 1988).

Our results suggest a novel role for the N-terminus in the regulation of tau solubility. These findings are particularly interesting in light of the numerous disease-related modifications of tau that affect the regions at either end of the molecule *in vivo*. The 18-42 and 392-421

sequences include residues which may be regulated by phosphorylation (G. Lee et al., 2004; Otvos et al., 1994) or nitration (Reynolds et al., 2005a). Our previous work has also shown that the N-terminus of tau in neurofibrillary tangles may be subject to regulation by enzymatic cleavage in early AD (Horowitz et al., 2004), and proteolysis after glutamic acid 391 (Novak, Jakes, Edwards, Milstein, & Wischik, 1991; Wischik, Novak, Edwards et al., 1988; Wischik, Novak, Thogersen et al., 1988) is known to occur at an advanced stage in AD tangle evolution (Garcia-Sierra et al., 2003; Ghoshal et al., 2002). It will be interesting to determine how these modifications influence the ability of the fragments to inhibit tau polymerization.

The inhibitory N-terminal constructs described here also bear an intriguing resemblance to a recently discovered group of alternatively spliced tau isoforms which lack the sequences encoding the MTBR region and C-terminal portion of the protein (Wei & Andreadis, 1998; Wei, Memmott, Screaton, & Andreadis, 2000). At least one of these alternatively spliced constructs (the 6d tau isoform, which contains residues 1-143 of canonical tau followed by 11 additional unique amino acids) is expressed in human brain tissue, and expression is particularly high in areas that are not affected by tau lesions in AD (cerebellum, spinal cord) and lowest in tangle-prone areas (hippocampus, cerebral cortex) (Luo et al., 2004). Even within affected areas, the 6d isoform does not colocalize with cells bearing tangles (Luo et al., 2004). In light of our results, it is tempting to speculate that expression of this alternatively spliced N-terminal fragment of tau could be responsible for preventing tau polymerization in these unaffected cells and brain regions *in vivo*.

## ACKNOWLEDGEMENT

Peleg Horowitz, Angela Guillozet-Bongaarts, Robert W. Berry, and Lester I. Binder co-authored this work. The authors would like to acknowledge Drs. Yifan Fu and Nupur Ghoshal for their work in generation and preliminary characterization of the Tau-7 antibody. We would also like to thank Dr. Matthew Reynolds for his technical assistance. This work was supported by NIH Awards NS49760 (P.M.H.), NS049834 (N.L.), AG14453 and AG09466 (L.I.B)

# CHAPTER THREE

## TAU 6D AND 6P ISOFORMS INHIBIT POLYMERIZATION OF FULL-LENGTH TAU *IN VITRO*

**In Preparation**

## ABSTRACT

Alzheimer's disease and a variety of frontotemporal dementias are characterized by the intraneuronal and/or intraglial accumulation of insoluble filaments of the microtubule-associated protein tau. We have previously shown that N-terminal fragments of tau inhibit polymerization of the full-length protein, potentially by stabilizing the C-terminus/MTBR interaction. Here we report that two short, naturally occurring tau isoforms, termed 6D and 6P, inhibit the polymerization of full-length tau (hTau40) in a similar manner. These isoforms are produced via alternative splice sites in exon 6 that cause a frame shift and introduce a stop codon prior to the start of the proline-rich region of the protein. Like the N-terminal fragments previously tested, these isoforms reduce the number and length of hTau40 filaments, and remain in the soluble fraction of the polymerization mixture. The efficacy of inhibition depends on whether the isoform is of the 6D or 6P variant, and on the presence of N-terminal exons 2 and 3. Because the amino terminus of the 6D/6P isoforms is identical to canonical tau, these isoforms contain the region previously identified as crucial to the inhibitory effect (residues 18-42). We demonstrate that changes in this region that mimic posttranslational modifications impair the ability of these isoforms to inhibit polymerization. Furthermore, similar changes in a specific C-terminal region of hTau40 (residues 392-421), thought to be the site of N-term/C-term interaction, also modulate the effectiveness of the 6D/6P isoforms. Taken together, these results suggest that the 6D/6P isoforms have the potential to act as endogenous inhibitors of tau filament formation, and suggest a mechanism by which this ability may be disrupted in disease.

## INTRODUCTION

Alzheimer's disease (AD) and other tauopathies are marked by the appearance of intracellular, filamentous aggregates of the microtubule-associated protein tau. The formation of tau pathology is thought to be intimately linked to neurodegeneration, in part because the appearance of tau pathology follows a spatial and temporal progression through the anatomical regions that underlie the clinical symptoms, beginning in areas associated with learning and memory, and spreading through much of the cerebral cortex (reviewed in (Binder et al., 2005)). Yet even in severe AD there are areas of the brain that remain unaffected, including the cerebellum and primary motor cortex (reviewed in (Mesulam, 1999)). One of the great unanswered questions is why some neurons develop tau pathology, while others are spared. Identifying the differences between susceptible and protected neuronal populations may be crucial to understanding this disease.

To identify factors that influence tau polymerization, it is important to understand the conformational changes in tau that take place during filament formation. Monomeric tau exhibits little detectable secondary structure (Schweers et al., 1994), and was once thought to exist in a largely extended state (Syme et al., 2002). However, recent evidence indicates that tau in solution exhibits a globally folded structure (Horowitz, LaPointe, Guillozet-Bongaarts, Berry, & Binder, 2006; Jeganathan et al., 2006). According to this model, the carboxy terminus discourages filament formation by folding over and protecting the microtubule-binding repeat (MTBR) region, which comprises the filament core. Evidence that the carboxy terminus promotes solubility in this manner comes from *in vitro* studies of filament assembly (Abraha et al., 2000; R. W. Berry et al., 2003). Additionally, cell culture work indicates that removal of the

C-terminus by caspase-3 stimulates filament assembly, and can occur as a result of exposure to ß-amyloid (T. C. Gamblin, F. Chen et al., 2003).

A second feature of this model of soluble tau conformation is the association of the N-terminus with the C-terminus. This feature is supported by work from our lab, in which we demonstrated that constructs containing only the N-terminus of tau inhibit the *in vitro* polymerization of the full-length protein by promoting tau solubility (Horowitz et al., 2006). This effect requires amino acids 18-42 in the N-terminal fragments and residues 392-421 of the full-length protein (Horowitz et al., 2006), regions that FRET analysis of soluble tau indicate are in close proximity (Jeganathan et al., 2006). We therefore proposed a scenario in which the N-terminal fragments promote tau solubility by associating with the C-terminus of full-length tau, stabilizing the C-terminus/MTBR interaction (Horowitz et al., 2006).

The inhibitory N-terminal fragments described by our lab (Horowitz et al., 2006) bear an intriguing resemblance to the N-terminal tau isoforms Tau6D and Tau6P, which are generated by the alternative splicing of exon 6. In the six canonical tau isoforms in the human central nervous system, exon 6 is entirely removed from the transcript prior to translation (reviewed in (Andreadis, 2005)). However, in addition to the usual 3' splice site of exon 6, there are two alternate splice sites within the exon itself. Use of either of these splice sites introduces a frame shift mutation in the message, such that the resulting isoforms contain eleven unique amino acids not found in canonical tau, followed by a stop codon. The specific amino acids introduced depend on whether the spice site is proximal (6P) or distal (6D) to the 5' end of exon 6. Because of the introduction of the stop codon, 6P and 6D isoforms lack the sequences encoding the MTBR region and C-terminal portion of the protein (Wei & Andreadis, 1998; Wei et al., 2000).

Previous work has demonstrated that mRNA corresponding to the Tau6D and 6P splice variants is present in human brain tissue, although levels are low relative to canonical isoforms (Leroy et al., 2006; Wei & Andreadis, 1998). Additionally, a polyclonal antibody raised to the unique amino acid sequence at the C-terminus of the Tau6D isoforms has been used to detect the presence of this isoform in human brain, demonstrating that the message for at least one of these splice variants is translated. Intriguingly, Tau6D protein expression is particularly high in areas that are not affected by tau lesions in AD (cerebellum, spinal cord) and lowest in tangle-prone areas (hippocampus, cerebral cortex). Even within affected areas, the anti-6D labeling does not colocalize with an antibody that labels neurofibrillary tangles (Tau5; (Luo et al., 2004).

In light of our recent results concerning the polymerization suppressive properties of N-terminal tau fragments and the preliminary Tau6D expression studies in human brain, we asked whether these tau isoforms might be responsible for preventing tau polymerization in these unaffected cells and brain regions. As a preliminary step toward answering this question, we examined the effects of 6D and 6P isoforms on filament formation in an *in vitro* polymerization assay (Gamblin, King, Dawson et al., 2000; King et al., 1999). We report that 6D and 6P isoforms are capable of inhibiting polymerization of full-length tau, and that this effect is isoform-dependent. We also demonstrate that this ability is influenced by posttranslational modifications in full-length tau or in the 6D and 6P isoforms themselves. Collectively, our results suggest that these short isoforms may represent endogenous regulators of filaments assembly, and suggest a basis for their disruption in disease.

## EXPERIMENTAL PROCEDURES

*Materials* – Arachidonic acid (AA) was obtained from Cayman Chemical (Ann Arbor, MI) and stored at -20°C. Working solutions were prepared in 100% ethanol immediately prior to use.

*Recombinant proteins* – The six canonical CNS tau isoforms contain zero, one, or two alternatively spliced N-terminal inserts (designated 0N, 1N, and 2N, respectively), and either three or four MTBRs (3R or 4R). The full-length tau used in this study (hTau40) is the longest isoform in the human central nervous system and contains 441 amino acids, including both alternatively spliced N-terminal exons (e2 and e3) and four microtubule binding repeats (m1-m4; Fig. 1A). The various 6D and 6P isoforms were generated by restriction digestion and ligation of cDNA constructs described previously (Luo et al., 2004) and hTau40 (2N4R) (Carmel et al., 1996), hTau23 (0N3R) and hTau37 (1N3R) (King et al., 2000). $6D^{Y}18/29^{F}$ and $6D^{Y}18/29^{E}$ were created by site-directed mutagenesis (Stratagene) on the 2N6D background. Mutations were verified by sequencing prior to protein purification. Other tau constructs used in this study have been described elsewhere: hTau40 (Carmel et al., 1996); 1-196 (Horowitz et al., 2006): $^{S}422^{E}$ (Angela L. Guillozet-Bongaarts et al., 2006); $^{S}396/404^{E}$ (Abraha et al., 2000): $^{Y}394^{E}$ (Reynolds et al., 2005b); $^{R}406^{W}$ (Gamblin, King, Dawson et al., 2000). A summary of all constructs used in this study is provided in Table 1. Proteins were expressed in E. coli and purified by means of an N-terminal poly-histidine tag (Abraha et al., 2000; Carmel et al., 1996). Protein concentrations were determined by the Lowry assay (Lowry, Rosenbrough, Farr, & Randall, 1951).

*Polymerization* – Tau polymerization was induced by arachidonic acid as previously described (Gamblin, King, Dawson et al., 2000). Briefly, tau protein (4 μM) was incubated at room

temperature in reaction buffer (final buffer conditions: 10 mM HEPES, pH 7.6, 100 mM NaCl, 0.1 mM EGTA, 5mM DTT) in the presence of 75 μM arachidonic acid (AA). The final volume of ethanol in these reactions was 3.8 %, and this volume was added to control reactions in the absence of AA. Unless otherwise noted, N-terminal constructs were added at a concentration of 8 μM to the polymerization reaction mixture prior to the addition of arachidonic acid. Reaction progress was monitored by the intensity of right angle laser-light scattering ($i_s$; (Gamblin, King, Dawson et al., 2000)). End-point (t = 300 min) laser light scatter data from at least three independent experiments were analyzed. Statistical significance was determined by comparing polymerization in the presence and absence of N-terminal constructs by student's two tailed t-tests. Time course data were fit with curves using GraphPad Prism 3.0 software. Error bars in all figures represent plus or minus one standard error of the mean.

*Electron Microscopy* – Polymerization reactions were allowed to proceed at least five hours, fixed with 2% glutaraldehyde (Electron Microscopy Sciences, EMS, Hatfield, PA), spotted onto 300 mesh formvar/carbon coated copper grids (EMS), and negatively stained with 2% uranyl acetate (EMS) as previously described (King et al., 1999). Grids were examined using a JEOL JEM-1220 electron microscope at 60kV and 12,000x magnification, and photographed using a MegaScan 794/20 digital camera and DigitalMicrograph software version 3.9.3 (Gatan). Optimas 6.0 imaging software (Media Cybernetics) was used to automatically identify and measure filaments (defined as objects > 20 nm in length). At least five separate fields from each grid were randomly chosen for quantitation under low illumination to prevent bias. In experiments where different constructs were analyzed for effects on hTau40, data from each experiment were normalized to control reactions containing hTau40 alone, and expressed the data as "percent of

the hTau40 value". Results from at least three independent experiments were analyzed by student's two-tailed t tests to determine if polymerization was significantly different from controls (GraphPad Prism 3.0 software).

*Filament Sedimentation* – Reaction mixtures were incubated for 5 h in the presence of arachidonic acid. Following assembly, a pretreatment sample was removed and the remainder of the reaction mixture was centrifuged at 100,000 x g for 20 minutes at 25° C over a 40% glycerol cushion. Samples of the starting material and supernatants were diluted in 2X Laemmli buffer and boiled. Pellets were resuspended in an amount of polymerization buffer equal to the starting volume prior to addition of Laemmli buffer. Proteins were separated by SDS-PAGE and transferred to nitrocellulose membranes where Tau6D and Tau6P were probed with the amino-terminal antibody Tau-12 (4 ng/mL) (Ghoshal et al., 2002), and full-length hTau40 was probed with the carboxy-terminal antibody Tau-7 (40 ng/mL) (Horowitz et al., 2006). HRP-conjugated goat anti-mouse secondary antibody (Vector Laboratories, Burlingame, CA) and ECL (GE Healthcare, Amersham, UK) was used to detect proteins.

## RESULTS

*6D and 6P isoforms share common features with N-terminal fragments that inhibit the polymerization of hTau40* – To examine the effects of the 6D and 6P isoforms on the polymerization of full-length tau (hTau40), several protein constructs were created and purified (Fig. 7A-B). These proteins contain the specific amino acid region (18-42) that we have identified as crucial for the inhibition of hTau40 polymerization (Horowitz et al., 2006). Like N-terminal protein constructs previously examined, the 6D and 6P constructs lack the region of tau necessary for filament formation (Abraha et al., 2000; von Bergen et al., 2000). Alternative splicing of exons 2 and 3 produces tau isoforms containing zero, one, or both of these N-terminal inserts (designated 0N, 1N, and 2N, respectively). To examine the effects of N-terminal processing, constructs containing 0, 1 or 2 alternately spliced N-terminal exons were created on the background of the 6P and 6D isoforms. An additional tau protein construct, 1-196, that has previously been shown to inhibit hTau40 polymerization (Horowitz et al., 2006) was included as a positive control.

*2N6D and 2N6P inhibit the polymerization of full-length hTau40* – To determine whether 6P and 6D influence tau polymerization, hTau40 (4 μM) was incubated in the presence or absence of a twice-molar excess of 2N6D, 2N6P, or 1-196. Polymerization was induced by the addition of arachidonic acid, and right angle laser-light scattering (LLS) was used to monitor filament formation (Fig. 8A). After five hours of polymerization, a similar degree of inhibition was apparent in the presence of 2N6P (71.37 ± 6.27% of control, $p < 0.05$) and 1-196 (66.60 ± 6.59% of control, $p < 0.05$). 2N6D also significantly inhibited hTau40 polymerization, albeit to a lesser extent (79.80 ± 2.85% of control, $p < 0.05$).

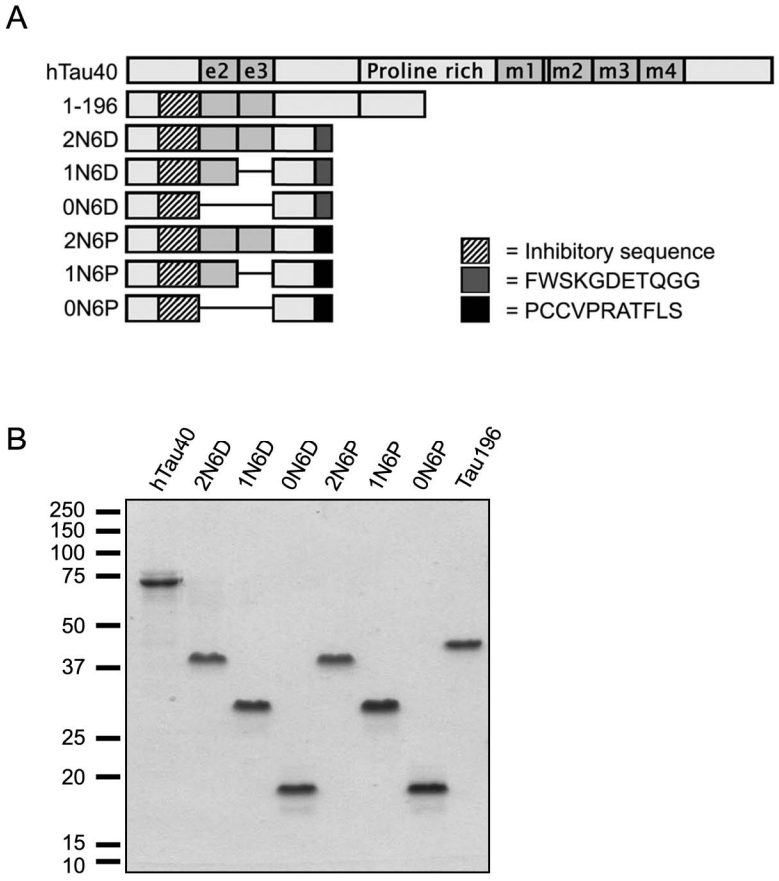


**Figure 7. Schematic of the tau constructs used in this study.** (A). A tau construct containing a stop codon at Y197 (1-196) has been described elsewhere (Horowitz et al., 2006). Constructs containing 0, 1 or 2 alternately spliced N-terminal exons (e2 and e3) we created on the background of the 6P and 6D isoforms. The key indicates the specific N-terminal sequence required to inhibit polymerization of full-length tau (residues 18-42), as well as sequences unique to 6P and 6D isoforms. (B) All purified proteins used in this study are shown separated by SDS-PAGE electrophoresis and stained with Coomassie dye.

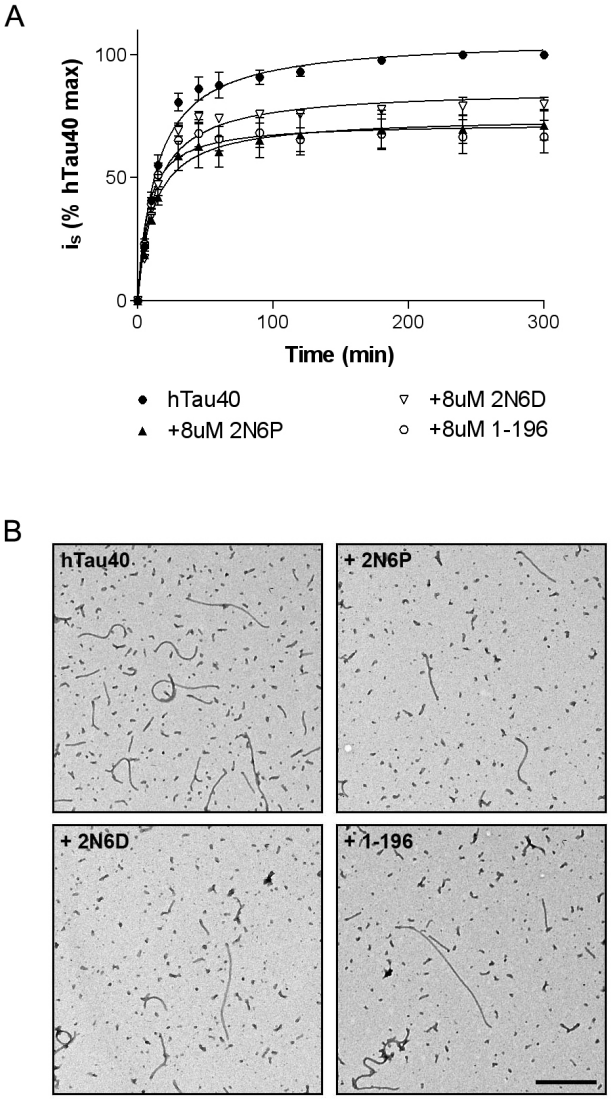


**Figure 8. 6D and 6P isoforms inhibit the polymerization of hTau40, as measured by laser-light scattering (LLS).** (A) LLS was used to monitor the polymerization of hTau40 in the absence (●) or presence of a twice-molar excess of 2N6P (▲), 2N6D (□). An N-terminal construct know to inhibit hTau40 polymerization, Tau1-196 (○), was included as an experimental control. (B) Representative electron micrographs of hTau40 filaments formed alone or in the presence of 8 μM 2N6P, 2N6D, or 1-196. Scale bar represents 500 nm.

To verify the results of the LLS experiments and to further characterize the effects of 2N6P and 2N6D on hTau40 polymerization, we performed electron microscopy (EM) on filaments formed under each experimental condition (Fig. 8B). Previous work from our lab demonstrated that incubation with N-terminal tau fragments reduced the overall mass of hTau40 filaments formed, with the primary effect being a reduction in the number of filaments per field (Horowitz et al., 2006). Quantitative analysis revealed similar effects in the present study (Fig. 9). Polymerization of hTau40 (4 μM) in the presence of 2N6P (8 μM) caused a significant reduction in the number of filaments per field (63.74 ± 2.36% of control; $p < 0.001$), which resulted in a reduced overall mass of polymerized material per field (57.20 ± 4.64% of control; $p < 0.001$). Filament number was also decreased by incubation with 2N6D (74.80 ± 4.62% of control; $p < 0.001$), as was polymer mass (69.88 ± 3.23% of control; $p < 0.001$). In agreement with our previous report (Horowitz et al., 2006), incubation with 1-196 reduced both the number and overall mass of filaments (54.93 ± 3.86% and 48.37 ± 3.27% of control, respectively; $p < 0.0001$). These results are consistent with the reduction in polymer mass observed by LLS. Taken together, the results of the LLS and EM experiments indicate that, like the N-terminal constructs previously examined, 2N6P and 2N6D are capable of inhibiting polymerization of full-length tau.

*The presence of alternatively-spliced N-terminal exons differentially impacts the effects of 6D and 6P constructs on hTau40 polymerization* – As stated previously, alternative splicing of exons 2 and 3 in the 6D/6P message may produce three isoforms (see Fig. 7A). Western blot analysis of human brain with the 6D antibody revealed several bands containing the 6D sequence, suggesting that multiple 6D isoforms may be expressed (Luo et al., 2004). To determine whether

alternative splicing of exons 2 and 3 affects the ability of these isoforms to inhibit hTau40 polymerization, we used quantitative EM to assess the effects off each splice variant on hTau40 polymerization (Fig. 9). Filament number was significantly reduced by 0N6P and 1N6P in a manner similar to 2N6P (57.28 ± 2.94% and 63.92 ± 2.45% of control, respectively; $p < 0.01$), as was filament mass (56.05 ± 3.22% and 59.62 ± 4.30% of control, respectively; $p < 0.01$, $p < 0.05$). In contrast, while 2N6D significantly reduced filament number and mass, 6D constructs containing zero or one N-terminal exons (0N6D and 1N6D) failed to significantly inhibit hTau40 polymerization. These experiments indicate that although alternative splicing has no effect on the ability of 6P isoforms to inhibit hTau40 polymerization, the absence of exons 2 and/or 3 reduces the effectiveness of 6D isoforms.

*6D and 6P isoforms remain in the soluble fraction* – In a previous study, we demonstrated that N-terminal tau fragments do not associate with hTau40 filaments in a co-sedimentation assay (Horowitz et al., 2006). This result was interpreted as evidence that the fragments act in the soluble fraction of the polymerization mixture to produce their effects. To determine whether 6D and 6P isoforms inhibit polymerization through a similar mechanism, we assembled hTau40 (4 μM) in the presence or absence of 2N6P, 2N6D, or 1-196 (8 μM), and then separated the mixtures into soluble and filamentous fractions through ultracentrifugation. The resulting supernatants and pellets were processed by gel electrophoresis, transferred to nitrocellulose membranes, and probed with antibodies against tau (Fig. 10). All three constructs, 2N6P, 2N6D and Tau196, remained in the supernatant fraction and were absent from the filamentous pellet, even at longer exposures (data not shown). These results suggest that 2N6P and 2N6D act in the

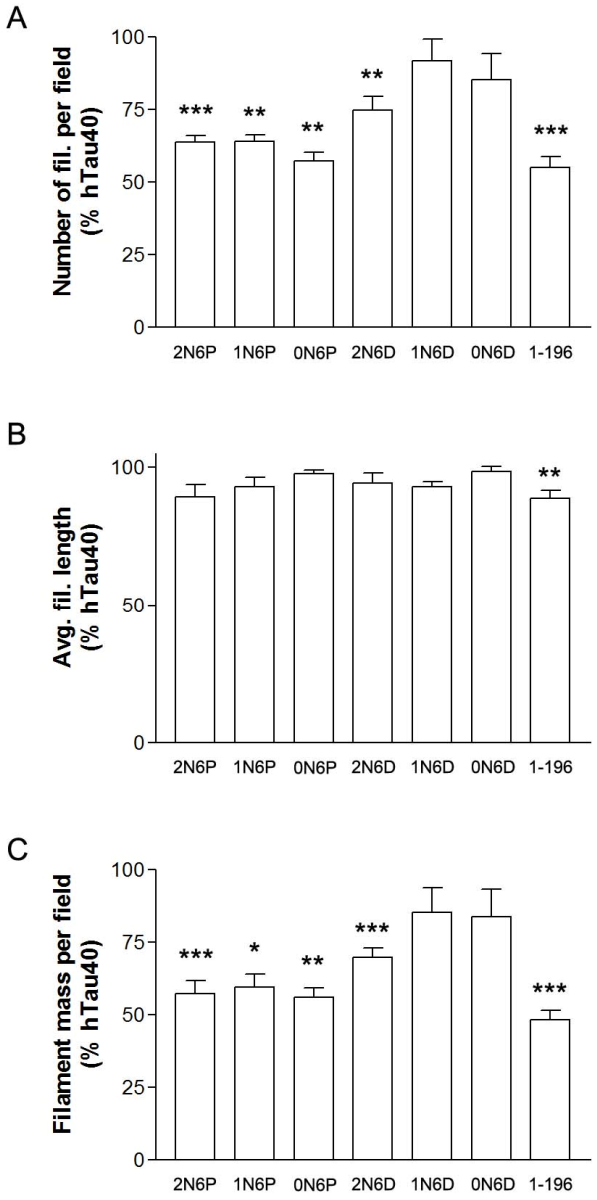


**Figure 9. The presence of alternatively-spliced N-terminal exons differentially impacts the effects of 6D and 6P constructs on hTau40 polymerization.** Incubation with 2N6P reduced the number (to 63.74 ± 2.36 % of control, $p < 0.0001$) and mass (to 57.20 ± 4.64 % of control, $p < 0.0001$) of hTau40 filaments per field. Filament number and mass were also reduced with 0N6P and 1N6P (see Results section). Although 2N6D significantly reduced filament number (to 74.80 ± 4.62 % of control, $p < 0.001$) and mass (to 69.88 ± 3.23 % of control, $p < 0.0001$), 6D constructs containing zero or one N-terminal exon (0N6D and 1N6D) failed to inhibit hTau40 polymerization. In agreement with our previous report (Horowitz et al., 2006), incubation with 1-196 reduced both the number and overall mass of filaments.

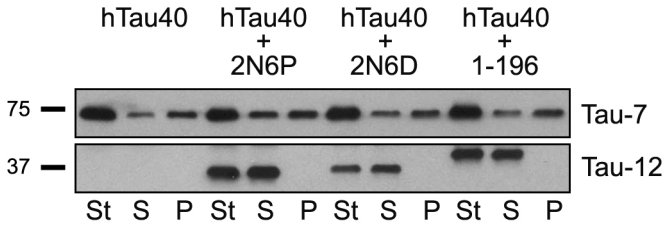


**Figure 10. Tau6D and 6P isoforms remain in the soluble fraction of the polymerization reaction.** Polymerized samples were subjected to ultracentrifugation over a 40% glycerol cushion and separated by gel electrophoresis. From left to right: hTau40 polymerization; hTau40 polymerization with twice molar 2N6P, 2N6D, or 1-196. St: pre-spin starting material; S: supernatant; P: pellet. Short N-terminal constructs were probed with the amino terminal antibody Tau-12, while full-length tau was probed with the carboxy terminal antibody Tau-7. Like 1-196, 2N6P and 2N6P do not pellet with the mass of polymerized hTau40, but instead remain in the supernatant.

soluble fraction to inhibit hTau40 polymerization, as did the N-terminal tau fragments previously studied.

*Modification of a crucial N-terminal motif modulates the effects of the short isoforms* – We have previously demonstrated that amino acids 18-42 are required for N-terminal tau fragments to inhibit hTau40 polymerization. Since 6D and 6P isoforms appear to inhibit full-length tau polymerization through the same mechanism, it is likely that amino acids 18-42 are crucial for their effect as well. Because of the importance of these residues, we examined whether posttranslational modifications here would affect the ability of these isoforms to inhibit polymerization.

The inhibitory 18-42 sequence contains tyrosine residues at positions 18 and 29, which are potential targets of protein tyrosine kinases. Tau is phosphorylated at Tyr18 by the src family

member fyn (G. Lee et al., 1998), and tau phosphorylated at Tyr18 tau has been detected in the neurofibrillary lesions of AD brain (G. Lee et al., 2004). Phosphorylation at Tyr29 has been detected in PHF tau isolated from AD brain as well (Williamson et al., 2002). To determine whether tyrosine phosphorylation influences the inhibitory ability of N-terminal isoforms, we generated a construct based on 2N6D in which both tyrosine residues were mutated to glutamic acid to mimic phosphorylation. As a control, we also generated a construct in which both residues were mutated in a manner that did not mimic phosphorylation ($^{Y}18/29^{F}$) (Table 2).

**Table 2.** Constructs containing modifications in the N- or C-terminus.

| **Name(s)** | **Description** | **Purpose** |
|---|---|---|
| $6D^{Y}18/29^{E}$ | 2N6D containing two Tyr→Glu mutations | Phosphorylation mimetic; used to test the effect of tyrosine phosphorylation |
| $6D^{Y}18/29^{F}$ | 2N6D containing two Tyr→Phe mutations | Used to make verify that effects of pseudophosphorylation were specific |
| $^{Y}394^{E}$ | hTau40 construct containing Tyr→Glu | Simulates phosphorylation at a.a. 394 |
| $^{394}$nY | hTau40 construct with Tyr→Phe at a.a. 18, 29, 197, and 310 | Assays effects of a single nitration event at 394 |
| $^{S}396/404^{E}$ | hTau40 construct containing Tyr→Glu at 396, 404 | Simulates phosphorylation at a.a. 396, 404 |
| $^{R}406^{W}$ | hTau40 construct containing Arg→Trp at 406 | FTDP-17 mutation |
| $^{S}422^{E}$ | hTau40 containing Ser→Glu | Simulates phosphorylation at a.a. 422 |

We polymerized hTau40 (4 μM) in the presence or absence of these constructs (8 μM), and measured the effects on filament number, average length, and mass by quantitative EM. Pseudophosphorylation at both tyrosine residues ($^{Y}18/29^{E}$) blocked the ability of 2N6D to inhibit hTau40 (Figure 11). However, the $^{Y}18/29^{F}$ control construct reduced hTau40 filament mass (64.72 ± 7.3% control; $P<0.05$) to a level not significantly different from wild-type 2N6D. These results suggest that tyrosine phosphorylation abolishes the inhibitory effects of the N-terminal isoforms. They also indicate that the same N-terminal region (18-42) identified in our earlier work (Horowitz et al., 2006) is important for the inhibitory effects of the 6D and 6P isoforms.

*Changes in the C-terminus of hTau40 modulate the effect of the short isoforms* – We have previously shown that the inhibitory effect of N-terminal fragments requires a sequence in the C-terminus of full-length tau (a.a. 391-421); if tau is truncated prior to this sequence, the fragments no longer inhibit (Horowitz et al., 2006). Because of the importance of this sequence, changes in this region may impact the inhibitory effect of the N-terminal isoforms. To address this question, we used recombinant tau constructs containing several disease-relevant modifications in or near this sequence (see Table 1). With the exception of pseudophosphorylation at position 394 ($^{Y}394^{E}$; (Reynolds et al., 2005b)), all of these C-terminal modifications alter the polymerization profile of hTau40 ($^{S}422^{E}$ (Angela L. Guillozet-Bongaarts et al., 2006); $^{S}396/404^{E}$ (Abraha et al., 2000): $^{394}$nY (Reynolds et al., 2005b); $^{R}406^{W}$ (Gamblin, King, Dawson et al., 2000)).

Full-length constructs containing C-terminal changes (4 μM) were incubated in the absence or presence 2N6P (8 μM). We used 2N6P rather than 2N6D for these experiments because of its

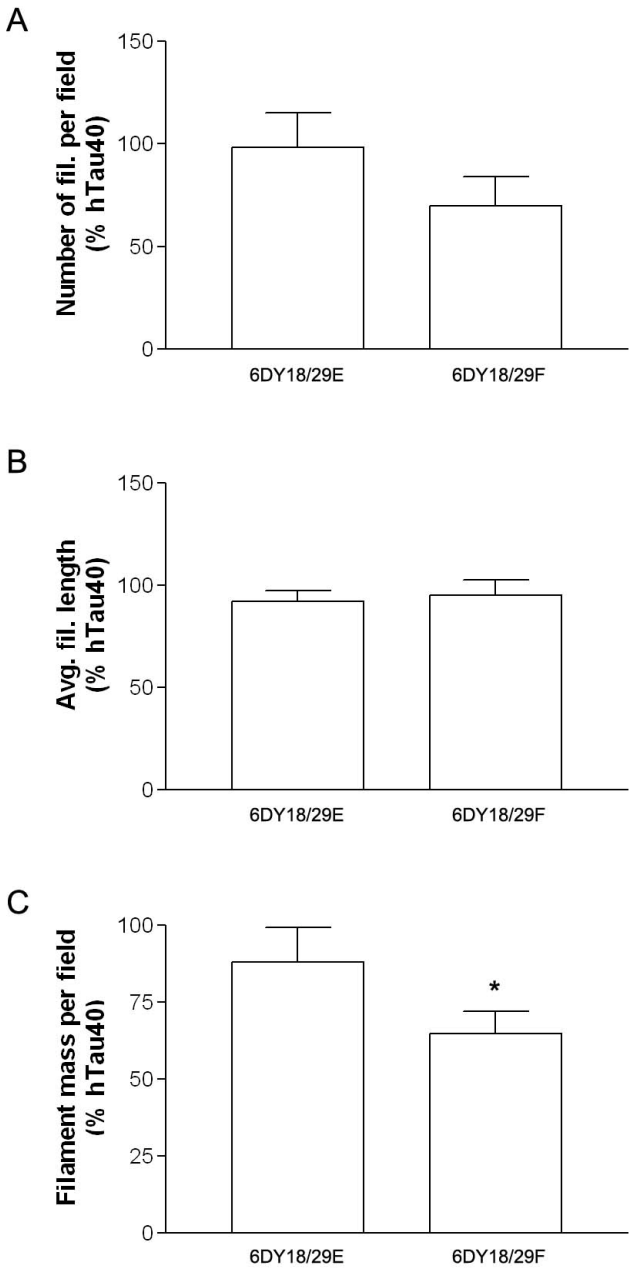


**Figure 11. Changes that mimic post-translational modifications impair the ability of 2N6D to influence hTau40 polymerization.** We polymerized hTau40 (4 μM) in the presence or absence of 8 μM wild-type 2N6D (data not shown), $^{Y}18/29^{E}$, or $^{Y}18/29^{F}$ and measured the effects on filament number, average length, and mass by quantitative EM. Pseudophosphorylation at both tyrosine residues ($^{Y}18/29^{E}$) blocked the ability of 2N6D to inhibit hTau40 polymerization. In contrast, $^{Y}18/29^{F}$ decreased filament mass and number similar to wild-type 2N6D.

**Figure 12. Modifications in the C-terminus of hTau40 modulate the effects of 2N6P.** Full-length constructs containing C-terminal changes (4 μM) were incubated with 2N6P (8 μM) for five hours, and filament number, average length, and mass were analyzed by quantitative EM. Although the effect on the number of $^{Y}394^{E}$ filaments (64.77 ± 7.51% of control) was similar to hTau40, 2N6P had a stronger effect on filament length (54.43 ± 2.53%; different from hTau40 at $P<0.01$) and mass for this construct (35.78 ± 5.76%; different from hTau40 at $P<0.05$). Interestingly, nitration at this same position ($^{394}$nY) appeared to reverse the effects of 2N6P, although the increase in filament length (to 116.5 ± 3.78% of the control) was the only parameter that reached significance. The reduction of $^{S}396/404^{E}$ filament mass (54.93 ± 0.70) was similar to hTau40, but 2N6P had a slightly stronger effect on filament number for this construct (53.16 ± 1.51; different from hTau40 at $P<0.05$). 2N6P reduced $^{R}406^{W}$ filament number (to 65.23 ± 6.00 % of control) and mass (to 61.86 ± 3.53 % control), and these effects were not statistically different from its effects on hTau40. Pseudophosphorylation at position 422 (pS422) abolished the effects of 2N6P on polymerization. Data were normalized prior to statistical analysis such that each treatment condition (with 2N6P) was expressed as a percentage of the non-treatment control (full-length tau alone).

**Figure 12**

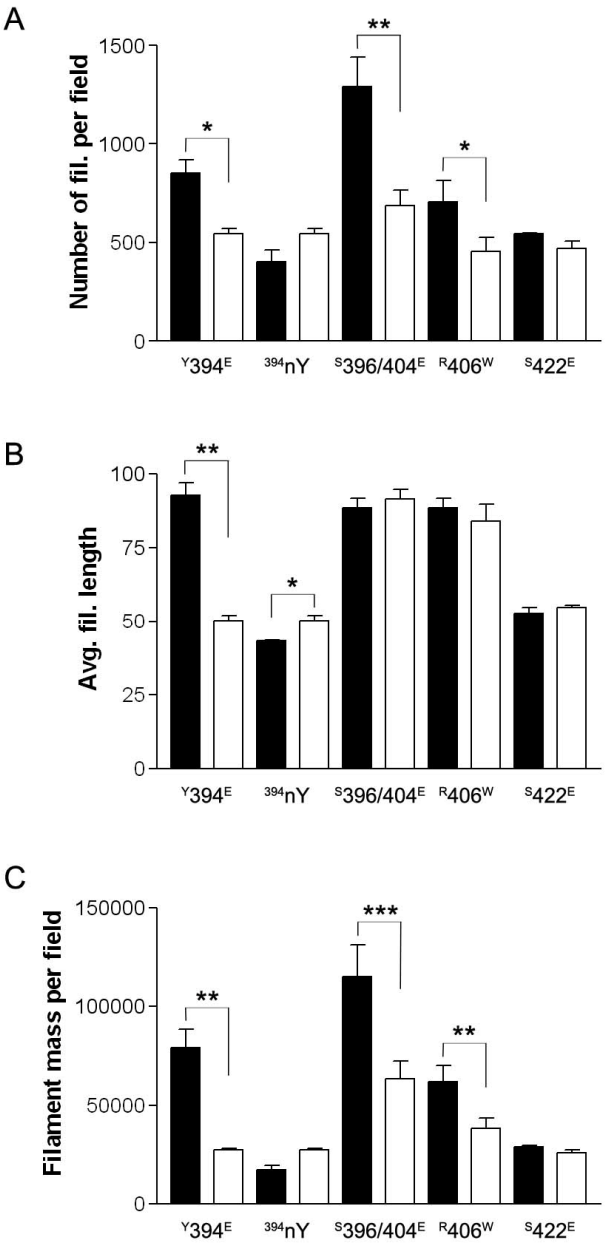
A
Number of fil. per field
1500
1000
500
0
*
**
*
Y394E
394nY
S396/404E
R406W
S422E
B
Avg. fil. length
100
75
50
25
0
**
*
Y394E
394nY
S396/404E
R406W
S422E
C
Filament mass per field
150000
100000
50000
0
**
***
**
Y394E
394nY
S396/404E
R406W
S422E

stronger inhibitory effect. Following five hours of polymerization, the filament number, average length, and mass were analyzed by quantitative EM (Fig. 12). To illustrate the polymerization differences among the various constructs, the raw data are presented in Figure 12. However, to facilitate comparisons with other experiments in this paper, data were normalized prior to statistical analysis such that each treatment condition (with 2N6P) was expressed as a percentage of the non-treatment control (full-length tau alone).

*Nitration at Tyr394:* Nitration is a potential link between tau pathology and the neuroinflammatory response that occurs during AD (reviewed in (Reynolds, Berry, & Binder, 2007)), and is an emerging area of interest in tau research. Reynolds et al. demonstrated previously that nitration at $^{394}$Y ($^{394}$nY) decreases the rate and extent of filament formation relative to hTau40. In that study, the length distribution of $^{394}$nY filaments formed was dramatically shifted relative to hTau40 filaments; short filaments and globular structures predominated, and long filaments were relatively rare.

To determine whether nitration at Tyr394 affects the ability of the N-terminal isoforms to inhibit tau polymerization, we polymerized hTau40 singly nitrated at Tyr394 ($^{394}$nY) in the presence or absence of 8 μM 2N6P. In contrast to the effects of 2N6P on hTau40 filament formation, incubation of 2N6P with $^{394}$nY had no effect on the number or mass of filaments produced, and slightly increased filament length (116.5 ± 3.78% of the control, $p < 0.05$).

*Pseudophosphorylation at Tyr394:* Tyrosine residues in tau are potential targets of phosphorylation events as well as nitration events, and tau in AD is characterized by a high

degree of phosphorylation (reviewed in (Buee et al., 2000) and (V. M. Lee et al., 2001)). Phosphorylation at Tyr394 can by mimicked by a tyrosine to glutamic acid substitution. In contrast to nitration at the same site, pseudophosphorylation at Tyr394 ($^{Y}394^{E}$) has no effect on tau polymerization (Reynolds et al., 2005b).

To determine whether pseudophosphorylation at this site affects the inhibitory ability of the N-terminal isoforms, we polymerized $^{Y}394^{E}$ in the presence or absence of 8 μM 2N6P. While the effect of 2N6P on the number of $^{Y}394^{E}$ filaments (64.77 ± 7.51% of control) was similar to hTau40, it had a stronger effect on filament length (54.43 ± 2.53%; $P<0.01$ vs. hTau40) and mass for this construct (35.78 ± 5.76%; $P<0.05$ vs. hTau40). Pseudophosphorylation introduces additional negative charge in the proposed interacting region of hTau40's carboxy terminus, which may account for the enhanced effectiveness of 2N6P on this construct. The difference between the effects of 2N6P on $^{Y}394^{E}$ and on hTau40 nitrated at this same site ($^{394}$nY) highlight the sensitivity of the inhibitory effect to posttranslational changes.

*Pseudophosphorylation at Ser396/404:* The antibody AD2 recognizes tau phosphorylated at serine 396 and 404, and this epitope is an early marker of AD neuropathology (Buee-Scherrer et al., 1996; Condamines et al., 1995). Pseudophosphorylation at these sites is mimicked by substituting glutamic acid for each serine residue by site-directed mutagenesis. The resulting mutant hTau40 construct, $^{S}396/404^{E}$, demonstrates enhanced polymerization in vitro (Abraha et al., 2000).

The effect of pseudophosphorylation at these sites was investigated by assembling $^{S}396/404^{E}$ in the presence of 8 μM 2N6P. The reduction in $^{S}396/404^{E}$ filament mass in the presence of 2N6P (54.93 ± 0.70) was not statistically different than hTau40. However, 2N6P had a stronger effect on filament number for this construct (53.16 ± 1.51; $P<0.05$ vs. hTau40). This result indicates that phosphorylation at these residues in AD increases the ability of the N-terminal isoforms to inhibit filament formation, which may partially offset the increased ability of $^{S}396/404^{E}$ tau to polymerize.

*$^{R}406^{W}$:* The FTDP-17 mutation $^{R}406^{W}$ causes an autosomal dominant form of dementia characterized by widespread neurofibrillary pathology and neuronal loss (Hutton et al., 1998; Reed et al., 1997). In vitro, the $^{R}406^{W}$ mutation increases the rate and extent of hTau40 filament formation (Barghorn et al., 2000; Gamblin, King, Dawson et al., 2000; Nacharaju et al., 1999).

To assess the impact of this mutation on the inhibitory effects of the N-terminus, we polymerized hTau40 containing this mutation ($^{R}406^{W}$) in the presence or absence of 8 μM 2N6P. The presence of 2N6P reduced $^{R}406^{W}$ filament number (to 65.23 ± 6.00 % of control) and mass (to 61.86 ± 3.53 % control). These effects were not statistically different from its effects on hTau40, indicating that this mutation has no effect on the ability of the N-terminal isoforms to promote tau solubility through assembly inhibition.

*Pseudophosphorylation at Ser422:* The C-terminus of tau is phosphorylated at serine 422 in AD (Augustinack, Schneider, Mandelkow, & Hyman, 2002; Ikegami et al., 1996; Kimura et al., 1996), and this phosphorylation may protect tau from cleavage by caspase 3 (Angela L.

Guillozet-Bongaarts et al., 2006). When hTau40 containing the $^{S}422^{E}$ mutation is polymerized in vitro, it forms many small aggregates, but relatively few extended filaments (unpublished observations).

Although Ser422 lies adjacent to the C-terminal region of interest rather than inside it, we investigated the effect of pseudophosphorylation at position 422 on the ability of 2N6P to inhibit polymerization. When incubated with this construct ($^{S}422^{E}$), 2N6P had no effect on filament number, average length, or mass. This indicates that phosphorylation at Ser422 interferes with the ability of 2N6P to inhibit tau polymerization. Phosphorylation at Ser422 occurs relative early in AD progression, and may represent an effort by the cell to prevent caspase cleavage at Asp421 (Angela L. Guillozet-Bongaarts et al., 2006). Since phosphorylation at this site interferes with N-terminal inhibition of polymerization, our results suggest that this phosphorylation event may have harmful effects in addition to the protective effects against caspase cleavage.

Collectively, these results demonstrate that disease-related changes in full-length tau modulate the inhibitory ability of the 2N6P isoform. They also indicate that the effect of the 6D and 6P isoforms requires the same C-terminal sequence as the N-terminal fragments previously studied.

# DISCUSSION

*6D and 6P isoforms as potential endogenous regulators of filament formation* - Alternative splicing of tau exon 6 produces isoforms, Tau6D and Tau6P, which contain the amino terminus of the canonical protein, but lack the proline rich region, MTBR region and the C-terminal tail of the molecule. Previous studies have demonstrated the presence of these splice variants in human brain tissue at the mRNA and protein levels (Leroy et al., 2006; Luo et al., 2004; Wei & Andreadis, 1998), although a physiological role has not been identified. The results presented here demonstrate that these N-terminal isoforms of tau can inhibit polymerization of full-length tau *in vitro*, and suggest a possible function for these isoforms as endogenous regulators of tau filament formation.

Exon 6 splicing is governed by a complex regulatory system (J. Wang, Tse, & Andreadis, 2007), and the pattern of expression is disrupted in myotonic dystrophy type 1, a disease marked by tau aggregation (Leroy et al., 2006). Our work revealed different inhibitory potential not only between the 6D and 6P isoforms, but also within these isoforms depending on the presence or absence of exons 2 and 3. It is therefore possible that the cell may fine tune tau aggregation through regulated splicing events.

Although our results demonstrate that the N-terminal isoforms can inhibit tau filament formation, it is unclear whether the *in vivo* levels of these isoforms reach the concentrations necessary to do so. Previous work has indicated that 6D and 6P mRNA levels in adult human brain are low relative to canonical tau isoforms (Leroy et al., 2006; Wei & Andreadis, 1998), as are 6D protein levels (Luo et al., 2004). In the *in vitro* polymerization assay employed in this study, the 6D/6P

isoforms were present at a two-fold molar excess relative to full-length tau, and the inhibitory effect reached only 30%-40% as assayed by quantitative EM (depending on the specific isoform). However, immunohistochemical labeling of human brain with an antibody against the 6D isoform revealed a robust presence of this variant in neuronal cells (Luo et al., 2004). Further studies are therefore necessary to determine whether these isoforms actually represent endogenous regulators of tau polymerization. It would also be interesting to determine whether these isoforms inhibit filament formation in cell culture models of tau aggregation and transgenic animal models of tauopathy.

*Posttranslational modifications of the 6D/6P isoforms* – Tau6D and 6P contain two tyrosine residues, Tyr18 and Try29, and our results indicate that phosphorylation at these sites reduces the isoforms' inhibitory potential. The effect of pseudophosphorylation at tyrosines 18 and 29 may be due to steric hindrance of the N-term C-term interaction, or the introduction of more negative charge in the crucial N-terminal interacting region. Alternatively, the N-terminus may have to adopt a specific conformation in order to inhibit polymerization, and this conformation may be disrupted by tyrosine phosphorylation.

Phosphorylation at each of these tyrosines has been observed in AD (G. Lee et al., 2004; Williamson et al., 2002). The tyrosine kinase that targets Tyr29 is unknown, but Tyr18 is phosphorylated by Fyn, a member of the Src family of non-receptor tyrosine kinases (G. Lee et al., 2004). Fyn may have a reduced affinity for Tau6D and 6P, because these isoforms lack the SH3-binding domain through which tau and fyn interact (Bhaskar, Yen, & Lee, 2005; G. Lee et al., 1998). If the 6D/6P isoforms represent endogenous inhibitors of filament formation, our

results indicate that phosphorylation at these tyrosine residues could contribute to disease progression by removing a barrier to tau aggregation.

In addition to phosphorylation, the amino terminus is the target of nitration events (Reynolds, Lukas, Berry, & Binder, 2006) (Reyes et al., in submission), and is also altered in the FTDP-17 mutations R5L (Poorkaj et al., 2002) and R5H (Hayashi et al., 2002). These changes may affect inhibition as well. Immunological studies indicate that the N-terminus of tau is lost early in AD progression, possibly due to cleavage by caspase 6 (Horowitz et al., 2004) or puromycin-sensitive aminopeptidase (Sengupta et al., 2006). If the 6D and 6P isoforms are also subject to cleavage, these events would be expected to remove their inhibitory effect on filament formation. Affinity purification of these isoforms with antibodies against the unique 6D and 6P sequences, followed by analysis with antibodies against specific tau modifications and cleavage events, may reveal if 6D and 6P are modified during AD progression.

*Changes in the C-terminus of tau alter the effects of the 6D and 6P isoforms* – The C-terminus of tau is subject to a number of posttranslational modifications in disease, including phosphorylation, nitration, and cleavage events. The C-terminus undergoes successive cleavage events during AD progression (reviewed in (A. L. Guillozet-Bongaarts et al., 2005)). The antibody MN423, which is specific for tau cleaved at position 392, recognizes a relatively late cleavage event (A. L. Guillozet-Bongaarts et al., 2005; Ugolini, Cattaneo, & Novak, 1997). We have previously shown that truncation of the C-terminus at position 391 abolishes inhibition by N-terminal fragments (Horowitz et al., 2006), and cleavage at this site should also prevent inhibition by 6D and 6P isoforms as well. In this paper, we demonstrate that certain other

modifications of the C-terminus also have an impact on the inhibitory ability of the 6D and 6P isoforms. The effect of two of these modification in particular, nitration at Tyr394 and phosphorylation at Ser396/404, have interesting implications for our working model of N-terminal inhibition.

Selective nitration at Tyr394 in full-length tau blocked the ability of the short isoforms to inhibit its polymerization. It is possible that the altered effect of Tau6P on $^{394}$nY polymerization is due to the increased ability of $^{394}$nY to adopt the Alz-50 conformation. The conformation-dependent antibody Alz-50 has a greater affinity for $^{394}$nY filaments than for hTau40 filaments, indicating that $^{394}$nY tau has a greater propensity to adopt a conformation in which the extreme amino terminus is in close proximity to the MTBR region (Reynolds et al., 2005b). This is somewhat counterintuitive, since the Alz50 conformation is thought to be a preliminary step in filament formation, and nitration at this site inhibits filament formation.

In our working model of soluble tau, the C-terminus associates with the MTBR region, and the N-terminus stabilizes this interaction by associating with the C-terminus. N-terminal stabilization may come in the form of the native amino terminus, N-terminal tau fragments, or the short isoforms 6D and 6P. The increased affinity of Alz-50 for $^{394}$nY suggests that the amino terminus of this construct is associated with the MTBR region (Carmel et al., 1996), potentially preventing association of the C-terminus with that part of the molecule. Since our model depends on the C-terminus/MTBR interaction, this could explain the reduced efficacy of the N-terminal isoforms to promote solubility of this protein. This is unlikely to be the entire explanation, however, since it does not explain the observed increase in $^{394}$nY filament length.

The effects of pseudophosphorylation at Ser396/404 on 2N6P inhibition were also interesting in light of our model. Tau pseudophosphorylated at these sites shows enhanced ability to polymerize relative to hTau40 (Abraha et al., 2000). In wild-type tau, filament formation is discouraged when the C-terminal tail of the molecule folds over the MTBR region (Abraha et al., 2000; R. W. Berry et al., 2003). It has been proposed that the $^{S}396/404^{E}$ mutations inhibit this folding event, keeping the C-terminus in an extended position (Abraha et al., 2000).

In our working model, the inhibitory effect of the N-terminus is accomplished by stabilizing the interaction between the C-terminus and MTBR region. Since the C-terminus/MTBR interaction is impaired in the $^{S}396/404^{E}$ mutant, we predicted that the effect of 2N6P on this construct would be reduced. However, 2N6P actually inhibited this construct to a greater extent than wild-type tau.

*Additional cell biological functions for Tau6D and 6P isoforms* - Several reports have indicated that the N-terminus of tau associates with the plasma membrane (Brandt et al., 1995; Maas et al., 2000), where it is potentially involved in signaling cascades (Hwang et al., 1996). Amino terminal tau constructs similar in length to 6P and 6D isoforms are neuroprotective in some circumstances (Amadoro et al., 2004). Conversely, smaller N-terminal fragments induce cell death through a mechanism involving the activation of N-methyl-D-aspartate (NMDA) receptors and calpain (Amadoro et al., 2006; Amadoro et al., 2004). The amino terminus has also been linked to the cellular response to beta-amyloid (Barbato et al., 2005; King et al., 2006). Finally, the unique eleven amino acids at the C-terminus of each 6D/6P protein may confer isoform-

specific cellular roles to these proteins. Further work is necessary to reveal the role of these truncated tau isoforms in human brain.

*Conclusions* – The results presented here suggest the short, naturally occurring tau 6D and 6P isoforms have the potential to act as endogenous regulators of tau filament formation. The neurofibrillary tangles of AD are not static entities, but rather undergo a sequence of modifications (e.g. truncations and phosphorylations) as they age, and great strides have been made toward establishing a timeline of these changes in recent years (reviewed in (Binder et al., 2005)). We demonstrate that certain of these modifications have an impact on the inhibitory ability of the 6D and 6P isoforms. By looking at a number of these markers in conjunction with antibodies to the 6D and 6P isoforms, future studies may determine how these short isoforms fit into the life story of a degenerating neuron.

## ACKNOWLEDGEMENT

I would like to thank Dr. Peleg Horowitz and Andres Silva for their contributions to this project, and Dr. Angela Guillozet-Bongaarts for her advice and critical reading of this manuscript. The authors would also like to thank Dr. Athena Andreadis for the kind gift of the Tau6D and 6P cDNA constructs. This work is supported by NIH Awards NS049834 (N.L.), AG14453 and AG09466 (L.I.B)

# CHAPTER FOUR

# THE AMINO TERMINUS OF TAU INHIBITS KINESIN-DEPENDENT AXONAL TRANSPORT: IMPLICATIONS FOR FILAMENT TOXICITY

**In submission at J. Neuroscience Research**

## ABSTRACT

The neuropathology of Alzheimer's disease (AD) and other tauopathies is characterized by filamentous deposits of the microtubule-associated protein tau, but the relationship between tau polymerization and neurotoxicity is unknown. Here, we examined effects of filamentous tau on fast axonal transport (FAT) using isolated squid axoplasm. Monomeric and filamentous forms of recombinant human tau were perfused in axoplasm, and their effects on kinesin- and dynein-dependent FAT rates evaluated by video microscopy. While perfusion of monomeric tau at physiological concentrations showed no effect, tau filaments at the same concentrations selectively inhibited anterograde (kinesin-dependent) FAT, triggering the release of conventional kinesin from axoplasmic vesicles. Pharmacological experiments indicated that the effect of tau filaments on FAT is mediated by protein phosphatase 1 (PP1) and glycogen synthase kinase-3 (GSK-3) activities. Moreover, deletion analysis suggested that these effects depend on a conserved 18-amino acid sequence at the amino terminus of tau. Interestingly, monomeric tau isoforms lacking the C-terminal half of the molecule (including the microtubule binding region) recapitulated the effects of full-length filamentous tau. Our results suggest that pathological tau aggregation contributes to neurodegeneration by altering a regulatory pathway for FAT.

## INTRODUCTION

Tau is a microtubule-associated protein (MAP) involved in microtubule dynamics and maintenance (Amos & Schlieper, 2005), and insoluble filamentous tau aggregates form in Alzheimer's disease (AD) and several other neurodegenerative tauopathies (reviewed in (T. C. Gamblin, R. W. Berry et al., 2003). Despite the strong positive correlation between the appearance of filamentous tau and neuronal dysfunction (reviewed in (Binder et al., 2005)), no toxic mechanism has been directly tied to these structures, and as a result the toxicity of tau filaments remains a subject of debate (King, 2005).

In AD, degenerating neurons exhibit alterations in synaptic function (Bell & Claudio Cuello, 2006; Yoshiyama et al., 2007), the appearance of neuritic varicosities, and the mislocalization of various membrane-bound organelles (MBOs), all of which indicate that intracellular transport is disrupted in this disease (reviewed in (Morfini, Pigino, Beffert, Busciglio, & Brady, 2002). Given these observations, and the central role of tau in AD pathology, a number of investigators have explored the effects of monomeric tau on microtubule-dependent fast axonal transport (FAT). Although reports have been published arguing both for (Ebneth et al., 1998; Seitz et al., 2002; Vershinin et al., 2007), and against (Morfini, Pigino, Mizuno et al., 2007) the idea that high levels of soluble tau can reduce anterograde FAT by interfering with the attachment of the molecular motor kinesin, there is no evidence that such levels of tau are seen in normal or pathological neurons. Remarkably, even though the hallmark of AD and other tauopathies is the presence of intracellular tau filaments, the biological effects of filamentous tau on FAT have not been assessed previously.

In this paper, we examined the effects of tau filaments on FAT using isolated squid axoplasm. Whereas at low, physiologically relevant, ratios of tau to tubulin, monomeric tau has

no effect, tau filaments selectively inhibit anterograde, conventional kinesin-dependent fast axonal transport (FAT). Furthermore, deletion experiments indicate that this effect requires the first 18 a.a. at the amino terminus of tau, which becomes abnormally exposed upon polymerization. Consistent with this notion, monomeric tau isoforms lacking the microtubule-binding region (MTBR) and the C-terminus mimicked the effect of tau filaments on FAT. Finally, we show that tau filaments do not act at the microtubule surface, but rather inhibit anterograde FAT by activating protein phosphatase 1 (PP1) and glycogen synthase kinase 3 (GSK-3). Taken together, our findings reveal a novel gain-of-function mechanism by which the formation of tau filaments may play a critical role in AD pathogenesis.

## EXPERIMENTAL PROCEDURES

*Reagents:* CREBpp was synthesized and purified (95%) by New England Peptide (Gardner, MA). Inhibitor-2 (I-2), SB203580, and okadaic acid were purchased from Calbiochem (San Diego, CA). Arachidonic acid (AA; Cayman Chemical, Ann Arbor, MI) was stored at -20°C, and working solutions were prepared in 100% ethanol immediately prior to use. Mammalian protease inhibitor cocktail was from Sigma (St. Louis, MO). ING-135 (see Supplemental Material) was synthesized as described previously (Kozikowski et al., 2007).

*Recombinant Proteins*: The full-length tau used in this study (hTau40) corresponds to the longest isoform in adult human brain, containing 441 amino acids and four microtubule-binding repeats (MTBRs). K23 is a tau construct lacking both alternatively-spliced N-terminal exons as well as all four MTBRs. Tau6D and Tau6P are tau isoforms lacking the MTBR region and the C-terminus of canonical tau. The alternative splicing that generates these isoforms occurs in exon 6, and introduces a unique 11 amino acid sequence followed by a stop codon. The specific 11 amino acids vary depending on whether the splice site is proximal or distal to the beginning of exon 6 (Luo et al., 2004). Tau6D and Tau6P isoforms were generated by restriction digestion and ligation of constructs previously described (Luo et al., 2004) and hTau40 (Carmel et al., 1996; Gustke et al., 1994). All other constructs used in this study have been described elsewhere:, Δ2-18 (T.C. Gamblin et al., 2003), 1-421 (T. C. Gamblin, F. Chen et al., 2003), K23 (Preuss, Biernat, Mandelkow, & Mandelkow, 1997). All proteins were expressed in E. coli and purified by means of an N-terminal poly-histidine tag (Abraha et al., 2000; Carmel et al., 1996).

*Immunoblots:* Tau constructs were spotted onto nitrocellulose membranes (1 ng/µL, 1 µL per spot), blocked with 5% non-fat dry milk in Tris-buffered saline, pH 7.4, and probed with the monoclonal antibodies Tau12 (2 ng/mL), Tau5 (20 ng/mL), and Tau46.1 (20 ng/mL), which recognize amino acids 9-18, 210-230, and 428-441, respectively (Carmel et al., 1996; Ghoshal et al., 2002; Kosik et al., 1988). Primary antibody binding was detected with HRP-conjugated anti-mouse secondary antibody (Vector Laboratories, Burlingame, CA) and ECL developing solution (GE Healthcare, Amersham, UK).

*Microtubule-binding Assays:* Squid optic lobes were dissected and flash frozen in liquid nitrogen (Morfini, Pigino, Mizuno et al., 2007). 1.5 grams of freshly thawed squid optic lobes was homogenized in 2.5 mL of BRB80 buffer (80 mM Pipes, 1 mM $MgCl_2$ and 1 mM EGTA) and 1/100 mammalian protease inhibitor cocktail (Sigma, St. Louis, MO), plus phosphatase and kinase inhibitors (Calbiochem, San Diego, CA) as follows: 1/200 phosphatase inhibitor cocktail II, 200 mM sodium orthovanadate, 200 nM mycrocystin RR, 50 nM okadaic acid, 100 nM K252a, 100 nM staurosporine. Squid optic lobe homogenate was prepared at $4^0$C using a glass Dounce homogeneizer. This homogenate was centrifuged at 12,500 x g for 20 min at $4^0$C. The supernatant fraction was transferred to a new tube, and centrifuged at 125,000 x g for 5 min at $4^0$C in a TL100.3 rotor (Beckman, Fullerton, CA). The supernantant (cytosol) was transferred to a new tube, adjusted to 20 µM taxol, and incubated at $37^0$ C for 15 min to allow for microtubule polymerization. After this step, 200 µL aliquots of microtubule-containing cytosol were incubated alone, or with htau40, or K23 tau constructs (5 µM final concentration) for 20 min at $37^0$ C. Samples were loaded on top of a 60 µL BRB80 buffer plus 20% sucrose cushion and 20 µM taxol using 1.5 mL microcentrifuge tubes, and centrifuged for 5 min at 125,000 x g at $4^0$C

using a TLA100.3 rotor (Beckman, Fullerton, CA). Microtubule pellets were resuspended in 200 µL of BRB80. Pellets and supernatant fractions were adjusted to 1X gel loading buffer (GLB) using a 5X GLB stock (0.35 M Tris-HCl pH 6.8, 10% w/v SDS (Sequanal grade, Pierce, Rockford, IL), 36% glycerol, 5% ß-mercaptoethanol, 0.01% bromophenol blue). Membranes were also probed with an antibody against tubulin (DM1a clone, Sigma) to demonstrate the presence of microtubules in the pellet samples.

*Tau Polymerization:* Tau polymerization was induced using arachidonic acid as previously described (King et al., 1999), except that KCl was substituted for NaCl in the polymerization buffer. This substitution did not prevent filament formation (see Fig. 5b-d). Briefly, tau protein (4 µM) was incubated at room temperature in reaction buffer (50 mM HEPES, pH 7.6, 50 mM KCl, 5 mM DTT) in the presence of 75 µM arachidonic acid (in ethanol vehicle). Samples of soluble tau were prepared for perfusion in the same manner, except that arachidonic acid was excluded from the polymerization buffer. Control mixtures containing AA but lacking tau were prepared in parallel. Final ethanol concentration in all samples was 3.8%.

*Electron Microscopy:* Polymerization reactions were allowed to proceed for six hours, fixed with 2% glutaraldehyde, spotted onto 300 mesh formvar/carbon coated copper grids (Electron Microscopy Sciences, Hatfield, PA), and negatively stained with 2% uranyl acetate (King et al., 1999). Samples were examined using a JEOL JEM-1220 electron microscope at 60kV and 12,000X magnification, and photographs were taken using a MegaScan 794/20 digital camera and DigitalMicrograph software version 3.9.3 (Gatan, Pleasanton, CA).

*Squid Axoplasm Motility Assays:* Axoplasm from squid giant axons (*Loligo pealii*; Marine Biological Laboratory, Woods Hole, MA) was extruded as previously described (Brady, Lasek, & Allen, 1985). All proteins and inhibitors were diluted in ATP-supplemented X/2 buffer (175 mM potassium aspartate, 65 mM taurine, 35 mM betaine, 25 mM glycine, 10 mM HEPES, 6.5 mM $MgCl_2$, 5 mM EGTA, 1.5 mM $CaCl_2$, 0.5 mM glucose, pH 7.2) for perfusion. For experiments involving tau and their controls, reaction mixtures (containing tau alone, tau and AA, and AA alone) were diluted 1:1 in ATP-supplemented X/2 buffer (final tau concentration 2 μM, when present). Motility was analyzed using a Zeiss Axiomat microscope equipped with a 100X, 1.3 N.A. objective and DIC optics. Organelle velocities were measured by matching calibrated cursor movements to the speed of vesicles moving in the axoplasm (Morfini et al., 2006).

*Purification of membrane vesicle fractions from squid axoplasms:* Two "sister" axoplasms were prepared from the same animal and incubated with the appropriate effectors (control buffer, active GSK-3β, monomeric tau or filamentous tau) as for motility assays in X/2 buffer plus 1 mM ATP in 25 μL final volume. Active GSK-3β was from Sigma (# G1663). After 40 min incubation, axoplasms were transferred, along with perfusion buffer, to low protein binding 1.5 mL centrifuge tubes containing 200 μL of homogenization buffer [0.25 mM sucrose, 1 mM EDTA, 10 mM Hepes, pH 7.4, 1/100 protease inhibitor cocktail (Sigma #P8340), 1/200 phosphatase inhibitor cocktail set II (Calbiochem # 524627), 2 μM K252a (Calbiochem # 420298), 1 μM PKI (Upstate # 12-151)], and carefully homogenized by 2 passages through a 23G syringe needle and 5 passages through a 27G syringe needle using a 1 mL Hamilton pipette.

Axoplasm homogenates were adjusted to 30% iodixanol by mixing 200 µL of axoplasm homogenates with 300 µL of solution D (50% (w/v) iodixanol, 10 mM $MgCl_2$ in 250 mM sucrose). A 500 µL layer of solution E (25% (w/v) iodixanol, 10 mM $MgCl_2$ in 250 mM sucrose) and a 100 µL layer of solution F (5% (w/v) iodixanol, 10 mM $MgCl_2$ in 250 mM sucrose) were loaded on top of the axoplasm homogenates. Samples were centrifuged at 250,000 x g max for 1 hour at $4^0$C in an RP55-S Sorvall rotor. 300 µL containing floating vesicles were collected from immediately below the 5% iodixanol interface, and 60 µl of 6X loading sample buffer added. In separate experiments, 0.1% Triton X-100 was added to the axoplasm homogenates prior to centrifugation to confirm the membranous nature of this fraction. Immunoblots were developed using antibodies against kinesin-1 heavy chain (H2, Pfister et al, 1989), dynein intermediate chain (rabbit polyclonal V3, a generous gift from Kevin Vaughan) and SNAP-25 (Synaptic Systems #111-002). Quantitative immunoblotting was performed as described before (Morfini et al, 2006).

*Statistical Analysis:* All experiments were repeated at least 3 times. Unless otherwise stated, the data was analyzed by ANOVA followed by post-hoc Student-Newman-Keul's test in order to make all possible comparisons. Comparison of transport data from axoplasm under different conditions was done using a two sample t-test of µ1-µ2 with Datadesk statistical software (Data Description, Inc; Ithaca, NY). Data was expressed as mean $\pm$ s.e.m. and significance was assessed at *p* values as noted.

# RESULTS

To evaluate the effect of tau on microtubule-dependent FAT, we used vesicle motility assays in isolated squid axoplasm. In this experimental system, the bi-directional transport of membrane-bound organelles (MBOs) can be directly observed by video-enhanced differential interference contrast (DIC) microscopy. This preparation preserves the ionic strength and complex environment of the cell, and because the axoplasm is isolated from the cell body, nuclear effects can be ignored (Brady et al., 1985). Also, the absence of plasma membrane in this preparation allows for the introduction of experimental agents at tightly controlled concentrations (Morfini, Pigino, Mizuno et al., 2007). This system was instrumental in the original discovery of kinesin-1 (Brady, 1985), novel regulatory pathways for FAT (Morfini et al., 2006; Morfini et al., 2004; Morfini, Szebenyi, Elluru, Ratner, & Brady, 2002), and axonal-specific phosphorylation events (Grant, Diggins, & Pant, 1999).

## *Monomeric hTau40 binds to squid microtubules, but does not affect FAT*

Alternative splicing produces six major tau isoforms in the adult human central nervous system. In a previous study, we assayed monomeric tau constructs derived from the shortest tau isoform (352 a.a., hTau23) and established their effects on FAT (Morfini, Pigino, Mizuno et al., 2007). In the present study, we chose to use the longest isoform (441 a.a., hTau40), because of its greater propensity to form filaments (T. C. Gamblin, R. W. Berry et al., 2003). Unlike hTau23, hTau40 contains two alternatively-spliced N-terminal exons (E2 and E3) and four microtubule binding repeats (R1-R4). A schematic of each tau construct used in the present study is shown in Fig. 13a.

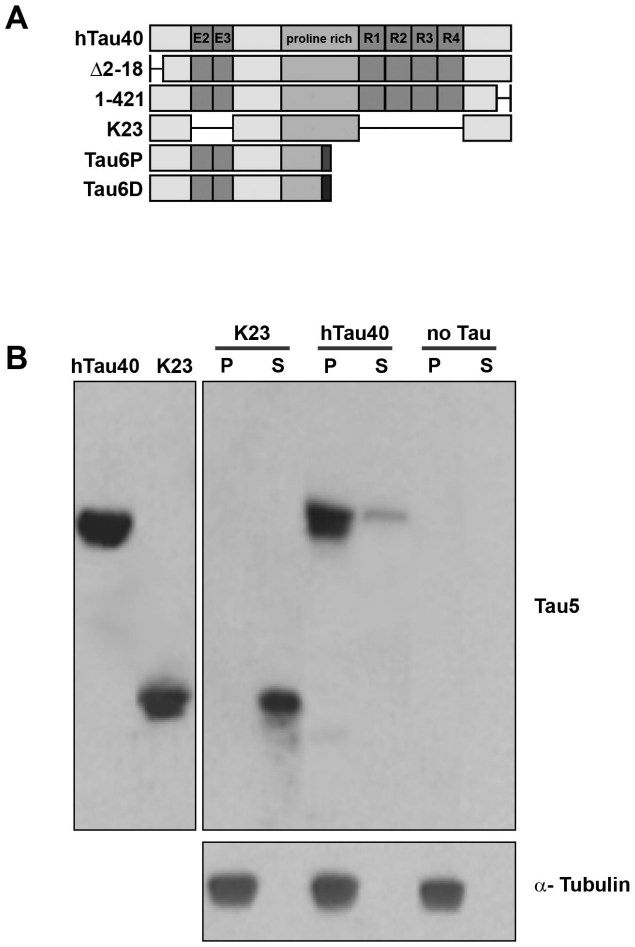


**Figure 13. Schematic and microtubule binding of tau constructs used in this study.** A) The longest isoform of tau in the human central nervous system is referred to as hTau40. Boxes represent alternatively spliced exons (E2 and E3), the proline rich region, and the microtubule-binding repeats (R1-R4). Δ2-18 and 1-421 are constructs containing N-terminal and C-terminal deletions, respectively, and K23 is a construct lacking N-terminal exons and microtubule-binding repeats. Tau6P and Tau6D are isoforms that are identical to canonical tau from amino acids 1-144, at which point alternative splicing introduces 11 unique amino acids (represented by dark boxes) followed by a stop codon. The specific amino acids differ between Tau6P and Tau6D. B) Tau constructs (5 μM) were incubated with microtubule-containing squid optic lobe cytosol as described in Materials and Methods. Microtubule pellets (P) and supernatant (S) fractions were prepared by centrifugation, and analyzed by immunoblot using antibodies against tau (Tau5) and tubulin. Note that the K23 tau construct lacking MTBRs is mostly recovered in supernatant fractions, consistent with its weak binding to microtubules. In contrast, hTau40 is recovered in association with microtubules. Neither construct was recovered in pellet fractions when centrifuged in the absence of squid microtubules (data not shown).

Previously, we demonstrated that monomeric hTau23 binds to axonal squid microtubules (Morfini, Pigino, Mizuno et al., 2007). To rule out species-related artifacts, we assayed the ability of monomeric hTau40 to interact with endogenous squid microtubules. Microtubule-enriched fractions fromsquid optic lobe were prepared in the presence or absence of hTau40. Following taxol-induced microtubule assembly, microtubules and associated proteins were sedimented by centrifugation, and the resulting fractions (supernatants and microtubule-enriched pellets) probed with anti-tau antibodies. A tau construct with low binding affinity (K23) was assayed in parallel to control for non-specific sedimentation. As observed previously (Morfini, Pigino, Mizuno et al., 2007), most K23 remained in the supernatant fraction. In contrast, hTau40 was depleted from the supernatant fraction and found in association with the microtubule-enriched pellet fraction (Fig. 13b), indicating that monomeric hTau40 can bind to endogenous squid microtubules.

Microtubule rigidity is increased when tau binds to the microtubule surface, and this effect is observable even at low, non-saturating tau concentrations (Felgner et al., 1997; Morfini, Pigino, Mizuno et al., 2007). As an additional indicator of hTau40's ability to interact with squid microtubules, we perfused axoplasm with tau and then examined the morphology of microtubules at the axoplasm periphery. In the absence of exogenous tau, many of these microtubules exhibited a curved appearance (Fig. 14a). However, perfusion of monomeric hTau40 (2 μM) caused peripheral microtubules to acquire a straight, rigid appearance (Fig. 14b), consistent with binding of hTau40 to the microtubule surface (Morfini, Pigino, Mizuno et al., 2007). Together with the sedimentation assay, these results demonstrate that hTau40 is capable of binding to squid microtubules.

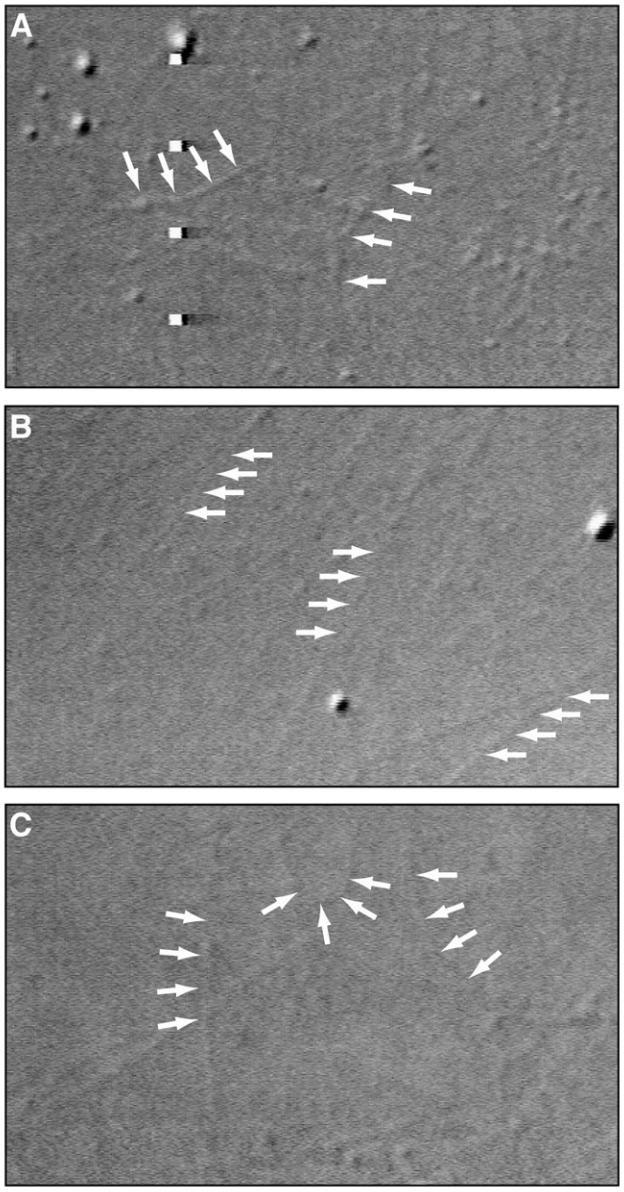


**Figure 14. The effect of hTau40 on the morphology of axoplasmic squid microtubules.** A) After perfusion of squid axoplasm with control buffer, individual microtubules can be observed at the axoplasm periphery. Many of these microtubules display a gently curving, freely bending morphology (white arrows). B) Perfusion of hTau40 at 2 μM dramatically changes the morphology of peripheral microtubules to a stiff, linear appearance (white arrows). This effect of tau and other MAPs on microtubule stiffness has been previously characterized *in vitro* (Felgner et al., 1997), and indicates direct binding of hTau40 to endogenous squid microtubules. C) In contrast to monomeric hTau40, perfusion of filamentous hTau40 at 2 μM does not change the morphology of peripheral microtubules.

We next examined the effects of monomeric hTau40 on FAT. We perfused axoplasm with hTau40 at 2 μM, which is within the physiological range for neurons (2-5 μM) (Drubin et al., 1985). The concentration of tubulin in squid axoplasm is 50 μM (Morris & Lasek, 1984), resulting in a tau to tubulin ratio of approximately 1:25. FAT rates measured between 30 and 50 min post-perfusion were pooled and compared to axoplasms perfused with control buffer alone. As observed for other monomeric tau constructs (Morfini, Pigino, Mizuno et al., 2007), perfusion of hTau40 at 2 μM showed no effect on either anterograde or retrograde FAT (Fig. 15a), demonstrating that physiological levels of monomeric hTau40 do not impair FAT in this system.

***Perfusion of filamentous tau selectively inhibits anterograde FAT***

Recombinant hTau40 forms filaments *in vitro* when incubated with arachidonic acid (reviewed in (T. C. Gamblin, R. W. Berry et al., 2003)), and these filaments are morphologically similar to those isolated from Alzheimer's disease neuronal tissue (King et al., 1999). To determine the effects of filamentous tau on FAT, we perfused hTau40 filaments (2 μM) into squid axoplasm and monitored anterograde and retrograde FAT rates. Unlike monomeric tau, hTau40 filaments inhibited anterograde, kinesin-dependent FAT rates (Fig. 15b, $p \leq 0.001$) when perfused at the same concentration as monomeric hTau40 (2μM). Perfusion of axoplasms with polymerization buffer alone (see Materials and Methods) had no effect on FAT (data not shown), demonstrating that the effects on FAT were due to the presence of filamentous tau. Significantly, retrograde FAT rates remained unaffected, suggesting that the effects of hTau40 filaments on anterograde FAT were not due to alterations in microtubule integrity. Supporting this idea, htau40 filaments (2 μM) did not produce changes in microtubule morphology when perfused into axoplasm, which also suggests that filamentous tau does not bind to microtubules

(Fig. 2c). Similarly, perfusion of equivalent amounts of polymerization buffer (containing arachidonic acid, but no tau) had no effect on FAT (not shown).

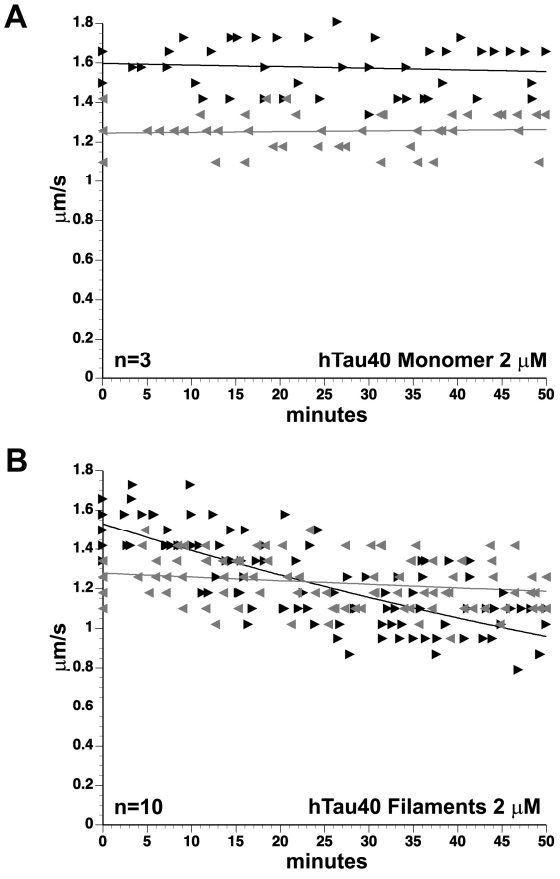


**Figure 15. Effects of soluble and filamentous tau on FAT.** Axoplasms were perfused with soluble or filamentous recombinant tau (hTau40), and FAT rates (μm/sec) monitored over a period of 50 min. Each arrowhead represents a measurement of the average velocity at which particles move in the anterograde (►) or retrograde (◄) direction. Graphs depict compiled data from at least three separate trials. While soluble hTau40 (2 μM) had no observable effect on either FAT direction (A), hTau40 filaments (2 μM) specifically inhibited anterograde FAT in a time-dependent manner (B).

***The effect of tau filaments on FAT depends upon the extreme N-terminus of tau***

Several studies suggest important functional roles for both the amino and carboxy terminus of tau (Amadoro et al., 2006; Amadoro et al., 2004; Brandt et al., 1995; G. Lee, 2005), and the study of selected modifications of these domains constitutes an emerging area of interest in AD (T. C. Gamblin, F. Chen et al., 2003; A. L. Guillozet-Bongaarts et al., 2005). To determine whether these domains are involved in FAT inhibition, we assayed two tau constructs, Δ2-18 and 1-421 containing deletions at the extreme amino- and carboxy-terminus, respectively (see Fig. 1a and Fig. 16a). These deletions do not normally prevent tau from forming filaments (R. W. Berry et al., 2003; T.C. Gamblin et al., 2003). However, the buffer conditions required for axoplasm perfusion (see Materials and Methods) differ from the buffer used in previous tau assembly assays. This led us to evaluate the formation of tau filaments under these experimental conditions using electron microscopic analysis. As shown in Fig. 16b-d, hTau40, Δ2-18 and 1-421 all form morphologically undistinguishable filaments under these buffer conditions (Fig. 16b-d).

We then evaluated the effects of Δ2-18 and 1-421 filaments on FAT. Axoplasms perfused with monomeric hTau40 (2 μM) were used as an experimental control, because this treatment results in FAT rates that are indistinguishable from control buffer alone (see Fig. 3a). Filaments composed of hTau40 (hTau40 F) and 1-421 (1-421 F) significantly reduced anterograde FAT rates, compared to hTau40 monomer (hTau40 M; *$p \leq 0.0001$ by a two-sample t test). In contrast, Δ2-18 filaments (Δ2-18 F) had no effect on FAT (Fig. 17a). Retrograde transport was unaffected in all conditions (Fig. 17b). These results suggest that the first 18 a.a. of tau are necessary for the inhibitory effect of tau filaments on anterograde FAT.

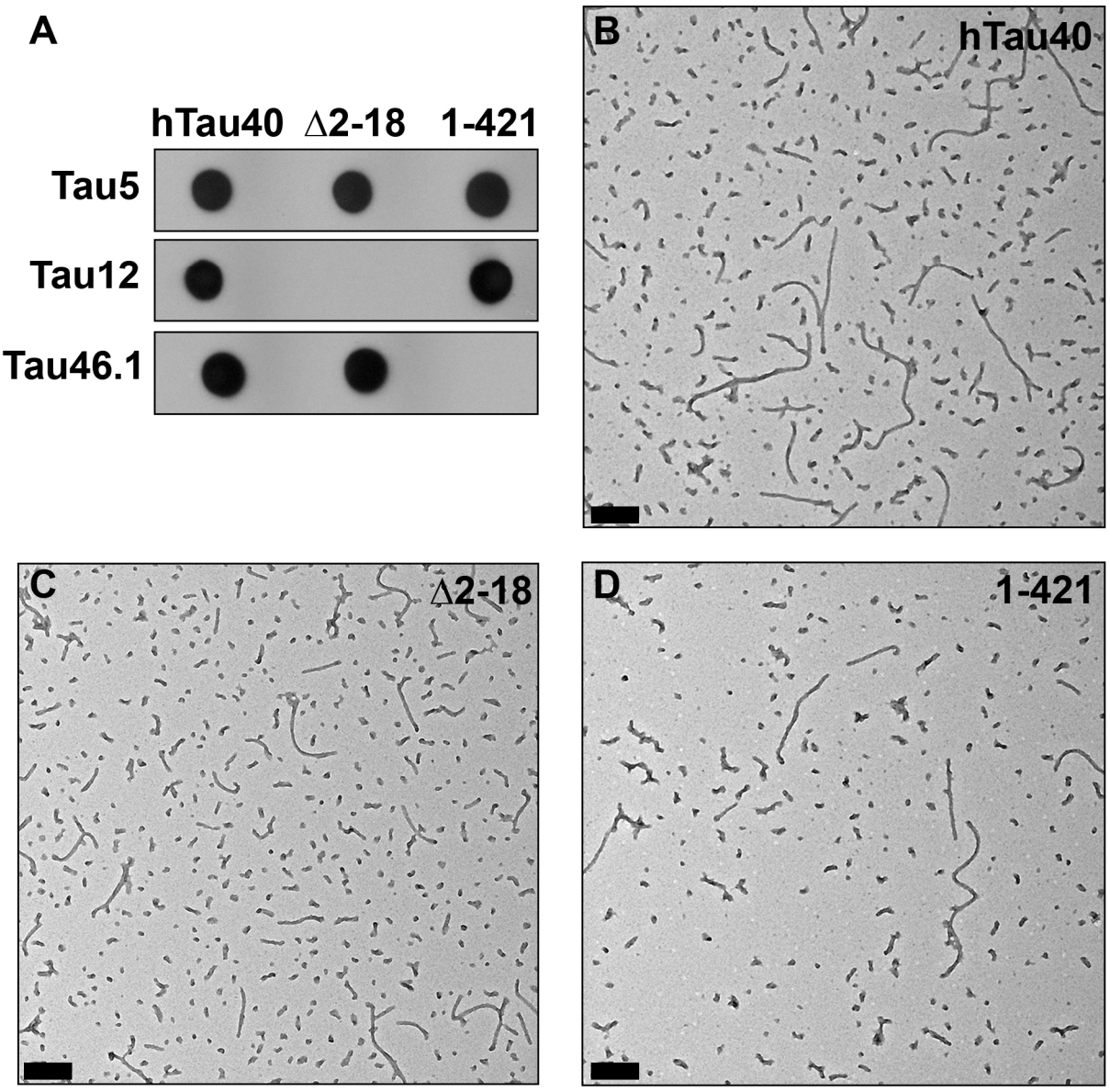


**Figure 16. Characterization of tau filaments.** Tau constructs hTau40, Δ2-18, and 1-421 were all recognized by Western blot analysis with the antibody Tau5, which recognizes an epitope near the middle of the protein (top panel). Δ2-18 is not recognized by the N-terminal antibody Tau12, and the C-terminal antibody Tau46.1 does not recognize 1-421 (lower panel) (A). Filaments generated from 4 μM hTau40 (B), Δ2-18 (C), and 1-421 (D) following five hours of polymerization with arachidonic acid. Fixed samples were negatively stained and viewed by electron microscopy. Representative digital micrographs are shown. Size bars represent 200 nm.

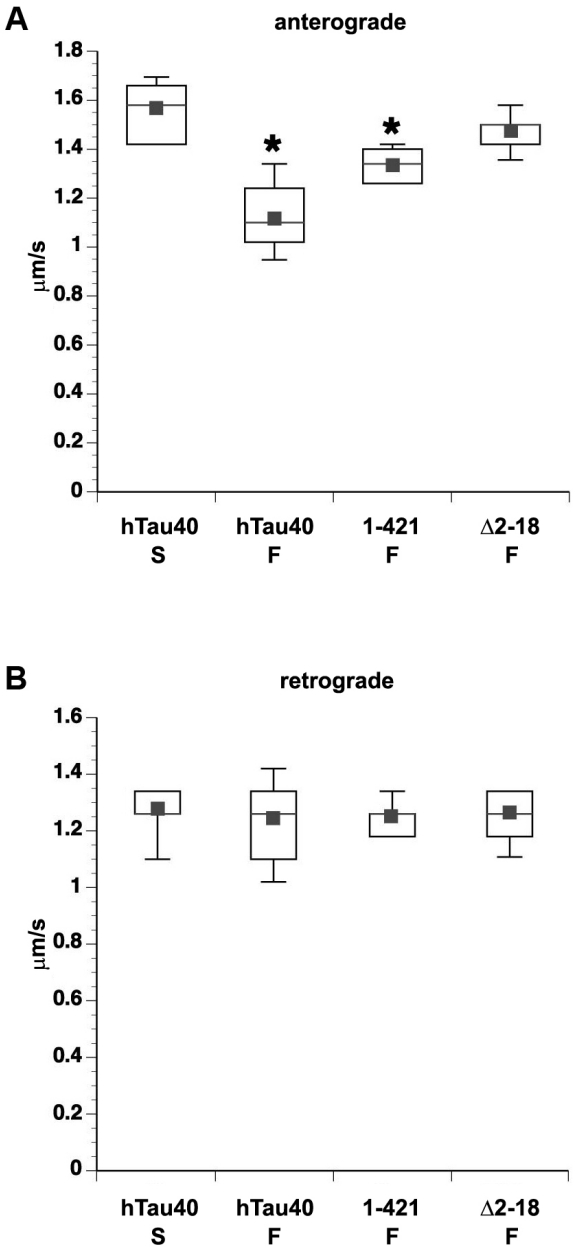


**Figure 17. Removal of the extreme N-terminus of tau abolishes the effects of tau filaments on FAT.** Box plots of FAT rates in axoplasm perfused with 2 μM soluble or filamentous tau. Data represent pooled measurements taken between 30 and 50 min of observation. Perfusion with filaments composed of hTau40 (hTau40 F) and 1-421 (1-421 F) significantly reduced anterograde FAT compared to hTau40 monomer (hTau40 M) rate at (*$p \leq 0.0001$ by a 2 sample t test). In contrast, Δ2-18 filaments (Δ2-18 F) failed to inhibit anterograde FAT (A). Retrograde FAT was unaffected in all conditions (B). Rates for monomeric hTau40 were indistinguishable from axoplasm perfused with buffer alone (data not shown).

***Monomeric tau constructs lacking the C-terminal half of the protein recapitulate the effects of tau filaments on FAT***

Results from deletion experiments above suggested that the first 18 a.a. at the amino terminus of tau are required to elicit the inhibitory effect of tau filaments on FAT. However, various full-length tau constructs including the amino terminal 18 a.a. domain do not affect FAT when perfused in monomeric, soluble form (Fig 15 and (Morfini, Pigino, Mizuno et al., 2007)), suggesting this domain is abnormally exposed in filamentous hTau40. Supporting this idea, biochemical studies identified a intramolecular interaction between the amino and C-terminus of monomeric tau constructs (Horowitz et al., 2006; Jeganathan et al., 2006). These observations led us to evaluate the effect of endogenous tau isoforms lacking the C-terminal half of the protein on FAT. These isoforms, Tau6P and Tau6D, are the products of two cryptic splice sites in exon 6 (see Fig. 13a). They are identical to canonical tau from amino acids 1-144, at which point splicing introduces a unique 11 amino acid sequence followed by a stop codon. The specific 11 amino acids differ depending on whether the splice site is proximal or distal to the beginning of exon 6 (Luo et al., 2004). Tau6P and Tau6D terminate prior to the MTBR region, and so are not expected to interact with microtubules (G. Lee, Neve, & Kosik, 1989) or form filaments (Abraha et al., 2000; von Bergen et al., 2000). When axoplasm was perfused with monomeric Tau6P or Tau6D (2 μM), anterograde FAT was inhibited ($p \leq 0.0001$), but retrograde transport remained unchanged. Since the effects of these two isoforms were indistinguishable, data from Tau6P and Tau6D were pooled (Fig. 18). The inhibitory effect of these tau isoforms was indistinguishable from that of hTau40 filaments, indicating that the amino terminus of tau is sufficient to trigger FAT inhibition (see Discussion).

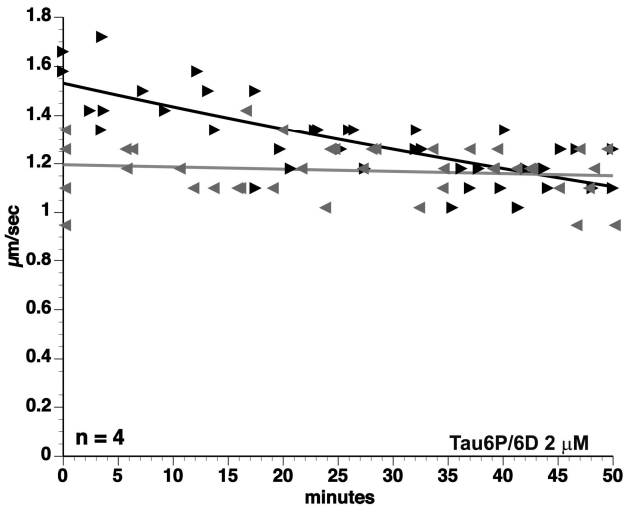


**Figure 18. The N-terminus of tau is sufficient to inhibit anterograde FAT.** Graph representing pooled data from axoplasms perfused with either Tau6P or Tau6D (2 μM). The N-terminus of both isoforms is identical to that of hTau40, but they lack the MTBR region and the C-terminus. When perfused as monomer into isolated axoplasm, these isoforms inhibit anterograde FAT. The effect was not statistically different from inhibition caused by hTau40 filaments.

***The effects of tau filaments on FAT are mediated by GSK-3 activity***.

The effect of tau filaments and monomeric 6P/6D tau isoforms on anterograde FAT raised questions about the underlying molecular mechanisms. The effect of tau filaments on FAT is unlikely to be due to steric hindrance of kinesin by tau at the microtubule surface, since filamentous tau is not expected to bind to microtubules (Fig. 14c) and Tau6P/6D isoforms lack a MTBR domain. Instead, we suspected that FAT inhibition might occur through one of the signaling pathways that regulate the activity of the major anterograde motor in this system, conventional kinesin.

Several axonal kinases have been identified that play a role in regulating conventional kinesin-dependent FAT, including JNK (Morfini et al., 2006), and GSK-3 (Morfini, Szebenyi et

al., 2002) kinases. JNK phosphorylates kinesin heavy chains (KHCs), which inhibits kinesin-1 binding to microtubules and results in reduced anterograde FAT (Morfini et al., 2006). The effects of abnormal JNK activation can be blocked by SB203580 (Morfini et al., 2006), a pharmacological inhibitor that acts on JNK2/3 and other members of the stress-activated protein kinase (SAPK)/JNK family (Coffey et al., 2002; Morfini et al., 2006). To determine whether tau filaments inhibit anterograde FAT through a mechanism involving JNK activation, we co-perfused tau filaments with SB203580 (5 μM). Co-perfusion of tau filaments with SB203580 did not block the effect of tau filaments on FAT (Fig. 19c; different from soluble tau at $p \leq 0.001$), indicating this effect is independent of JNK and other SAPK/JNK kinases (i.e., p38s).

To evaluate whether tau filaments inhibit anterograde FAT through a mechanism involving GSK-3 activation, we co-perfused hTau40 filaments (2 μM) with cAMP response element-binding protein phosphopeptide (CREBpp; 0.5 mM). While many kinases phosphorylate intact CREB protein, the peptide fragment employed here (KRREILSRRPpSYR) is selectively phosphorylated by GSK-3, and therefore acts as a competitive inhibitor of other GSK-3 substrates (Q. M. Wang, Roach, & Fiol, 1994). Perfusion of CREBpp in squid axoplasm alone has no effect on FAT, although it effectively blocks the effects of active GSK-3 on kinesin-1-based motility (Morfini et al., 2004; Morfini, Szebenyi et al., 2002). Remarkably, co-perfusion of tau filaments and CREBpp blocked tau filament-induced effects on FAT (Fig. 19a), suggesting that the effects of the filaments are dependent on GSK-3 activation. To confirm that GSK-3 activity is required for tau filaments to inhibit kinesin-dependent FAT, we co-perfused tau filaments with the lithium mimetic ING-135 (100 nM), a highly specific inhibitor of GSK-3 (Kozikowski et al., 2007) (for the structure of this compound in complex with GSK-3β, see

**Figure 19. The effect of tau filaments is mediated by the activity of GSK-3.** Co-perfusion of hTau40 filaments with phospho-CREB peptide (0.5 mM), a competitive inhibitor of GSK-3, blocked the effects of hTau40 filaments on FAT (A). The inhibitory effect of tau filaments on FAT was also blocked by co-perfusion with another specific GSK-3 inhibitor, ING-135 (100 nM; B). SB203580 (5 μM), a stress-activated protein kinase inhibitor, did not prevent the effects of hTau40 filaments on FAT (C). Perfusion of any of these inhibitors alone showed no effect on FAT (data not shown).

**Figure 19**

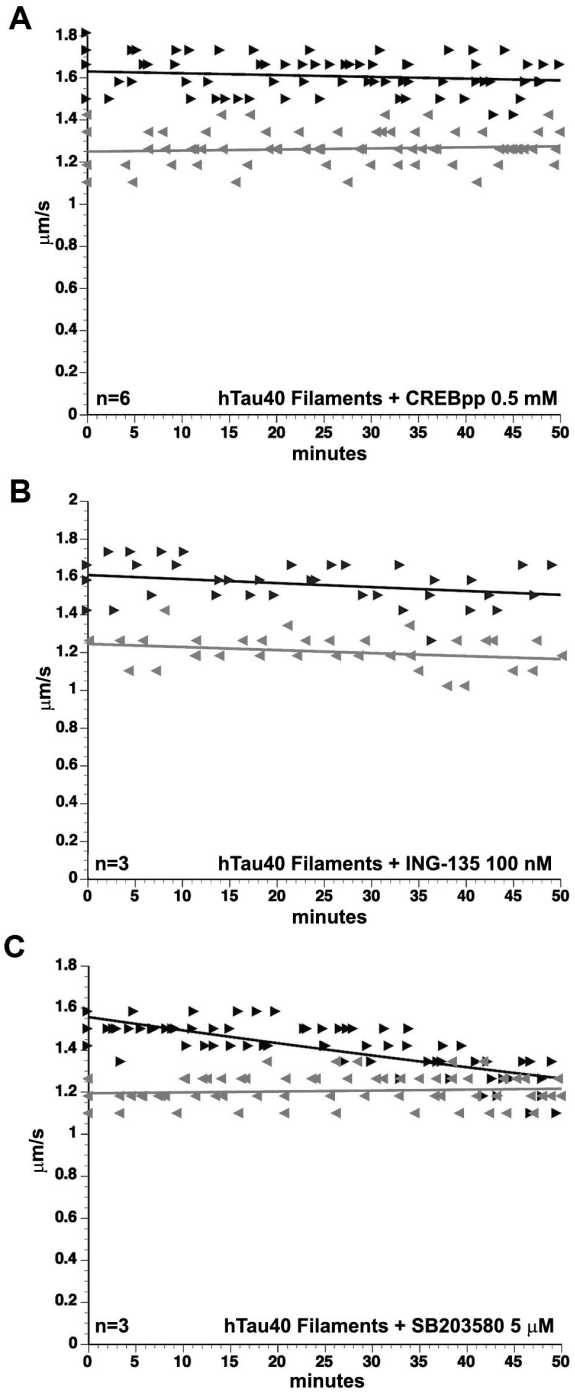
A
µm/s
n=6
hTau40 Filaments + CREBpp 0.5 mM
minutes
B
µm/s
n=3
hTau40 Filaments + ING-135 100 nM
minutes
C
µm/s
n=3
hTau40 Filaments + SB203580 5 µM
minutes

(Figure 23). As with CREBpp, co-perfusion with ING-135 blocked the effect of tau filaments (Fig. 19b), and perfusion of ING-135 alone had no effect on FAT (data not shown). Together, these results suggest that the effect of tau filaments on anterograde FAT involves activation of axonal GSK-3.

Phosphorylation of kinesin light chains (KLCs) by GSK-3 triggers the chaperone-dependent dissociation of kinesin-1 from its cargo (Morfini, Szebenyi et al., 2002; Pigino et al., 2003). To determine whether tau filaments induce the dissociation of kinesin-1 from cargo, we obtained "sister" axoplasms from individual animals and treated them with monomeric or filamentous hTau40 (2 μM). For comparison, we treated other axoplasm pairs with control buffer or with recombinant, active GSK-3β. After 40 min of incubation, we isolated axoplasmic vesicle fractions and evaluated kinesin-1 levels with an antibody against kinesin heavy chains (KHCs). Antibodies recognizing the synaptic integral membrane protein SNAP-25 served as a control for equal vesicle protein loading. The recovery of SNAP-25, kinesin-1 and dynein from vesicles was blocked by addition of 0.1% Triton X-100 to axoplasm homogenates prior to centrifugation, confirming the membranous nature of this fraction (not shown). Perfusion of either filamentous tau or active GSK-3β resulted in ≈50% decrease in the amount of kinesin-1 associated with vesicles relative to monomeric tau or control buffer, respectively ($p \leq 0.05$ for filamentous tau). In contrast, levels of dynein intermediate chain were unaffected (Fig. 20). These results demonstrate that both tau filaments and GSK-3 selectively inhibit anterograde FAT by leading to dissociation of conventional kinesin-1, but not dynein, from its transported vesicular cargo.

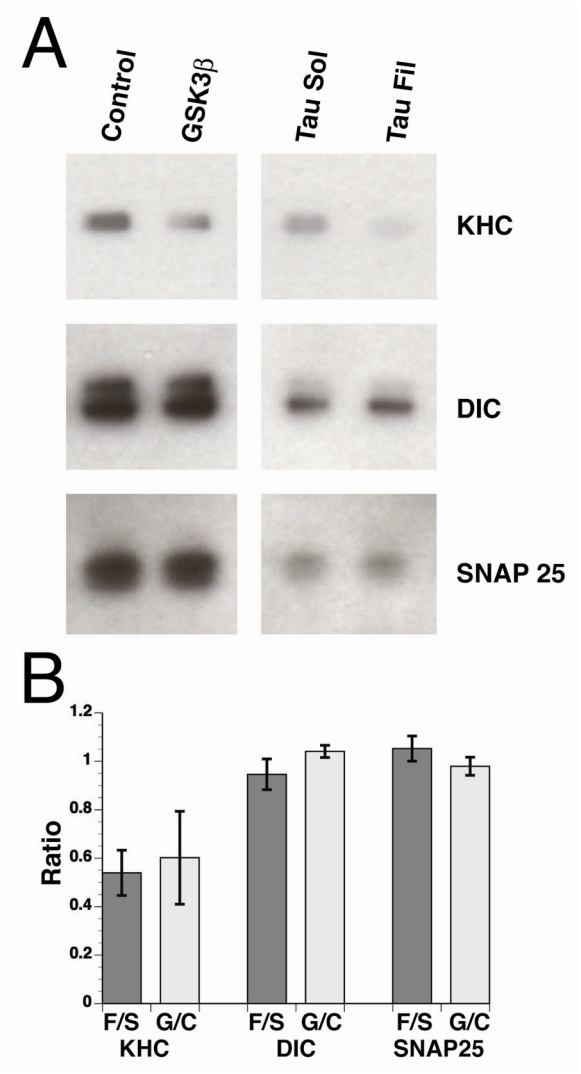


**Figure 20. Perfusion of active GSK-3β or filamentous tau induces kinesin-1 release from squid vesicle fractions.** (A) Purified vesicle fractions from individual axoplasms perfused with buffer control or active GSK-3β, and with soluble tau or filamentous tau were immunobloted for kinesin-1 heavy chain (KHC), dynein intermediate chain (DIC) and SNAP-25 antibodies. Note the dramatic reduction of kinesin-1 from membrane fractions of axoplasms perfused with GSK-3β and filamentous tau. B) Perfusion of active GSK-3β and filamentous tau reduces kinesin-1 membrane association by ≅ 50%. Membrane binding values of KHC, DIC and SNAP-25 are expressed as the ratio between axoplasms perfused with active GSK-3β over buffer control and fibrillar over soluble tau. Values were obtained by using the Image J software from NIH and represent the mean ± SEM from three independent experiments. The difference between soluble and filamentous tau was significant at $p \leq 0.05$ using a two sample t-test of $\mu 1$-$\mu 2$.

***PP1 activity mediates the inhibitory effect of tau filaments on FAT***

GSK-3 is inactive when phosphorylated (Q. M. Wang, Fiol, DePaoli-Roach, & Roach, 1994), and can be activated by axonal phosphatases (Morfini et al., 2004; Q. M. Wang, Fiol et al., 1994). This prompted us to evaluate whether the inhibitory effects of tau filaments involve the activity of axoplasmic phosphatases. To this end, we co-perfused axoplasm with tau filaments and okadaic acid (100 nM). Okadaic acid inhibits two major serine-threonine phosphatases, namely protein phosphatase 1 (PP1) and protein phosphatase 2A (PP2A). Concentrations of okadaic acid alone up to 1 μM have no effect on FAT (Bloom, Richards, Leopold, Ritchey, & Brady, 1993). Remarkably, okadaic acid blocked the effect of tau filaments on FAT (Fig. 21a), suggesting that tau filament-mediated inhibition of anterograde FAT involves the activity of a major serine-threonine phosphatase. To distinguish between PP1 and PP2A activity, we co-perfused filaments with 50 nM inhibitor-2 (I-2). I-2 selectively inhibits PP1, but has no effect on PP2A, even at micromolar concentrations (Cohen, 1991). When co-perfused with tau filaments, I-2 prevented FAT inhibition (Fig. 21b), suggesting that axonal PP1 activity mediates the effect of tau filaments on FAT.

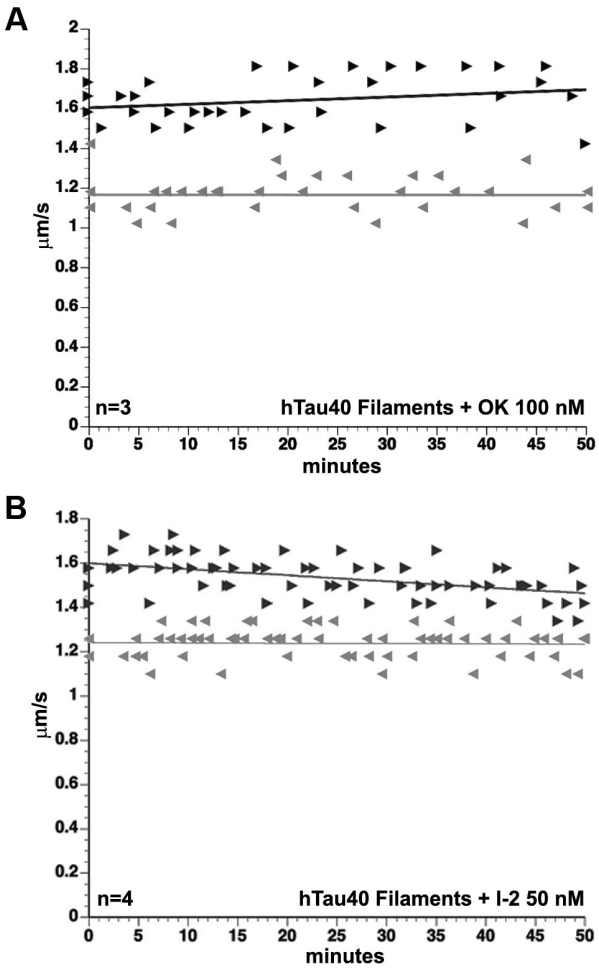


**Figure 21. The effect of tau filaments depends upon PP1 activity.** The inhibitory effect of tau filaments on FAT was blocked by co-perfusion with (A) the serine-threonine phosphatase inhibitor okadaic acid (100 nM), and (B) the PP1-specific inhibitor I-2 (50 nM). Perfusion of either of these inhibitors alone had no effect on FAT (data not shown).

# DISCUSSION

We have demonstrated that hTau40 filaments selectively impair anterograde FAT in isolated axoplasm, whereas monomeric hTau40 has no effect at the same concentration. Our results provide a novel link between tau aggregation and neuronal dysfunction, and identify a specific gain of function mechanism conferred by the aggregation process. Further, our studies suggest that inhibition of kinesin-1-based motility represents an important pathogenic event in AD and other tauopathies.

We have previously described a signaling pathway that regulates conventional kinesin-based motility. In this pathway, increased PP1 activity results in the dephosphorylation and activation of axonal GSK-3 (Morfini et al., 2004). Activated GSK-3 phosphorylates kinesin light chains (KLCs), prompting a chaperone-dependent dissociation of kinesin-1 and cargo (Morfini et al., 2004; Morfini, Szebenyi et al., 2002). Results presented here suggest that tau filaments inhibit anterograde FAT by triggering this pathway (Fig. 22). It is possible that tau filaments directly activate PP1 in this cascade, since tau reportedly binds to PP1 and stimulates its activity (Liao et al., 1998). However, more work is necessary to determine whether tau filaments act directly on PP1, or if additional intermediate components remain undiscovered. Additionally, some feedback from GSK-3 is conceivable, since GSK-3 is a major tau kinase that can also bind directly to tau (Sun et al., 2002), and is reported to be abnormally activated in AD (Ferrer et al., 2005).

We demonstrated that the inhibitory effect of tau filaments on FAT requires the extreme amino terminus of the protein. A pivotal role for this part of the protein is consistent with studies in other experimental systems. For example, overexpression of tau amino terminus induces cell death in cultured neurons through a mechanism involving abnormal kinase activity (Amadoro et

al., 2006; Amadoro et al., 2004), and expression of the N-terminus of tau induced microtubule disassembly in cells exposed to beta-amyloid (King et al., 2006). Immunological studies indicate that loss of the N-terminus is an early event in the maturation of tau fibrillar lesions in AD (Horowitz et al., 2004). Our results suggest that such cleavage events may

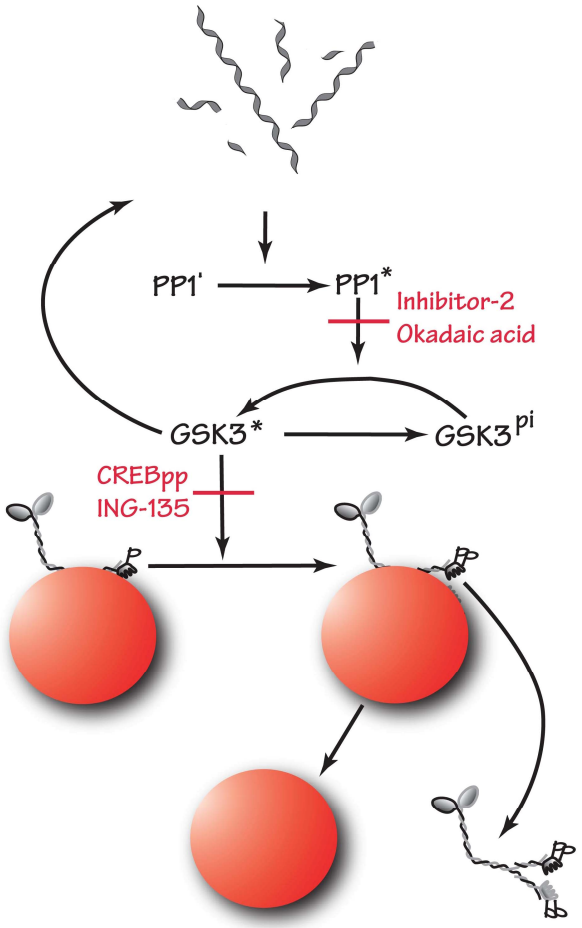


**Figure 22. Schematic of a potential mechanism underlying tau filament-induced inhibition of anterograde FAT.** Pharmacological experiments presented here indicate that FAT inhibition requires the activity of PP1 and GSK-3. We have previously described a pathway in which PP1 dephosphorylates and activates GSK-3, which subsequently phosphorylates kinesin light chains (KLCs). Phosphorylation of KLCs, promotes a chaperone-mediated detachment of kinesin-1 from its transported cargo. Our results suggest that tau can trigger this cascade when the amino terminus of tau is abnormally exposed in the filamentous form.

modulate the toxicity of filamentous tau  on FAT (I change this paragraph because with the new 6P/6D data, it is also conveivable (yet unlikely), that cleavage exacerbate the effect further. Regardless, it is better to play conservative on this until we know more).  The amino terminus is also the site of AD-related phosphorylation (G. Lee et al., 2004) and nitration (Reynolds, Lukas et al., 2006) events, and of the FTDP-17-associated mutations R5L (Poorkaj et al., 2002) and R5H (Hayashi et al., 2002).  Analysis of how these modifications influence the effects of tau filaments on FAT may provide further insights into disease progression.

Although hTau40 monomer had no effect on FAT at the concentrations tested, monomers of Tau6P and Tau6D inhibited anterograde FAT as effectively as hTau40 filaments.  This result demonstrates that the N-terminus of tau is sufficient to produce the observed effects on FAT, since these isoforms lack the MTBR region and the C-terminal tail of canonical tau. Additionally, it raises the question of why hTau40 monomer failed to show the same inhibitory effect, even though it contains an intact amino terminus.  Although monomeric hTau40 was first thought to exist in an extended conformation (Schweers et al., 1994; Syme et al., 2002), recent evidence suggests that tau in solution adopts a globally folded conformation in which the N-terminus folds in close proximity to the C-terminus (Horowitz et al., 2006; Jeganathan et al., 2006).  It is possible that this conformation shields the extreme amino terminus, thus preventing hTau40 monomer from inhibiting FAT.  In this scenario, polymerization would freeze hTau40 in a different conformation in which the N-terminus is exposed.

With these results, tau joins a growing list of proteins whose pathogenic forms alter regulatory pathways for FAT.  Like tau filaments, AD-associated mutations in presenilin-1 inhibit kinesin-1-based motility through GSK-3 activation (Pigino et al., 2003), whereas pathogenic forms of androgen receptor and huntingtin inhibit kinesin-1 dependent transport

through JNK activation (Morfini et al., 2006). The current study suggests that AD represents an example of a dysferopathy, where alterations in FAT lead to a dying back neuropathy (Morfini, Pigino, Opalach et al., 2007), providing further evidence that alterations in regulatory pathways for FAT represent a common pathogenic event in multiple, otherwise apparently unrelated neurodegenerative diseases (Morfini, Pigino et al., 2002; Morfini, Pigino, & Brady, 2005).

## ACKNOWLEDGEMENT

Gerardo Morfini, Gustavo Pigino, Irina N. Gaisina, Alan P. Kozikowski, Lester I. Binder, and Scott T. Brady co-authored this manuscript. The authors would like to thank Natalia Marangoni, Sarah Pollema, Kelly Monk and Hannah Brown for assistance with axoplasm experiments, and Dr. Athena Andreadis for the Tau6P and Tau6D constructs. Special thanks to Dr. Angela Guillozet-Bongaarts for a critical reading of the manuscript. Research supported by NIH awards NS049834 (N.E.L.), AG14453 (L.I.B.), NINDS grants NS23868, NS23320, NS41170 and NS43408 (S.B.), MDA (S.B.), ALSA (G.M, S.B), and HDSA (G.M.).

**SUPPLEMENTAL MATERIAL**

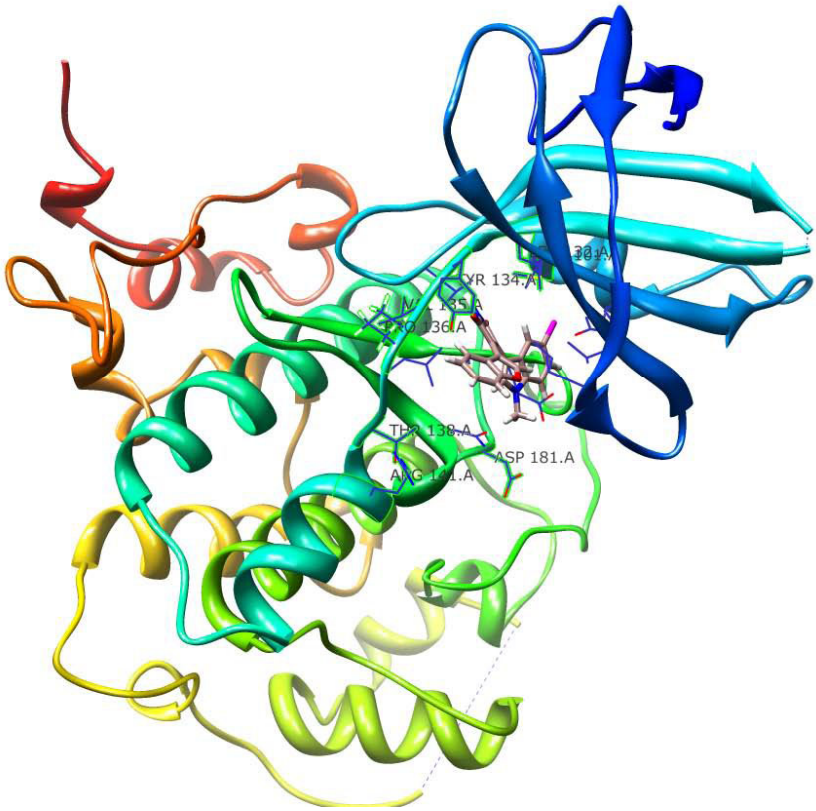


**Figure 23. Rendering of 5-ING-135 in complex with GSK-3β.** This complex structure was generated from the available x-ray structure of the protein co-crystallized with staurosporine (PDB:1Q3D) with docking of the inhibitor performed using Molegro Virtual Docker program.

# CHAPTER FIVE

# DISCUSSION

The work presented in this dissertation represents a significant advance in the study of tau in neurodegeneration, especially regarding the role of the amino terminus. Although the amino terminus has traditionally been regarded as a factor that promotes filament formation, we demonstrate that it can also inhibit this process, likely by stabilizing tau in a soluble conformation. Polymerization of full-length tau is inhibited when an excess of amino terminus is added to the reaction mixture, either in the form of recombinant N-terminal tau constructs or as the short, naturally occurring 6D and 6P isoforms. We show that this inhibitory effect requires sequences in the amino (18-42) and carboxy (391-421) termini of the protein, a result consistent with a published model of soluble tau conformation (Jeganathan et al., 2006), in which the amino terminus and the carboxy terminus of the protein are in close proximity.

We also demonstrate that the amino terminus of tau can trigger a signaling cascade resulting in the phosphorylation of kinesin light chains and the inhibition of anterograde microtubule-dependent transport. This effect is present in soluble 6D and 6P tau isoforms, which lack the C-terminal half of canonical tau, but is absent from the soluble full-length (hTau40) monomer. The folded conformation described above may explain why soluble full-length tau had no effect on transport in this system. In contrast, full-length tau triggered the inhibition of kinesin-dependent transport when in filamentous form, suggesting that filament formation locks canonical tau in a conformation in which the N-terminus is perhaps more accessible. Collectively, this dissertation suggests that the toxic effects of tau filaments result when the amino terminus is repositioned during polymerization.

Our results demonstrate that the amino terminus of tau can have beneficial or toxic effects, depending on its context and/or modification. A similarly dichotomous role for the amino terminus was discovered in cell culture work performed by Amadoro et al. In their

studies, expression of a tau construct consisting of the amino terminus and the beginning of the proline-rich region (a.a. 1-230) promoted neuronal survival in the face of pro-apoptotic stimuli (Amadoro et al., 2004). However, shorter tau constructs representing the amino terminus only (a.a. 1-44) triggered calpain activation and cell death (Amadoro et al., 2006; Amadoro et al., 2004). The mechanism at work in each case is incompletely understood, but the evidence suggests that the two constructs triggered different downstream signaling effects. Interestingly, the protective tau construct (1-230) bears some resemblance to the 6D/6P tau isoforms. Like filamentous tau, these short isoforms inhibited kinesin-dependent transport in isolated axoplasm, an effect that contrasts with the protective effects of the 1-230 construct in cell culture. There are some differences between the short tau isoforms and the 1-230 construct; the construct used by Amadoro et al. is almost a hundred amino acids longer than the 6D/6P isoforms, and the 6D/6P isoforms have a short amino acid sequence at their C-terminus that does not occur in canonical tau. However, the high degree of similarity is intriguing in light of their apparently opposite effects on neuronal survival. These results indicate that even outside the context of a filament, the regulation of interactions between the N-terminus and signaling proteins is a complicated affair.

Our work not only reveals a novel role for the amino terminus in the regulation of filament formation, but highlights the consequences of aggregation by demonstrating that filament formation ”unmasks” the amino terminus of the tau protein. The following sections will provide a synthesis suggested by the results presented in this dissertation, and clarify future research directions.

## IMPLICATIONS FOR FILAMENT TOXICITY

The precise relationship between tau aggregation and neuronal cell death remains a matter of debate, in part because of a lack of mechanistic links between the two. In Chapter Four, we demonstrate that tau filament formation inhibits kinesin-dependent transport. This effect is likely relevant to the pathogenesis of AD, because AD neurons exhibit changes consistent with disruptions in intracellular transport. These include morphological changes like synapse loss, the appearance of neuritic varicosities, and the "dying back" of the dentritic arbor (E. Braak et al., 1994; Hall, Lee, Lee, & Yao, 2001; Terry, 1998), as well as functional changes at synapses and the mislocalization of membrane bound organelles (reviewed in (Morfini, Pigino et al., 2002)). Disruption of transport may also increase the vulnerability of neuronal processes to oxidative stress (Stamer et al., 2002), and interfere with the transport of materials necessary for neuronal survival (reviewed in (Morfini, Pigino et al., 2002)). Impaired anterograde transport in one neuron may contribute to dysfunction in connected neurons by interfering with the transport of material to the presynaptic terminal, and hence proper firing. Cells connected to neurons containing filamentous tau might then receive a reduced level of input, which could result in synapse loss and cellular dysfunction. If aberrant signaling in turn triggers tau aggregation, the pathological cycle would begin again. This mechanism may help explain the spread of tau pathology in AD described by Mesulam and colleagues, in which the sequential appearance of filamentous tau pathology in different brain areas follows pathways of synaptic connectivity (Mesulam, 1999).

Soluble canonical tau has no effect on transport in isolated axoplasm, suggesting that filament formation results in a toxic gain-of-function. The inability of soluble canonical tau to inhibit transport suggests that the amino terminus, which is necessary for the effect on transport, is inaccessible when the protein is in monomeric form. According to the model presented in

Chapter Two, the amino terminus is shielded by the carboxy terminus in soluble canonical tau monomer. However, once tau assembles into filaments, the amino terminus becomes capable of triggering a signaling cascade that results in phosphorylation of kinesin light chains and the inhibition of anterograde microtubule-dependent transport. In contrast to canonical tau, monomers of the tau isoforms 6D and 6P inhibit axonal transport. These isoforms lack most of the proline rich region, the MTBR region, and the C-terminal tail of canonical tau, and the resulting accessibility of the amino terminus may explain their effects in the axoplasm. These results suggest that tau filament toxicity arises from the repositioning of the amino terminus during polymerization (Fig. 24).

The amino terminus of tau has been implicated in several other signaling cascades (Amadoro et al., 2006; Amadoro et al., 2004; Hwang et al., 1996), including the response to beta-amyloid (Barbato et al., 2005; King et al., 2006). Our results suggest that the conformational rearrangement of tau that accompanies filament formation may alter the way in which the amino terminus interacts with components of these pathways. The resulting changes may represent other avenues by which filamentous tau leads to neurodegeneration.

In recent years several studies have looked at the consequences of tau aggregation in cultured cells. However, because full-length tau does not aggregate readily under physiological conditions, some authors have used tau constructs representing only the MTBR region of the protein (Khlistunova et al., 2006; Y. P. Wang et al., 2007). Our results suggest that studies using tau constructs that do not represent the entire protein risk overlooking potentially important effects of filament formation.

It has been estimated that neurons bearing NFT may survive for years (H. Braak, 1996; Angela L. Guillozet-Bongaarts et al., 2006), and it is difficult to reconcile that longevity with the

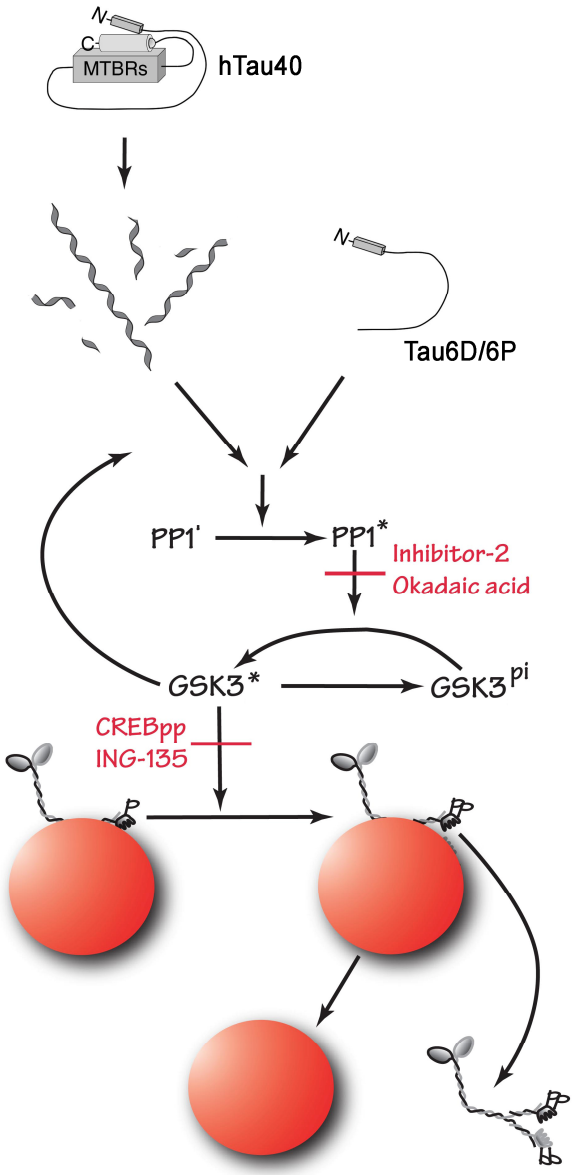


**Figure 24. Filament toxicity may result from the unmasking of the amino terminus.** Our model suggests that when full-length tau (hTau40) is soluble, the N- and C-termini of the protein are in close proximity. The amino terminus becomes capable of triggering the disruption of anterograde transport when hTau40 is in a filamentous state, suggesting that the conformational changes that accompany filament formation make that portion of the protein more accessable. In contrast, Tau 6D and 6P isoforms, which lack the C-terminal half of the protein, can trigger transport disruption when in soluble form.

acute effects of tau filaments observed in isolated axoplasm. However, tau in NFT and other fibrillar aggregates undergoes a series of modifications during the course of AD, including truncation and phosphorylation events (reviewed in (Binder et al., 2005)), and it is possible that some of these modifications block the effects of the filaments on axonal transport. For instance, we demonstrated that removal of the crucial 2-18 amino sequence abolished the transport toxicity. In AD, removal of the amino terminus is an early event (Binder et al., 2005; Horowitz et al., 2004), which may be effected by caspases (Horowitz et al., 2004) or by the aminopeptidase PSA (Sengupta et al., 2006). This part of tau is also subject to phosphorylation (G. Lee et al., 2004) and nitration events ((Reynolds, Reyes et al., 2006) and Reyes et al., in preparation) events. It will be interesting to determine whether these changes prevent tau filaments from inhibiting microtubule-dependent transport.

**TAU OLIGOMERS AS A TOXIC SPECIES**

Our results indicate that tau filaments inhibit microtubule-dependent transport, a process that is crucial to proper neuronal function and survival. However, the possibility exists that the filamentous tau mixture used in these experiments contained other aggregated tau species, such as tau oligomers. The structure of tau oligomers is unknown, and it is possible that the accessibility of the N-terminus in these aggregates is different than in filaments. Our experiments were not designed to differentiate tau filaments from other aggregated species. However, the fact remains that tau incubated with AA produced an effect on transport that was not present with tau or AA alone. AA induces a conformational change in tau that promotes tau aggregation and filament formation (reviewed in (Carlson et al., 2007; T. C. Gamblin, R. W.

Berry et al., 2003; Kuret et al., 2005)), so, at the very least, a pathological conformational change in tau would appear to be responsible for the effects of the polymerization mixture on transport.

There is reason to suspect that tau oligomers may have a hand in neurodegeneration. In a Drosophila model of tauopathy, observations of toxicity in the absence of detectable neurofibrillary pathology support the existence of a toxic oligomeric tau species (Wittmann et al., 2001). However, short tau filaments may have escaped detection in this system. Additionally, the appearance of an oligomeric tau species correlated with functional deficits and memory loss in two mouse models of tauopathy (Berger et al., 2007). Oligomers have been implicated as toxic species in other neurodegenerative diseases (reviewed in (Caughey & Lansbury, 2003)), and tau oligomers have been detected in human AD (Berger et al., 2007; Maeda et al., 2007; Maeda et al., 2006) and FTDP-17 tissue (Berger et al., 2007).

It may be possible to design experiments to compare the effects of tau filaments and oligomers in isolated axoplasm, although there are challenges. Recent experiments by Carlson et al. demonstrate that tau polymerization can be driven toward the formation of small aggregates or extended filaments by adjusting the ratio of tau to AA (Carlson et al., 2007). While it is not certain if these small tau aggregates are identical to the oligomers isolated from diseased brain tissue, it may be relevant to test their effects in axoplasm. An alternative approach is to use ultracentrifugation to separate the polymerization mixture into a supernatant containing monomer and small oligomers, and a filamentous pellet, and then to examine the effects of each fraction on axoplasmic transport. This approach would require extensive optimization. Biochemical analysis would be needed to verify that oligomers were formed and remained in the

supernatant fraction, and that filaments in the pellet did not depolymerize when resuspended following centrifugation.

That said, the toxic tau species may be tau filaments containing full-length tau. Our NFT evolution studies have demonstrated that tau filaments are altered nearly simultaneously with tangle coelescence in neurons *in situ*, losing both their amino and carboxy termini (Horowitz et al., 2004), which may reconcile the longevity of these neurons with our results. Furthermore, many of the neuropil threads (pathological neurites filled with tau filaments) are likely made of full length tau as antibodies recognizing the amino and carboxy termini of tau often stain these structures in human brain.

**THE ROLE OF THE N-TERMINUS IN FILAMENT FORMATION**

In combination with earlier results, a more complex picture of the role of the amino terminus in filament formation is beginning to emerge. The conformation-dependent antibody Alz-50 recognizes a discontinuous epitope comprising residues in the extreme amino terminus and the MTBR region. The affinity of this antibody is nearly 100–fold higher for filaments than for monomeric tau, indicating that polymerization brings these two regions into close proximity (Carmel et al., 1996). This fact, in combination with the observation that Alz-50 recognizes prefibrillar tau pathology (Garcia-Sierra et al., 2003; Hyman et al., 1988), led to the hypothesis that folding of the N-terminus over the MTBRs is one of the earliest events in filament formation. Further evidence of the importance of the amino terminus comes from a comparative study of the assembly capabilities of the six canonical tau isoforms, where those lacking the alternatively-spliced N-terminal exons 2 and 3 exhibited impaired ability to form elongated filaments (King et al., 2000). Finally, subsequent *in vitro* analysis of recombinant tau protein

revealed that removal of the N-terminal portion of the Alz-50 epitope, a.a. 2-18, dramatically reduced the ability of tau to polymerize (T.C. Gamblin et al., 2003).

The results presented in Chapter Two add an additional layer of complexity to the involvement of the amino terminus in filament formation. We demonstrate that the amino terminus inhibits polymerization of full-length tau when present in excess. Our data indicate that the amino terminus acts by stabilizing full-length tau in a soluble conformation, and suggest that the two ends of the protein are in close proximity when tau is in solution. Although this model of soluble tau is supported by FRET analysis (Jeganathan et al., 2006), other data suggests that this conformation is only present a portion of the time, and that tau in solution switches rapidly between a number of possible conformations (reviewed in (E. Mandelkow, von Bergen, Biernat, & Mandelkow, 2007)). This may explain the relatively high concentration of excess N-terminus required to inhibit filament formation. Clearly, much work remains before the conformational state of soluble tau is fully understood.

## POSTTRANSLATIONAL MODIFICATIONS AND THE AMINO TERMINUS

The results presented in this dissertation demonstrate that posttranslational modifications can modulate the beneficial effects of the N-terminus, as well as the negative effects. For instance, we demonstrate that posttranslational modifications in the amino and carboxy termini alter the ability of 6D/6P isoforms to inhibit filament formation, and show that truncation of the amino terminus abolishes the effects of tau filaments on axonal transport. Our results also suggest that modifications that encourage tau to adopt a filamentous conformation are potentially toxic to the cell, because they unmask the amino terminus. Isolated axoplasm is an ideal

experimental system in which to determine whether a particular posttranslational modification produces a toxic conformation of monomeric tau, or alters the toxicity of tau filaments.

Nitration is one potential modification that may affect the properties of the amino terminus. The amino terminus contains two of the five nitration sites in tau, and nitration at any of the sites in tau inhibits filament formation. Nitration also increases the affinity of the Alz-50 antibody for tau; this result is somewhat counterintuitive, given that adoption of the Alz-50 conformation is regarded as an initial step in filament formation, and nitration inhibits polymerization (Reynolds et al., 2005b). Other factors that modify tau structure include phosphorylation (reviewed in (Brandt et al., 2005)), the prolyl isomerase Pin1 (reviewed in (Balastik, Lim, Pastorino, & Lu, 2007), caspase cleavage (R. W. Berry et al., 2003; T. C. Gamblin, F. Chen et al., 2003), and glycosylation (reviewed in (Brandt et al., 2005)). Examining the effects of these changes may provide further insights into the role of the amino terminus in tauopathies.

## ISOFORM-SPECIFIC DIFFERENCES IN TAU STRUCTURE AND FUNCTION

The six canonical isoforms of tau have different conformational properties apparent in their ability to form filaments and to interact with microtubules. Isoforms lacking N-terminal exons 2 and 3 fail to form elongated filaments in the presence of arachidonic acid, and polymerization is also impaired in isoforms lacking exon 10 (King et al., 2000). Tau also shows isoform-specific differences in microtubule binding; the contribution made by the individual MTBRs, the inter-repeat regions, and the flanking regions vary according to whether tau has

three or four repeats. This suggests that there are isoform-specific differences in the conformations adopted by tau on the microtubule surface (Goode et al., 2000).

Our study of the 6D and 6P isoforms reveals additional complexity in the relationship between tau isoforms and function. These isoforms do not contain the MTBR region or the C-terminal tail of the canonical tau isoforms. As a result, the amino terminus of the 6D and 6P isoforms lacks two potential intramolecular interacting sites. Possibly due to the resulting accessibility of the amino terminus, these isoforms trigger the inhibition of kinesin-dependent transport in monomeric form, unlike canonical tau. The unique structure of 6D and 6P may result in additional signaling capabilities not available to canonical tau isoforms under normal physiological conditions.

The ability of the N-terminus to inhibit tau filament formation may be affected by alternative splicing. The results described in Chapter Three indicate that the effectiveness of the 6D isoforms is decreased when exons 2 and 3 are absent. However, that effect was not observed for the 6P isoforms, or for the N-terminal tau fragments described in Chapter Two. We did not examine whether the presence of exons 2, 3, and 10 in full-length tau influence the ability of the N-terminus to inhibit polymerization. This represents a potential area of exploration for future experiments.

## TAU 6D AND 6P ISOFORMS: POTENTIAL ROLES AND REGULATION

The results presented in Chapter Three indicate that the 6D and 6P isoforms have the potential to inhibit tau filament formation. This result is especially intriguing in light of the expression pattern of the 6D variant in human brain. Luo et al. found that 6D levels are highest in the cerebellum, which is relatively protected from the development of filamentous tau

pathology in AD. Conversely, 6D expression is low in areas prone to developing tau pathology, including the cerebral cortex and hippocampus. Furthermore, in AD brain immunoreactivity to a 6D antibody did not colocalize with markers of filamentous tau pathology on a cell-by-cell basis (Luo et al., 2004).

When this immunohistochemical data is looked at in combination with our *in vitro* results, it is tempting to suggest that expression of 6D and 6P isoforms may protect neurons from developing filamentous tau pathology. However, these isoforms are present at low levels relative to canonical tau isoforms (Leroy et al., 2006; Luo et al., 2004; Wei & Andreadis, 1998), and our work indicates that a two-fold excess of these isoforms is required to see appreciable inhibition *in vitro* (Chapters Two and Three).

Further work is necessary to determine whether 6D and 6P isoforms act as endogenous regulators of filament formation. It would be interesting to study these isoforms in a cell culture system that exhibits tau aggregation, such as the one described by Fath et al. (Fath et al., 2002). However, that particular model uses tau constructs carrying a number of pseudophosphorylation mutations, which could potentially disrupt the effects of the 6D/6P isoforms. It would also be interesting to determine whether expression of these short isoforms can inhibit tau aggregation in a transgenic animal model of tauopathy. Additionally, an in-depth immunohistochemical study of the expression of 6D and and 6P isoforms in the context of tau pathology in AD is indicated. Analysis of how levels of these isoforms change during AD progression, as well as their colocalization with markers of NFT maturity (i.e. early vs. late), may provide further insight into their involvement in disease.

**Regulation of 6D and 6P**

As the results presented in Chapter Four demonstrate, 6D and 6P inhibit kinesin-dependent transport, and this ability may result from the innate accessibility of the amino terminus in these isoforms. The amino terminus of tau is potentially involved in many aspects of neuronal function. This portion of the protein can promote cell survival in the presence of proapoptotic stimuli (Amadoro et al., 2004), or trigger cell death through a mechanism involving the activation of N-methyl-D-aspartate (NMDA) receptors and calpain (Amadoro et al., 2006; Amadoro et al., 2004). The amino terminus is also implicated in the response to beta-amlyoid (Barbato et al., 2005; King et al., 2006), and is necessary for the association of tau with the neural plasma membrane (Brandt et al., 1995; Maas et al., 2000), where it is potentially involved in signaling cascades (Hwang et al., 1996). While the amino terminus of canonical tau may be inaccessible part of the time, and so unable to participate in these cellular functions, the 6D and 6P isoforms may be constitutively active. As a result, 6D and 6P isoforms may be simultaneously very useful to the cell, and very dangerous. If these isoforms are expressed in healthy cells despite their toxic potential, there must be regulatory mechanisms in place.

It seems probable that posttranslational modifications of 6D/6P isoforms regulate their cellular activity. These isoforms can potentially be phosphorylated by serine/threonine kinases as well as tyrosine kinases, and are also targets for tyrosine nitration. It will be interesting to determine if these modifications affect the ability of the 6D and 6P isoforms to trigger the inhibition of axonal transport.

A second likely regulatory mechanism occurs at the level of protein expression. Alternative splicing of exon 6 is governed by a number of complex factors (Wei & Andreadis, 1998), and the low levels of these isoforms in adult brain suggests that their production is tightly regulated (Luo et al., 2004; Wei & Andreadis, 1998). The expression of at least one of these

isoforms (6D) is developmentally regulated, with levels falling in adulthood (Luo et al., 2004), further suggesting that alternative splicing of exon 6 is finely tuned. Finally, the pattern of exon 6 splicing is upset in myotonic dystrophy type 1, implying that disruption of normal regulation can contribute to neurodegeneration.

## PHYSIOLOGICAL ROLES FOR THE FILAMENTOUS CONFORMATION

### Regulation of microtubule-dependent transport

The cell uses several signaling cascades to regulate microtubule-dependent transport of cellular material. Components of those pathways that inhibit kinesin are localized at sites requiring targeted cargo delivery, such as growth cones (Morfini et al., 2004). One question raised by our results is whether the effects of filamentous tau in the axon represent a toxic gain-of-function that is purely pathological, or if tau regularly plays a part in the regulation of kinesin-dependent transport. The fact that full-length tau monomer had no effect in the axoplasm suggests that it must be modified in some way in order to take part in transport regulation under nonpathological conditions. Perhaps some of the posttranslational changes that induce a filamentous conformation in tau may be involved. It will be interesting to see if such modifications cause tau monomer to recapitulate the effects of tau filaments in the axon.

### Microtubule binding

Another area in which a filamentous conformation may play a role in physiological tau function is tau-microtubule binding. As covered in Chapter One, research suggests that tau adopts an induced fit conformation when it binds to the microtubule surface. Several lines of evidence suggest that this conformation shares features with the conformation that tau adopts in

filaments. For instance, the same regions flanking the MTBRs that come together to strengthen tau-microtubule binding (Gustke et al., 1994) make up the epitope of the conformation-specific antibody SM134, which recognizes fibrillar tau pathology in AD (Lichtenberg-Kraag et al., 1992). In addition, the MTBR region exhibits similar conformational shifts when it interacts with tubulin as it does in the presence of heparin (Marx et al., 2006). Furthermore, certain phosphorylation events that prevent tau from binding to microtubules also prevent filament formation, even though they lie outside of the MTBR region (Schneider et al., 1999). Finally, the microtubule surface can support the formation of tau oligomers (Makrides et al., 2003), further suggesting a relationship between microtubule binding and a filamentous tau conformation.

**Tau conformation and PLCγ**

Tau may adopt a filamentous conformation in order to interact with certain other cellular proteins. A potential example of this is the interaction of tau with the gamma isoform of phospholipase C (PLCγ) at the neural plasma membrane. Tau binds directly to PLCγ, likely through the interaction of it src homology 3 (SH3) domain with a sequence in the proline-rich region of tau ($^{233}$PKSP$^{236}$) (Hwang et al., 1996; G. Lee et al., 1998).

The hydrolysis of phosphatidylinositol 4,5-bisphosphate ($PIP_2$) by PLC produces the intracellular messengers inositol 1,4,5-trisphosphate ($IP_3$) and diacylglycerol. As such, it is an important step in a number of signaling cascades (Noh, Shin, & Rhee, 1995). PLCγ activity toward $PIP_2$ is slightly increased in the presence of tau. However, when AA is present tau increases the activity of PLCγ activity toward $PIP_2$ nearly 10–fold. In contrast, AA has no effect on PLCγ activity in the absence of tau (Hwang et al., 1996). Hwang et al. suggest that this

synergistic effect arises when tau and AA bind to PLCγ simultaneously, although it is not known whether AA binds to PLCγ (Hwang et al., 1996). However, the fact that AA has no effect on PLCγ activity in the absence of tau argues against this hypothesis.

It seems more likely that the synergistic effect is due to the interaction between tau and AA. AA induces a conformational change in tau causing it to adopt the Alz-50 conformation, which is associated with filament formation (reviewed in (Carlson et al., 2007; T. C. Gamblin, R. W. Berry et al., 2003; Kuret et al., 2005)). It is possible that tau in this "filamentous" conformation has an enhanced ability to bind to and/or stimulate PLCγ. In support of this hypothesis, other unsaturated fatty acids that induce tau polymerization also enhanced tau's effect on PLCγ activity, but saturated fatty acids, which are poor polymerization inducers, were not effective (Hwang et al., 1996; D. M. Wilson & Binder, 1997). If filamentous tau is indeed more capable of triggering PLCγ, this may represent a signaling mechanism that is disrupted in tauopathies, where cells contain high levels of filamentous tau.

Tau interacts with the SH3 domain of PLCγ, and our interpretation of the preceding results suggests that the affinity of tau for SH3 domains may be increased when tau adopts a "filamentous" conformation (i.e. Alz-50). There is some evidence in the literature that tau conformation influences its interaction with SH3 domains. A study by Bhaskar et al. found that the interaction between tau and the SH3 domain of the non-receptor tyrosine kinase fyn was affected by changes at sites in tau far removed from the PXXP interacting sequence, and suggested that conformational changes might be involved (Bhaskar et al., 2005). The idea that conformational changes induced by AA affect this interaction would be relatively simple to test, and may reveal an important principle of tau-SH3 domain interactions and another potential physiological role for a "filamentous" tau conformation.

## SUMMARY

This dissertation highlights the relationship between tau structure and function. We present evidence that the amino terminus is associated with the carboxy terminus when tau is in solution, and that the transition from soluble monomer to filament unmasks of this portion of the protein. We also demonstrate the consequences of this conformational rearrangement for kinesin-dependent transport, a cellular process critical for neuronal survival. Therefore this work represents a mechanism by which filament formation may lead to neurodegeneration in tauopathies. We also examine the roles of tau 6D and 6P isoforms in the context of filament formation and transport toxicity, and our results shed light on these little-studied tau isoforms. Collectively, the work presented in this dissertation represents a significant contribution to the tau field.

## REFERENCES


Abraha, A., Ghoshal, N., Gamblin, T. C., Cryns, V., Berry, R. W., Kuret, J., et al. (2000). C-terminal inhibition of tau assembly in vitro and in Alzheimer's disease. *J Cell Sci*, *113*, 3737-3745.

Alonso, A., Zaidi, T., Novak, M., Grundke-Iqbal, I., & Iqbal, K. (2001, Jun 5). Hyperphosphorylation induces self-assembly of tau into tangles of paired helical filaments/straight filaments. *Proc Natl Acad Sci U S A*, *98*(12), 6923-6928.

Amadoro, G., Ciotti, M. T., Costanzi, M., Cestari, V., Calissano, P., & Canu, N. (2006, Feb 21). NMDA receptor mediates tau-induced neurotoxicity by calpain and ERK/MAPK activation. *Proc Natl Acad Sci U S A*, *103*(8), 2892-2897.

Amadoro, G., Serafino, A. L., Barbato, C., Ciotti, M. T., Sacco, A., Calissano, P., et al. (2004, Feb). Role of N-terminal tau domain integrity on the survival of cerebellar granule neurons. *Cell Death Differ*, *11*(2), 217-230.

Amos, L. A., & Schlieper, D. (2005). Microtubules and maps. *Adv Protein Chem*, *71*, 257-298.

Andreadis, A. (2005, Jan 3). Tau gene alternative splicing: expression patterns, regulation and modulation of function in normal brain and neurodegenerative diseases. *Biochim Biophys Acta*, *1739*(2-3), 91-103.

Arriagada, P. V., Growdon, J. H., Hedley-Whyte, E. T., & Hyman, B. T. (1992). Neurofibrillary tangles but not senile plaques parallel duration and severity of Alzheimer's disease. *Neurology*, *42*(3 Pt 1), 631-639.

Arriagada, P. V., Marzloff, K., & Hyman, B. T. (1992, Sep). Distribution of Alzheimer-type pathologic changes in nondemented elderly individuals matches the pattern in Alzheimer's disease. *Neurology*, *42*(9), 1681-1688.

Augustinack, J. C., Schneider, A., Mandelkow, E. M., & Hyman, B. T. (2002, Jan). Specific tau phosphorylation sites correlate with severity of neuronal cytopathology in Alzheimer's disease. *Acta Neuropathol (Berl)*, *103*(1), 26-35.

Balastik, M., Lim, J., Pastorino, L., & Lu, K. P. (2007, Apr). Pin1 in Alzheimer's disease: multiple substrates, one regulatory mechanism? *Biochim Biophys Acta*, *1772*(4), 422-429.

Ballatore, C., Lee, V. M., & Trojanowski, J. Q. (2007, Sep). Tau-mediated neurodegeneration in Alzheimer's disease and related disorders. *Nat Rev Neurosci*, *8*(9), 663-672.

Bandyopadhyay, B., Li, G., Yin, H., & Kuret, J. (2007, Jun 1). Tau aggregation and toxicity in a cell culture model of tauopathy. *J Biol Chem*, *282*(22), 16454-16464.

Barbato, C., Canu, N., Zambrano, N., Serafino, A., Minopoli, G., Ciotti, M. T., et al. (2005, Mar). Interaction of Tau with Fe65 links tau to APP. *Neurobiol Dis*, *18*(2), 399-408.

Barghorn, S., Davies, P., & Mandelkow, E. (2004). Tau paired helical filaments from Alzheimer's disease brain and assembled in vitro are based on beta-structure in the core domain. *Biochemistry*, *43*(6), 1694-1703.

Barghorn, S., & Mandelkow, E. (2002, Dec 17). Toward a unified scheme for the aggregation of tau into Alzheimer paired helical filaments. *Biochemistry*, *41*(50), 14885-14896.

Barghorn, S., Zheng-Fischhofer, Q., Ackmann, M., Biernat, J., von Bergen, M., & Mandelkow, E. (2000). Structure, microtubule interactions, and paired helical filament aggregation by tau mutants of frontotemporal dementias. *Biochemistry*, *39*(38), 11714-11721.

Bell, K. F., & Claudio Cuello, A. (2006, Sep 1). Altered synaptic function in Alzheimer's disease. *Eur J Pharmacol*, *545*(1), 11-21.

Berger, Z., Roder, H., Hanna, A., Carlson, A., Rangachari, V., Yue, M., et al. (2007, Apr 4). Accumulation of pathological tau species and memory loss in a conditional model of tauopathy. *J Neurosci*, *27*(14), 3650-3662.

Berry, R. W., Abraha, A., Lagalwar, S., LaPointe, N., Gamblin, T. C., Cryns, V. L., et al. (2003, Jul 15). Inhibition of tau polymerization by its carboxy-terminal caspase cleavage fragment. *Biochemistry*, *42*(27), 8325-8331.

Berry, R. W., Quinn, B., Johnson, N., Cochran, E. J., Ghoshal, N., & Binder, L. I. (2001). Pathological glial tau accumulations in neurodegenerative disease: review and case report. *Neurochem Int*, *39*(5-6), 469-479.

Berry, R. W., Sweet, A. P., Clark, F. A., Lagalwar, S., Lapin, B. R., Wang, T., et al. (2004). Tau epitope display in progressive supranuclear palsy and corticobasal degeneration. *J Neurocytology*, *33*, 287-295.

Bhaskar, K., Yen, S. H., & Lee, G. (2005, Oct 21). Disease-related modifications in tau affect the interaction between Fyn and Tau. *J Biol Chem*, *280*(42), 35119-35125.

Binder, L. I., Frankfurter, A., & Rebhun, L. I. (1985). The distribution of tau in the mammalian central nervous system. *J Cell Biol*, *101*(4), 1371-1378.

Binder, L. I., Guillozet-Bongaarts, A. L., Garcia-Sierra, F., & Berry, R. W. (2005, Jan 3). Tau, tangles, and Alzheimer's disease. *Biochim Biophys Acta*, *1739*(2-3), 216-223.

Bloom, G. S., Richards, B. W., Leopold, P. L., Ritchey, D. M., & Brady, S. T. (1993, Jan). GTP gamma S inhibits organelle transport along axonal microtubules. *J Cell Biol*, *120*(2), 467-476.

Braak, E., Braak, H., & Mandelkow, E. M. (1994). A sequence of cytoskeleton changes related to the formation of neurofibrillary tangles and neuropil threads. *Acta Neuropathol*, *87*(6), 554-567.

Braak, H. (1996, July 24-29, 1996). Evolution of Alzheimer's disease related intraneuronal changes. *Fifth International Conference: On Alzheimer's Disease And Related Disorders*. Osaka, Japan.

Braak, H., & Braak, E. (1995). Staging of Alzheimer's disease-related neurofibrillary changes. *Neurobiol Aging*, *16*(3), 271-278; discussion 278-284.

Brady, S. T. (1985, Sep 5-11). A novel brain ATPase with properties expected for the fast axonal transport motor. *Nature*, *317*(6032), 73-75.

Brady, S. T., Lasek, R. J., & Allen, R. D. (1985). Video microscopy of fast axonal transport in extruded axoplasm: a new model for study of molecular mechanisms. *Cell Motil*, *5*(2), 81-101.

Bramblett, G. T., Goedert, M., Jakes, R., Merrick, S. E., Trojanowski, J. Q., & Lee, V. M. (1993). Abnormal tau phosphorylation at Ser396 in Alzheimer's disease recapitulates development and contributes to reduced microtubule binding. *Neuron*, *10*(6), 1089-1099.

Brandt, R., Hundelt, M., & Shahani, N. (2005, Jan 3). Tau alteration and neuronal degeneration in tauopathies: mechanisms and models. *Biochim Biophys Acta*, *1739*(2-3), 331-354.

Brandt, R., Leger, J., & Lee, G. (1995). Interaction of tau with the neural plasma membrane mediated by tau's amino-terminal projection domain. *J Cell Biol*, *131*(5), 1327-1340.

Brito, R. M., & Vaz, W. L. (1986). Determination of the critical micelle concentration of surfactants using the fluorescent probe N-phenyl-1-naphthylamine. *Anal Biochem*, *152*(2), 250-255.

Buee-Scherrer, V., Condamines, O., Mourton-Gilles, C., Jakes, R., Goedert, M., Pau, B., et al. (1996). AD2, a phosphorylation-dependent monoclonal antibody directed against tau proteins found in Alzheimer's disease. *Brain Res Mol Brain Res*, *39*(1-2), 79-88.

Buee, L., Bussiere, T., Buee-Scherrer, V., Delacourte, A., & Hof, P. R. (2000). Tau protein isoforms, phosphorylation and the role in neurodegenerative disorders. *Brain Res Brain Res Rev*, *33*(1), 95-130.

Butner, K. A., & Kirschner, M. W. (1991). Tau protein binds to microtubules through a flexible array of distributed weak sites. *J Cell Biol*, *115*(3), 717-730.

Carlson, S. W., Branden, M., Voss, K., Sun, Q., Rankin, C. A., & Gamblin, T. C. (2007, Jul 31). A complex mechanism for inducer mediated tau polymerization. *Biochemistry*, *46*(30), 8838-8849.

Carmel, G., Mager, E. M., Binder, L. I., & Kuret, J. (1996). The structural basis of monoclonal antibody Alz50's selectivity for Alzheimer's disease pathology. *J Biol Chem*, *271*(51), 32789-32795.

Caughey, B., & Lansbury, P. T. (2003). Protofibrils, pores, fibrils, and neurodegeneration: separating the responsible protein aggregates from the innocent bystanders. *Annu Rev Neurosci*, *26*, 267-298.

Chau, M. F., Radeke, M. J., de Ines, C., Barasoain, I., Kohlstaedt, L. A., & Feinstein, S. C. (1998, Dec 22). The microtubule-associated protein tau cross-links to two distinct sites on each alpha and beta tubulin monomer via separate domains. *Biochemistry*, *37*(51), 17692-17703.

Chirita, C., Necula, M., & Kuret, J. (2004). Ligand-dependent inhibition and reversal of tau filament formation. *Biochemistry*, *43*(10), 2879-2887.

Chirita, C. N., Congdon, E. E., Yin, H., & Kuret, J. (2005). Triggers of full-length tau aggregation: a role for partially folded intermediates. *Biochemistry*, *44*(15), 5862-5872.

Chirita, C. N., & Kuret, J. (2004). Evidence for an intermediate in tau filament formation. *Biochemistry*, *43*(6), 1704-1714.

Chirita, C. N., Necula, M., & Kuret, J. (2003). Anionic micelles and vesicles induce tau fibrillization in vitro. *Journal of Biological Chemistry.*, *278*(28), 25644-25650.

Cleveland, D. W., Hwo, S. Y., & Kirschner, M. W. (1977). Purification of tau, a microtubule-associated protein that induces assembly of microtubules from purified tubulin. *J Mol Biol*, *116*(2), 207-225.

Coffey, E. T., Smiciene, G., Hongisto, V., Cao, J., Brecht, S., Herdegen, T., et al. (2002, Jun 1). c-Jun N-terminal protein kinase (JNK) 2/3 is specifically activated by stress, mediating c-Jun activation, in the presence of constitutive JNK1 activity in cerebellar neurons. *J Neurosci*, *22*(11), 4335-4345.

Cohen, P. (1991). Classification of protein-serine/threonine phosphatases: identification and quantitation in cell extracts. *Methods Enzymol*, *201*, 389-398.

Condamines, O., Buee-Scherrer, V., Boissier, L., Wattez, A., Delacourte, A., Pau, B., et al. (1995). New immunoassay for the mapping of neurofibrillary degeneration in Alzheimer's disease using two monoclonal antibodies against human paired helical filament tau proteins. *Neurosci Lett*, *192*(2), 81-84.

Desai, A., & Mitchison, T. J. (1997). Microtubule polymerization dynamics. *Annu Rev Cell Dev Biol*, *13*, 83-117.

Drewes, G., Ebneth, A., & Mandelkow, E. M. (1998). MAPs, MARKs and microtubule dynamics. *Trends Biochem Sci*, *23*(8), 307-311.

Drewes, G., Ebneth, A., Preuss, U., Mandelkow, E. M., & Mandelkow, E. (1997, Apr 18). MARK, a novel family of protein kinases that phosphorylate microtubule-associated proteins and trigger microtubule disruption. *Cell*, *89*(2), 297-308.

Drubin, D. G., Feinstein, S. C., Shooter, E. M., & Kirschner, M. W. (1985). Nerve growth factor-induced neurite outgrowth in PC12 cells involves the coordinate induction of microtubule assembly and assembly-promoting factors. *J Cell Biol*, *101*(5 Pt 1), 1799-1807.

Duyckaerts, C., Colle, M. A., Dessi, F., Piette, F., & Hauw, J. J. (1998). Progression of Alzheimer histopathological changes. *Acta Neurol Belg*, *98*(2), 180-185.

Ebneth, A., Godemann, R., Stamer, K., Illenberger, S., Trinczek, B., & Mandelkow, E. (1998). Overexpression of tau protein inhibits kinesin-dependent trafficking of vesicles, mitochondria, and endoplasmic reticulum: implications for Alzheimer's disease. *J Cell Biol*, *143*(3), 777-794.

Eliezer, D., Barre, P., Kobaslija, M., Chan, D., Li, X., & Heend, L. (2005). Residual structure in the repeat domain of tau: echoes of microtubule binding and paired helical filament formation. *Biochemistry*, *44*(3), 1026-1036.

Esposito, G., Viglino, P., Novak, M., & Cattaneo, A. (2000, Nov). The solution structure of the C-terminal segment of tau protein. *J Pept Sci*, *6*(11), 550-559.

Fath, T., Eidenmuller, J., & Brandt, R. (2002, Nov 15). Tau-mediated cytotoxicity in a pseudohyperphosphorylation model of Alzheimer's disease. *J Neurosci*, *22*(22), 9733-9741.

Felgner, H., Frank, R., Biernat, J., Mandelkow, E. M., Mandelkow, E., Ludin, B., et al. (1997, Sep 8). Domains of neuronal microtubule-associated proteins and flexural rigidity of microtubules. *J Cell Biol*, *138*(5), 1067-1075.

Ferrer, I., Gomez-Isla, T., Puig, B., Freixes, M., Ribe, E., Dalfo, E., et al. (2005, Jan). Current advances on different kinases involved in tau phosphorylation, and implications in Alzheimer's disease and tauopathies. *Curr Alzheimer Res*, *2*(1), 3-18.

Friedhoff, P., von Bergen, M., Mandelkow, E., & Davies, P. (1998). A nucleated assembly mechanism of alzheimer paired helical filaments. *Proc Natl Acad Sci U S A*, *95*(26), 15712-15717.

Fulga, T. A., Elson-Schwab, I., Khurana, V., Steinhilb, M. L., Spires, T. L., Hyman, B. T., et al. (2007, Feb). Abnormal bundling and accumulation of F-actin mediates tau-induced neuronal degeneration in vivo. *Nat Cell Biol*, *9*(2), 139-148.

Gamblin, T. C., Berry, R. W., & Binder, L. I. (2003). Modeling tau polymerization in vitro: a review and synthesis. *Biochemistry*, *42*(51), 15009-15017.

Gamblin, T. C., Berry, R. W., & Binder, L. I. (2003). Tau polymerization: role of the amino terminus. *Biochemistry*, *42*, 2252-2257.

Gamblin, T. C., Chen, F., Zambrano, A., Abraha, A., Lagalwar, S., Guillozet, A. L., et al. (2003, Aug 19). Caspase cleavage of tau: linking amyloid and neurofibrillary tangles in Alzheimer's disease. *Proc Natl Acad Sci U S A*, *100*(17), 10032-10037.

Gamblin, T. C., King, M. E., Dawson, H., Vitek, M. P., Kuret, J., Berry, R. W., et al. (2000). In vitro polymerization of tau protein monitored by laser light scattering: Method and application to the study of FTDP-17 mutants. *Biochemistry*, *39*(20), 6136-6144.

Gamblin, T. C., King, M. E., Kuret, J., Berry, R. W., & Binder, L. I. (2000). Oxidative regulation of fatty acid-induced tau polymerization. *Biochemistry*, *39*(46), 14203-14210.

Garcia-Sierra, F., Berry, R. W., Lagalwar, S., Ghoshal, N., Quinn, B., Cryns, V. L., et al. (2002). Cleavage of tau protein at Asp-421 caspase site and truncation at Glu-391 during the formation and evolution of neurofibrillary tangles. *2002 Abstract Viewer/Itinerary Planner- Society for Neuroscience*

Garcia-Sierra, F., Ghoshal, N., Quinn, B., Berry, R. W., & Binder, L. I. (2003, Apr). Conformational changes and truncation of tau protein during tangle evolution in Alzheimer's disease. *J Alzheimer's Dis*, *5*(2), 65-77.

Ghoshal, N., Garcia-Sierra, F., Fu, Y., Beckett, L. A., Mufson, E. J., Kuret, J., et al. (2001, Jun). Tau-66: Evidence for a novel tau conformation in Alzheimer's disease. *J Neurochem*, *77*(5), 1372-1385.

Ghoshal, N., Garcia-Sierra, F., Wuu, J., Leurgans, S., Bennett, D. A., Berry, R. W., et al. (2002). Tau Conformational Changes Correspond to Impairments of Episodic Memory in Mild Cognitive Impairment and Alzheimer’s Disease. *Exp Neurol*, *177*(2), 475-493.

Goedert, M., & Jakes, R. (2005, Jan 3). Mutations causing neurodegenerative tauopathies. *Biochim Biophys Acta*, *1739*(2-3), 240-250.

Goedert, M., Jakes, R., Crowther, R. A., Six, J., Lubke, U., Vandermeeren, M., et al. (1993). The abnormal phosphorylation of tau protein at Ser-202 in Alzheimer disease recapitulates phosphorylation during development. *Proc Natl Acad Sci U S A*, *90*(11), 5066-5070.

Goedert, M., Spillantini, M. G., & Davies, S. W. (1998). Filamentous nerve cell inclusions in neurodegenerative diseases. *Curr Opin Neurobiol*, *8*(5), 619-632.

Goode, B. L., Chau, M., Denis, P. E., & Feinstein, S. C. (2000, Dec 8). Structural and functional differences between 3-repeat and 4-repeat tau isoforms. Implications for normal tau function and the onset of neurodegenetative disease. *J Biol Chem*, *275*(49), 38182-38189.

Goode, B. L., & Feinstein, S. C. (1994, Mar). Identification of a novel microtubule binding and assembly domain in the developmentally regulated inter-repeat region of tau. *J Cell Biol*, *124*(5), 769-782.

Grant, P., Diggins, M., & Pant, H. C. (1999, Jul). Topographic regulation of cytoskeletal protein phosphorylation by multimeric complexes in the squid giant fiber system. *J Neurobiol*, *40*(1), 89-102.

Gray, E. G., Paula-Barbosa, M., & Roher, A. (1987). Alzheimer's disease: paired helical filaments and cytomembranes. *Neuropathol Appl Neurobiol*, *13*(2), 91-110.

Grundke-Iqbal, I., Iqbal, K., Tung, Y. C., Quinlan, M., Wisniewski, H. M., & Binder, L. I. (1986). Abnormal phosphorylation of the microtubule-associated protein tau (tau) in Alzheimer cytoskeletal pathology. *Proc Natl Acad Sci U S A*, *83*(13), 4913-4917.

Guillozet-Bongaarts, A. L., Cahill, M. E., Cryns, V. L., Reynolds, M. R., Berry, R. W., & Binder, L. I. (2006). Pseudophosphorylation of tau at serine422 inhibits caspase cleavage: in vitro evidence and implications for tangle formation in vivo. *Journal of Neurochemistry*, *97*(4), 1005-1014.

Guillozet-Bongaarts, A. L., Garcia-Sierra, F., Reynolds, M. R., Horowitz, P. M., Fu, Y., Wang, T., et al. (2005, Jul). Tau truncation during neurofibrillary tangle evolution in Alzheimer's disease. *Neurobiol Aging*, *26*(7), 1015-1022.

Gunawardena, S., & Goldstein, L. S. (2004, Feb 5). Cargo-carrying motor vehicles on the neuronal highway: transport pathways and neurodegenerative disease. *J Neurobiol*, *58*(2), 258-271.

Gustke, N., Trinczek, B., Biernat, J., Mandelkow, E. M., & Mandelkow, E. (1994). Domains of tau protein and interactions with microtubules. *Biochemistry*, *33*(32), 9511-9522.

Hagiwara, H., Yorifuji, H., Sato-Yoshitake, R., & Hirokawa, N. (1994, Feb 4). Competition between motor molecules (kinesin and cytoplasmic dynein) and fibrous microtubule-associated proteins in binding to microtubules. *J Biol Chem*, *269*(5), 3581-3589.

Hall, G. F., Lee, V. M., Lee, G., & Yao, J. (2001). Staging of neurofibrillary degeneration caused by human tau overexpression in a unique cellular model of human tauopathy. *Am J Pathol*, *158*(1), 235-246.

Hayashi, S., Toyoshima, Y., Hasegawa, M., Umeda, Y., Wakabayashi, K., Tokiguchi, S., et al. (2002, Apr). Late-onset frontotemporal dementia with a novel exon 1 (Arg5His) tau gene mutation. *Ann Neurol*, *51*(4), 525-530.

Hoffmann, R., Lee, V. M. Y., Leight, S., Varga, I., & Otvos, L., Jr. (1997). Unique Alzheimer's disease paired helical filament specific epitopes involve double phosphorylation at specific sites. *Biochemistry*, *36*(26), 8114-8124.

Hogg, M., Grujic, Z. M., Baker, M., Demirci, S., Guillozet, A. L., Sweet, A. P., et al. (2003). The L266V tau mutation is associated with frontotemporal dementia and Pick-like 3R and 4R tauopathy. *Acta Neuropathologica*, *106*(4), 323-336.

Horowitz, P. M., LaPointe, N., Guillozet-Bongaarts, A. L., Berry, R. W., & Binder, L. I. (2006, Oct 24). N-terminal fragments of tau inhibit full-length tau polymerization *in vitro*. *Biochemistry*, *45*(42), 12859-12866

Horowitz, P. M., Patterson, K. R., Guillozet-Bongaarts, A. L., Reynolds, M. R., Carroll, C. A., Weintraub, S. T., et al. (2004, Sep 8). Early N-terminal changes and caspase-6 cleavage of tau in Alzheimer's disease. *J Neurosci*, *24*(36), 7895-7902.

Hutton, M. (2001, Jun). Missense and splice site mutations in tau associated with FTDP-17: multiple pathogenic mechanisms. *Neurology*, *56*(11 Suppl 4), S21-25.

Hutton, M., Lendon, C. L., Rizzu, P., Baker, M., Froelich, S., Houlden, H., et al. (1998). Association of missense and 5'-splice-site mutations in tau with the inherited dementia FTDP-17. *Nature*, *393*(6686), 702-705.

Hwang, S. C., Jhon, D. Y., Bae, Y. S., Kim, J. H., & Rhee, S. G. (1996). Activation of phospholipase C-gamma by the concerted action of tau proteins and arachidonic acid. *J Biol Chem*, *271*(31), 18342-18349.

Hyman, B. T., Van Hoesen, G. W., Wolozin, B. L., Davies, P., Kromer, L. J., & Damasio, A. R. (1988). Alz-50 antibody recognizes Alzheimer-related neuronal changes. *Ann Neurol*, *23*(4), 371-379.

Ikegami, K., Kimura, T., Katsuragi, S., Ono, T., Yamamoto, H., Miyamoto, E., et al. (1996). Immunohistochemical examination of phosphorylated tau in granulovacuolar degeneration granules. *Psychiatry Clin Neurosci*, *50*(3), 137-140.

Jeganathan, S., von Bergen, M., Brutlach, H., Steinhoff, H. J., & Mandelkow, E. (2006). Global hairpin folding of tau in solution. *Biochemistry*, *45*(7), 2283-2293.

Jicha, G. A., Berenfeld, B., & Davies, P. (1999). Sequence requirements for formation of conformational variants of tau similar to those found in Alzheimer's disease. *J Neurosci Res*, *55*(6), 713-723.

Johnson, G. V. W., & Hartigan, J. A. (1998). Tau protein in normal and Alzheimer's disease brain: An update. *Alzheimer's Disease Review*, *3*, 125-141.

Johnson, G. V. W., & Jenkins, S. M. (1996). Tau protein in normal and Alzheimer's disease brain. *Alzheimer's Disease Review*, *1*, 38-54.

Kanemaru, K., Takio, K., Miura, R., Titani, K., & Ihara, Y. (1992). Fetal-type phosphorylation of the tau in paired helical filaments. *J Neurochem*, *58*(5), 1667-1675.

Khatoon, S., Grundke-Iqbal, I., & Iqbal, K. (1992). Brain levels of microtubule-associated protein tau are elevated in Alzheimer's disease: a radioimmuno-slot-blot assay for nanograms of the protein. *J Neurochem*, *59*(2), 750-753.

Khlistunova, I., Biernat, J., Wang, Y., Pickhardt, M., von Bergen, M., Gazova, Z., et al. (2006, Jan 13). Inducible expression of Tau repeat domain in cell models of tauopathy: aggregation is toxic to cells but can be reversed by inhibitor drugs. *J Biol Chem*, *281*(2), 1205-1214.

Kimura, T., Ono, T., Takamatsu, J., Yamamoto, H., Ikegami, K., Kondo, A., et al. (1996). Sequential changes of tau-site-specific phosphorylation during development of paired helical filaments. *Dementia*, *7*(4), 177-181.

King, M. E. (2005, Jan 3). Can tau filaments be both physiologically beneficial and toxic? *Biochim Biophys Acta*, *1739*(2-3), 260-267.

King, M. E., Ahuja, V., Binder, L. I., & Kuret, J. (1999). Ligand-dependent tau filament formation: Implications for Alzheimer's disease progression. *Biochemistry*, *38*(45), 14851-14859.

King, M. E., Gamblin, T. C., Kuret, J., & Binder, L. I. (2000). Differential assembly of human tau isoforms in the presence of arachidonic acid. *J Neurochem*, *74*(4), 1749-1757.

King, M. E., Kan, H. M., Baas, P. W., Erisir, A., Glabe, C. G., & Bloom, G. S. (2006, Nov 20). Tau-dependent microtubule disassembly initiated by prefibrillar beta-amyloid. *J Cell Biol*, *175*(4), 541-546.

Kosik, K. S., Joachim, C. L., & Selkoe, D. J. (1986). Microtubule-associated protein tau (tau) is a major antigenic component of paired helical filaments in Alzheimer disease. *Proc Natl Acad Sci U S A*, *83*(11), 4044-4048.

Kosik, K. S., Orecchio, L. D., Binder, L., Trojanowski, J. Q., Lee, V. M., & Lee, G. (1988). Epitopes that span the tau molecule are shared with paired helical filaments. *Neuron*, *1*(9), 817-825.

Kozikowski, A. P., Gaisina, I. N., Yuan, H., Petukhov, P. A., Blond, S. Y., Fedolak, A., et al. (2007, Jul 4). Structure-Based Design Leads to the Identification of Lithium Mimetics That Block Mania-like Effects in Rodents. Possible New GSK-3beta Therapies for Bipolar Disorders. *J Am Chem Soc*, *129*(26), 8328-8332.

Kuret, J., Chirita, C. N., Congdon, E. E., Kannanayakal, T., Li, G., Necula, M., et al. (2005, Jan 3). Pathways of tau fibrillization. *Biochim Biophys Acta*, *1739*(2-3), 167-178.

Lee, G. (2005, Jan 3). Tau and src family tyrosine kinases. *Biochim Biophys Acta*, *1739*(2-3), 323-330.

Lee, G., Neve, R. L., & Kosik, K. S. (1989, Jun). The microtubule binding domain of tau protein. *Neuron*, *2*(6), 1615-1624.

Lee, G., Newman, S. T., Gard, D. L., Band, H., & Panchamoorthy, G. (1998). Tau interacts with src-family non-receptor tyrosine kinases. *J Cell Sci*, *111*(Pt 21), 3167-3177.

Lee, G., Thangavel, R., Sharma, V. M., Litersky, J. M., Bhaskar, K., Fang, S. M., et al. (2004). Phosphorylation of tau by fyn: implications for Alzheimer's disease. *J Neurosci*, *24*(9), 2304-2312.

Lee, V. M., Goedert, M., & Trojanowski, J. Q. (2001). Neurodegenerative tauopathies. *Annu Rev Neurosci*, *24*, 1121-1159.

Leroy, O., Wang, J., Maurage, C. A., Parent, M., Cooper, T., Buee, L., et al. (2006, Apr). Brain-specific change in alternative splicing of Tau exon 6 in myotonic dystrophy type 1. *Biochim Biophys Acta*, *1762*(4), 460-467.

Levy, S. F., Leboeuf, A. C., Massie, M. R., Jordan, M. A., Wilson, L., & Feinstein, S. C. (2005, Apr 8). Three- and four-repeat tau regulate the dynamic instability of two distinct microtubule subpopulations in qualitatively different manners. Implications for neurodegeneration. *J Biol Chem*, *280*(14), 13520-13528.

Liao, H., Li, Y., Brautigan, D. L., & Gundersen, G. G. (1998). Protein phosphatase 1 is targeted to microtubules by the microtubule-associated protein Tau. *J Biol Chem*, *273*(34), 21901-21908.

Lichtenberg-Kraag, B., Mandelkow, E. M., Biernat, J., Steiner, B., Schroter, C., Gustke, N., et al. (1992, Jun 15). Phosphorylation-dependent epitopes of neurofilament antibodies on tau protein and relationship with Alzheimer tau. *Proc Natl Acad Sci U S A*, *89*(12), 5384-5388.

Loomis, P. A., Howard, T. H., Castleberry, R. P., & Binder, L. I. (1990). Identification of nuclear tau isoforms in human neuroblastoma cells. *Proc Natl Acad Sci U S A*, *87*(21), 8422-8426.

LoPresti, P., Szuchet, S., Papasozomenos, S. C., Zinkowski, R. P., & Binder, L. I. (1995). Functional implications for the microtubule-associated protein tau: localization in oligodendrocytes. *Proc Natl Acad Sci U S A*, *92*(22), 10369-10373.

Lowry, O. H., Rosenbrough, N. J., Farr, A. L., & Randall, R. J. (1951). Protein measurement with the Folin phenol reagent. *J Biol Chem*, *193*, 265-275.

Luo, M. H., Tse, S. W., Memmott, J., & Andreadis, A. (2004). Novel isoforms of tau that lack the microtubule-binding domain. *Journal of Neurochemistry*, *90*(2), 340-351.

Maas, T., Eidenmuller, J., & Brandt, R. (2000). Interaction of tau with the neural membrane cortex is regulated by phosphorylation at sites that are modified in paired helical filaments. *J Biol Chem*, *275*(21), 15733-15740.

Maeda, S., Sahara, N., Saito, Y., Murayama, M., Yoshiike, Y., Kim, H., et al. (2007, Mar 27). Granular tau oligomers as intermediates of tau filaments. *Biochemistry*, *46*(12), 3856-3861.

Maeda, S., Sahara, N., Saito, Y., Murayama, S., Ikai, A., & Takashima, A. (2006, Mar). Increased levels of granular tau oligomers: an early sign of brain aging and Alzheimer's disease. *Neurosci Res*, *54*(3), 197-201.

Makrides, V., Massie, M. R., Feinstein, S. C., & Lew, J. (2004, Apr 27). Evidence for two distinct binding sites for tau on microtubules. *Proc Natl Acad Sci U S A*, *101*(17), 6746-6751.

Makrides, V., Shen, T. E., Bhatia, R., Smith, B. L., Thimm, J., Lal, R., et al. (2003, Aug 29). Microtubule-dependent oligomerization of tau. Implications for physiological tau function and tauopathies. *J Biol Chem*, *278*(35), 33298-33304.

Mandelkow, E., von Bergen, M., Biernat, J., & Mandelkow, E. M. (2007, Jan). Structural principles of tau and the paired helical filaments of Alzheimer's disease. *Brain Pathol*, *17*(1), 83-90.

Mandelkow, E. M., Thies, E., Trinczek, B., Biernat, J., & Mandelkow, E. (2004, Oct 11). MARK/PAR1 kinase is a regulator of microtubule-dependent transport in axons. *J Cell Biol*, *167*(1), 99-110.

Margolis, R. L., & Wilson, L. (1998, Oct). Microtubule treadmilling: what goes around comes around. *Bioessays*, *20*(10), 830-836.

Marx, A., Muller, J., Mandelkow, E. M., Hoenger, A., & Mandelkow, E. (2006). Interaction of kinesin motors, microtubules, and MAPs. *J Muscle Res Cell Motil*, *27*(2), 125-137.

Mesulam, M. M. (1999). Neuroplasticity failure in Alzheimer's disease: bridging the gap between plaques and tangles. *Neuron*, *24*(3), 521-529.

Minoura, K., Mizushima, F., Tokimasa, M., Hiraoka, S., Tomoo, K., Sumida, M., et al. (2005). Structural evaluation of conformational transition state responsible for self-assembly of tau microtubule-binding domain. *Biochemical & Biophysical Research Communications*, *327*(4), 1100-1104.

Minoura, K., Tomoo, K., Ishida, T., Hasegawa, H., Sasaki, M., & Taniguchi, T. (2002, Jun 7). Amphipathic helical behavior of the third repeat fragment in the tau microtubule-binding domain, studied by (1)H NMR spectroscopy. *Biochem Biophys Res Commun*, *294*(2), 210-214.

Minoura, K., Yao, T. M., Tomoo, K., Sumida, M., Sasaki, M., Taniguchi, T., et al. (2004). Different associational and conformational behaviors between the second and third repeat fragments in the tau microtubule-binding domain. *European Journal of Biochemistry*, *271*(3), 545-552.

Mitchell, T. W., Mufson, E. J., Schneider, J. A., Cochran, E. J., Nissanov, J., Han, L. Y., et al. (2002, Feb). Parahippocampal tau pathology in healthy aging, mild cognitive impairment, and early Alzheimer's disease. *Ann Neurol*, *51*(2), 182-189.

Morfini, G., Pigino, G., Beffert, U., Busciglio, J., & Brady, S. T. (2002). Fast axonal transport misregulation and Alzheimer's disease. *Neuromolecular Med*, *2*(2), 89-99.

Morfini, G., Pigino, G., & Brady, S. T. (2005, Feb). Polyglutamine expansion diseases: failing to deliver. *Trends Mol Med*, *11*(2), 64-70.

Morfini, G., Pigino, G., Mizuno, N., Kikkawa, M., & Brady, S. T. (2007, Jan 30). Tau binding to microtubules does not directly affect microtubule-based vesicle motility. *J Neurosci Res*

Morfini, G., Pigino, G., Opalach, K., Serulle, Y., Moreira, J. E., Sugimori, M., et al. (2007, Feb 13). 1-Methyl-4-phenylpyridinium affects fast axonal transport by activation of caspase and protein kinase C. *Proc Natl Acad Sci U S A*, *104*(7), 2442-2447.

Morfini, G., Pigino, G., Szebenyi, G., You, Y., Pollema, S., & Brady, S. T. (2006, Jul). JNK mediates pathogenic effects of polyglutamine-expanded androgen receptor on fast axonal transport. *Nat Neurosci*, *9*(7), 907-916.

Morfini, G., Szebenyi, G., Brown, H., Pant, H. C., Pigino, G., DeBoer, S., et al. (2004, Jun 2). A novel CDK5-dependent pathway for regulating GSK3 activity and kinesin-driven motility in neurons. *Embo J*, *23*(11), 2235-2245.

Morfini, G., Szebenyi, G., Elluru, R., Ratner, N., & Brady, S. T. (2002, Feb 1). Glycogen synthase kinase 3 phosphorylates kinesin light chains and negatively regulates kinesin-based motility. *Embo J*, *21*(3), 281-293.

Morishima-Kawashima, M., Hasegawa, M., Takio, K., Suzuki, M., Yoshida, H., Titani, K., et al. (1995). Proline-directed and non-proline-directed phosphorylation of PHF-tau. *J Biol Chem*, *270*(2), 823-829.

Morris, J. R., & Lasek, R. J. (1984, Jun). Monomer-polymer equilibria in the axon: direct measurement of tubulin and actin as polymer and monomer in axoplasm. *J Cell Biol*, *98*(6), 2064-2076.

Mukrasch, M. D., von Bergen, M., Biernat, J., Fischer, D., Griesinger, C., Mandelkow, E., et al. (2007, Apr 20). The "jaws" of the tau-microtubule interaction. *J Biol Chem*, *282*(16), 12230-12239.

Nacharaju, P., Lewis, J., Easson, C., Yen, S., Hackett, J., Hutton, M., et al. (1999). Accelerated filament formation from tau protein with specific FTDP-17 missense mutations. *FEBS Lett*, *447*(2-3), 195-199.

Neve, R. L., Harris, P., Kosik, K. S., Kurnit, D. M., & Donlon, T. A. (1986). Identification of cDNA clones for the human microtubule-associated protein tau and chromosomal localization of the genes for tau and microtubule-associated protein 2. *Brain Res*, *387*(3), 271-280.

Noble, W., Planel, E., Zehr, C., Olm, V., Meyerson, J., Suleman, F., et al. (2005, May 10). Inhibition of glycogen synthase kinase-3 by lithium correlates with reduced tauopathy and degeneration in vivo. *Proc Natl Acad Sci U S A*, *102*(19), 6990-6995.

Noh, D. Y., Shin, S. H., & Rhee, S. G. (1995, Dec 18). Phosphoinositide-specific phospholipase C and mitogenic signaling. *Biochim Biophys Acta*, *1242*(2), 99-113.

Novak, M., Jakes, R., Edwards, P. C., Milstein, C., & Wischik, C. M. (1991). Difference between the tau protein of Alzheimer paired helical filament core and normal tau revealed by epitope analysis of monoclonal antibodies 423 and 7.51. *Proc Natl Acad Sci U S A*, *88*(13), 5837-5841.

Novak, M., Kabat, J., & Wischik, C. M. (1993). Molecular characterization of the minimal protease resistant tau unit of the Alzheimer's disease paired helical filament. *Embo J*, *12*(1), 365-370.

Odawara, T., Iseki, E., Kosaka, K., Akiyama, H., Ikeda, K., & Yamamoto, T. (1995). Investigation of tau-2 positive microglia-like cells in the subcortical nuclei of human neurodegenerative disorders. *Neurosci Lett*, *192*(3), 145-148.

Otvos, L., Jr., Feiner, L., Lang, E., Szendrei, G. I., Goedert, M., & Lee, V. M. (1994). Monoclonal antibody PHF-1 recognizes tau protein phosphorylated at serine residues 396 and 404. *J Neurosci Res*, *39*(6), 669-673.

Panda, D., Goode, B. L., Feinstein, S. C., & Wilson, L. (1995, Sep 5). Kinetic stabilization of microtubule dynamics at steady state by tau and microtubule-binding domains of tau. *Biochemistry*, *34*(35), 11117-11127.

Papasozomenos, S. C., & Binder, L. I. (1987). Phosphorylation determines two distinct species of Tau in the central nervous system. *Cell Motil Cytoskeleton*, *8*(3), 210-226.

Perez, M., Hernandez, F., Lim, F., Diaz-Nido, J., & Avila, J. (2003, Aug). Chronic lithium treatment decreases mutant tau protein aggregation in a transgenic mouse model. *J Alzheimers Dis*, *5*(4), 301-308.

Pigino, G., Morfini, G., Pelsman, A., Mattson, M. P., Brady, S. T., & Busciglio, J. (2003, Jun 1). Alzheimer's presenilin 1 mutations impair kinesin-based axonal transport. *J Neurosci*, *23*(11), 4499-4508.

Poorkaj, P., Muma, N. A., Zhukareva, V., Cochran, E. J., Shannon, K. M., Hurtig, H., et al. (2002, Oct). An R5L tau mutation in a subject with a progressive supranuclear palsy phenotype. *Ann Neurol*, *52*(4), 511-516.

Preuss, U., Biernat, J., Mandelkow, E. M., & Mandelkow, E. (1997, Mar). The 'jaws' model of tau-microtubule interaction examined in CHO cells. *J Cell Sci*, *110 ( Pt 6)*, 789-800.

Rankin, C. A., Sun, Q., & Gamblin, T. C. (2005, Jul 29). Pseudo-phosphorylation of tau at Ser202 and Thr205 affects tau filament formation. *Brain Res Mol Brain Res*, *138*(1), 84-93.

Reed, L. A., Grabowski, T. J., Schmidt, M. L., Morris, J. C., Goate, A., Solodkin, A., et al. (1997). Autosomal dominant dementia with widespread neurofibrillary tangles [see comments]. *Ann Neurol*, *42*(4), 564-572.

Reynolds, M. R., Berry, R. W., & Binder, L. I. (2005a). Site-specific nitration and oxidative dityrosine bridging of the tau protein by peroxynitrite: implications for Alzheimer's disease. *Biochemistry*, *44*(5), 1690-1700.

Reynolds, M. R., Berry, R. W., & Binder, L. I. (2005b). Site-specific nitration differentially influences tau assembly in vitro. *Biochemistry*, *44*(42), 13997-14009.

Reynolds, M. R., Berry, R. W., & Binder, L. I. (2007, Jun 26). Nitration in neurodegeneration: deciphering the "Hows" "nYs". *Biochemistry*, *46*(25), 7325-7336.

Reynolds, M. R., Lukas, T. J., Berry, R. W., & Binder, L. I. (2006). Peroxynitrite-mediated tau modifications stabilize preformed filaments and destabilize microtubules through distinct mechanisms. *Biochemistry*, *45*(13), 4314-4326.

Reynolds, M. R., Reyes, J. F., Fu, Y., Bigio, E. H., Guillozet-Bongaarts, A. L., Berry, R. W., et al. (2006, Oct 18). Tau nitration occurs at tyrosine 29 in the fibrillar lesions of Alzheimer's disease and other tauopathies. *J Neurosci*, *26*(42), 10636-10645.

Santacruz, K., Lewis, J., Spires, T., Paulson, J., Kotilinek, L., Ingelsson, M., et al. (2005). Tau suppression in a neurodegenerative mouse model improves memory function. *Science*, *309*(5733), 476-481.

Schneider, A., Biernat, J., von Bergen, M., Mandelkow, E., & Mandelkow, E. M. (1999). Phosphorylation that detaches tau protein from microtubules (Ser262, Ser214) also protects it against aggregation into Alzheimer paired helical filaments. *Biochemistry*, *38*(12), 3549-3558.

Schweers, O., Schonbrunn-Hanebeck, E., Marx, A., & Mandelkow, E. (1994). Structural studies of tau protein and Alzheimer paired helical filaments show no evidence for beta-structure. *J Biol Chem*, *269*(39), 24290-24297.

Seitz, A., Kojima, H., Oiwa, K., Mandelkow, E. M., Song, Y. H., & Mandelkow, E. (2002). Single-molecule investigation of the interference between kinesin, tau and MAP2c. *EMBO Journal*, *21*(18), 4896-4905.

Sengupta, S., Horowitz, P. M., Karsten, S. L., Jackson, G. R., Geschwind, D. H., Fu, Y., et al. (2006, Dec 19). Degradation of tau protein by puromycin-sensitive aminopeptidase in vitro. *Biochemistry*, *45*(50), 15111-15119.

Sobue, K., Agarwal-Mawal, A., Li, W., Sun, W., Miura, Y., & Paudel, H. K. (2000, Jun 2). Interaction of neuronal Cdc2-like protein kinase with microtubule-associated protein tau. *J Biol Chem*, *275*(22), 16673-16680.

Sontag, E., Nunbhakdi-Craig, V., Lee, G., Brandt, R., Kamibayashi, C., Kuret, J., et al. (1999). Molecular interactions among protein phosphatase 2A, tau, and microtubules. Implications for the regulation of tau phosphorylation and the development of tauopathies. *J Biol Chem*, *274*(36), 25490-25498.

Stamer, K., Vogel, R., Thies, E., Mandelkow, E., & Mandelkow, E. M. (2002, Mar 18). Tau blocks traffic of organelles, neurofilaments, and APP vesicles in neurons and enhances oxidative stress. *J Cell Biol*, *156*(6), 1051-1063.

Sun, W., Qureshi, H. Y., Cafferty, P. W., Sobue, K., Agarwal-Mawal, A., Neufield, K. D., et al. (2002, Apr 5). Glycogen synthase kinase-3beta is complexed with tau protein in brain microtubules. *J Biol Chem*, *277*(14), 11933-11940.

Syme, C. D., Blanch, E. W., Holt, C., Jakes, R., Goedert, M., Hecht, L., et al. (2002). A Raman optical activity study of rheomorphism in caseins, synucleins and tau. New insight into the structure and behaviour of natively unfolded proteins. *European Journal of Biochemistry*, *269*(1), 148-156.

Terry, R. D. (1998). The cytoskeleton in Alzheimer disease. *J Neural Transm Suppl*, *53*, 141-145.

Timasheff, S. N. (1981). The Self-Assembly of Long Rodlike Structures. In C. Frieden & L. W. Nichol (Eds.), *Protein/Protein Interactions* (pp. 315-336). New York: John Wiley & Sons.

Tokimasa, M., Minoura, K., Hiraoka, S., Tomoo, K., Sumida, M., Taniguchi, T., et al. (2005). Importance of local structures of second and third repeat fragments of microtubule-binding domain for tau filament formation. *FEBS Letters*, *579*(17), 3481-3486.

Ugolini, G., Cattaneo, A., & Novak, M. (1997). Co-localization of truncated tau and DNA fragmentation in Alzheimer's disease neurones. *Neuroreport*, *8*(17), 3709-3712.

Vershinin, M., Carter, B. C., Razafsky, D. S., King, S. J., & Gross, S. P. (2007, Jan 2). Multiple-motor based transport and its regulation by Tau. *Proc Natl Acad Sci U S A*, *104*(1), 87-92.

von Bergen, M., Barghorn, S., Biernat, J., Mandelkow, E. M., & Mandelkow, E. (2005, Jan 3). Tau aggregation is driven by a transition from random coil to beta sheet structure. *Biochim Biophys Acta*, *1739*(2-3), 158-166.

von Bergen, M., Friedhoff, P., Biernat, J., Heberle, J., & Mandelkow, E. (2000). Assembly of tau protein into Alzheimer paired helical filaments depends on a local sequence motif (306VQIVYK311) forming beta structure. *Proc Natl Acad Sci U S A*, *97*(10), 5129-5134.

Wang, J., Tse, S. W., & Andreadis, A. (2007, Jan). Tau exon 6 is regulated by an intricate interplay of trans factors and cis elements, including multiple branch points. *J Neurochem*, *100*(2), 437-445.

Wang, Q. M., Fiol, C. J., DePaoli-Roach, A. A., & Roach, P. J. (1994, May 20). Glycogen synthase kinase-3 beta is a dual specificity kinase differentially regulated by tyrosine and serine/threonine phosphorylation. *J Biol Chem*, *269*(20), 14566-14574.

Wang, Q. M., Roach, P. J., & Fiol, C. J. (1994, Aug 1). Use of a synthetic peptide as a selective substrate for glycogen synthase kinase 3. *Anal Biochem*, *220*(2), 397-402.

Wang, Y. P., Biernat, J., Pickhardt, M., Mandelkow, E., & Mandelkow, E. M. (2007, Jun 12). Stepwise proteolysis liberates tau fragments that nucleate the Alzheimer-like aggregation of full-length tau in a neuronal cell model. *Proc Natl Acad Sci U S A*, *104*(24), 10252-10257.

Wei, M. L., & Andreadis, A. (1998). Splicing of a regulated exon reveals additional complexity in the axonal microtubule-associated protein tau. *J Neurochem*, *70*(4), 1346-1356.

Wei, M. L., Memmott, J., Screaton, G., & Andreadis, A. (2000). The splicing determinants of a regulated exon in the axonal MAP tau reside within the exon and in its upstream intron. *Brain Res Mol Brain Res*, *80*(2), 207-218.

Weingarten, M. D., Lockwood, A. H., Hwo, S. Y., & Kirschner, M. W. (1975). A protein factor essential for microtubule assembly. *Proc Natl Acad Sci U S A*, *72*(5), 1858-1862.

Williamson, R., Scales, T., Clark, B. R., Gibb, G., Reynolds, C. H., Kellie, S., et al. (2002, Jan 1). Rapid tyrosine phosphorylation of neuronal proteins including tau and focal adhesion kinase in response to amyloid-beta peptide exposure: involvement of Src family protein kinases. *J Neurosci*, *22*(1), 10-20.

Wilson, D. M., & Binder, L. I. (1997). Free fatty acids stimulate the polymerization of tau and amyloid beta peptides. In vitro evidence for a common effector of pathogenesis in Alzheimer's disease. *Am J Pathol*, *150*(6), 2181-2195.

Wilson, L., Panda, D., & Jordan, M. A. (1999, Oct). Modulation of microtubule dynamics by drugs: a paradigm for the actions of cellular regulators. *Cell Struct Funct*, *24*(5), 329-335.

Wischik, C. M., Novak, M., Edwards, P. C., Klug, A., Tichelaar, W., & Crowther, R. A. (1988). Structural characterization of the core of the paired helical filament of Alzheimer disease. *Proc Natl Acad Sci U S A*, *85*(13), 4884-4888.

Wischik, C. M., Novak, M., Thogersen, H. C., Edwards, P. C., Runswick, M. J., Jakes, R., et al. (1988). Isolation of a fragment of tau derived from the core of the paired helical filament of Alzheimer disease. *Proc Natl Acad Sci U S A*, *85*(12), 4506-4510.

Wittmann, C. W., Wszolek, M. F., Shulman, J. M., Salvaterra, P. M., Lewis, J., Hutton, M., et al. (2001). Tauopathy in Drosophila: neurodegeneration without neurofibrillary tangles. *Science*, *293*(5530), 711-714.

Wood, J. G., Mirra, S. S., Pollock, N. J., & Binder, L. I. (1986). Neurofibrillary tangles of Alzheimer disease share antigenic determinants with the axonal microtubule-associated protein tau (tau) [published erratum appears in Proc Natl Acad Sci U S A 1986 Dec;83(24):9773]. *Proc Natl Acad Sci U S A*, *83*(11), 4040-4043.

Yoshiyama, Y., Higuchi, M., Zhang, B., Huang, S. M., Iwata, N., Saido, T. C., et al. (2007, Feb 1). Synapse Loss and Microglial Activation Precede Tangles in a P301S Tauopathy Mouse Model. *Neuron*, *53*(3), 337-351.

Zhang, B., Maiti, A., Shively, S., Lakhani, F., McDonald-Jones, G., Bruce, J., et al. (2005, Jan 4). Microtubule-binding drugs offset tau sequestration by stabilizing microtubules and reversing fast axonal transport deficits in a tauopathy model. *Proc Natl Acad Sci U S A*, *102*(1), 227-231.

Zheng-Fischhofer, Q., Biernat, J., Mandelkow, E. M., Illenberger, S., Godemann, R., & Mandelkow, E. (1998). Sequential phosphorylation of Tau by glycogen synthase kinase-3beta and protein kinase A at Thr212 and Ser214 generates the Alzheimer-specific epitope of antibody AT100 and requires a paired-helical-filament-like conformation. *Eur J Biochem*, *252*(3), 542-552.